THE APPLIED COMPUTATIONAL ELECTROMAGNETICS SOCIETY JOURNAL AND NEWSLETTER

Vol.3 No.1 Spring 1988

THE APPLIED COMPUTATIONAL ELECTROMAGNETICS SOCIETY
JOURNAL and NEWSLETTER

Vol. 3 No.1 Spring 1988

APPLIED COMPUTATIONAL ELECTROMAGNETICS SOCIETY

OFFICERS AND COMMITTEE CHAIRMEN

OFFICERS:

James C. Logan
President (1990)
NOSC, Code 822
271 Catalina Blvd.
San Diego, CA 92152
Office: (619) 553-3780

Stan Kubina
Vice President (1990)
Concordia University
7141 Sherbrooke St WEST
Montreal, Quebec
CANADA H4B 1RG
Office: (514) 848-3093

Richard W. Adler
Secretary (1990)
Naval Postgraduate School
Code 62AB
Monterey, CA 93943
Office: (408) 646-2352

James K. Breakall
Treasurer (1990)
Naval Postgraduate School
Code 62BK
Monterey, CA 93943
Office: (408) 646-2383

MEMBERS AT LARGE:

Robert Bevensee
Lawrence Livermore National Lab
PO Box 5504
Livermore, CA 94550
Term: 3 years (expires 1989)
Office: (415) 422-6787

Lee Corrington
COMMANDER
USAISE C/ASB SET-P
Ft. Hauchuca, AZ 85613-5300
Term: 3 years (expires 1990)
Office: (602) 538-7682

Pete Cunningham
COMMANDER
USACECOM AMSEL-RD-C3-TA-1
Ft. Monmouth, NJ 07703
Term: 3 years (expires 1991)
Office: (201) 544-5415

APPLIED COMPUTATIONAL ELECTROMAGNETICS SOCIETY
OFFICERS AND COMMITTEE CHAIRMEN

PAST PRESIDENT:

E.K. Miller
Rockwell Science Center
Box 1085
Thousand Oaks, CA 91365
Office: (805) 373-4297

NEWSLETTER COMMITTEE:
(Publications Committee)

David Stein
Transactions Editor
P.O. Box 530685
Grand Prairie, TX 75073
Office: (214) 266-4958

Michael Thorburn
Advertising Editor
Electrical & Comp. Engr Dept
Oregon State University
Corvallis, OR 97331-3202
Office: (503) 754-3617

MEETINGS COMMITTEE:

Bob Noel, Chairman
Rockwell International
3370 Miraloma Ave
Mail Stop OA13
Anaheim, CA 92803
Office: (714) 779-3073

COMMITTEE ON LONG RANGE PLANNING:
(Technical Activities Committee)

R. Dawson Coblin, Chairman
Lockheed
Missiles & Space Co. Inc.
O/62-42 B/o76
111 Lockheed Way
Sunnyvale, CA 94089-3504
Office: (408) 742-2689

APPLIED COMPUTATIONAL ELECTROMAGNETICS SOCIETY

OFFICERS AND COMMITTEE CHAIRMEN

CONSTITUTION AND BYLAWS COMMITTEE:

Janet McDonald, Chairman
COMMANDER
USAIASE C/ASB-SET-P
Ft. Hauchuca, AZ 85613-5300

Office: (602) 538-7639

SOFTWARE EXCHANGE COMMITTEE:

(Previously established under E. Miller)

C.H. Vandament, Chairman
Rockwell International
802 Brentwood
RIchardson, TX 75080

Office: (214) 705-3952

SOFTWARE PERFORMANCE STANDARDS COMMITTEE:
(Established by ADCOM 3-24-88)

Ed Miller, Chairman
Rockwell Science Center
Box 1085
Thousand Oaks, CA 91365

Office: (805) 373-4297

NOMINATING COMMITTEE:
(For replacement of one Member at Large, to be elected at next general meeting.)

R. Bevensee
Lawrence Livermore National
Laboratory L-156
P.O. Box 5504
Livermore, CA 94550

Office: (408) 412-6787

APPLIED COMPUTATIONAL ELECTROMAGNETICS SOCIETY
OFFICERS AND COMMITTEE CHAIRMEN

AWARDS COMMITTEE:

Lee Corrington, Chairman
COMMANDER
USAISE C/ASB SET-P
Ft. Hauchuca, AZ 85613-5300

Office: (602) 538-7682

1989 SYMPOSIUM PROGRAM COMMITTEE:

Michael Thorburn, Chairman
Electrical and Computer Engineering
Oregon State University
Corvallis, OR 97331-3202

Office: (503) 743-3617

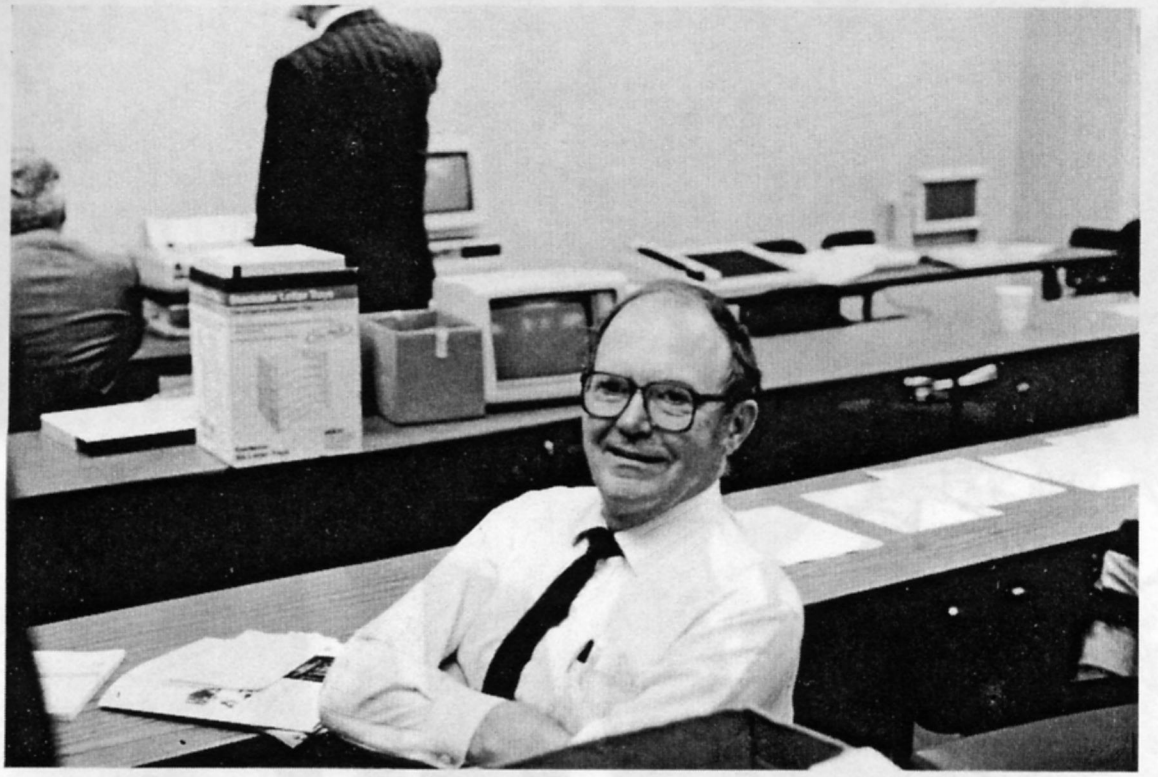

Ed Miller

First president, from date ACES was launched, March 1986 (2nd Annual Review) to Mar 1988, when Jim Logan was elected president at the 4th Annual Review.

Jim Logan **Dave Stein**

Jim Logan - Vice president from Mar 1986 to Mar 1988, when he became president. Dave Stein became Newsletter editor early 1987 & later chairman of Publicity Committee.

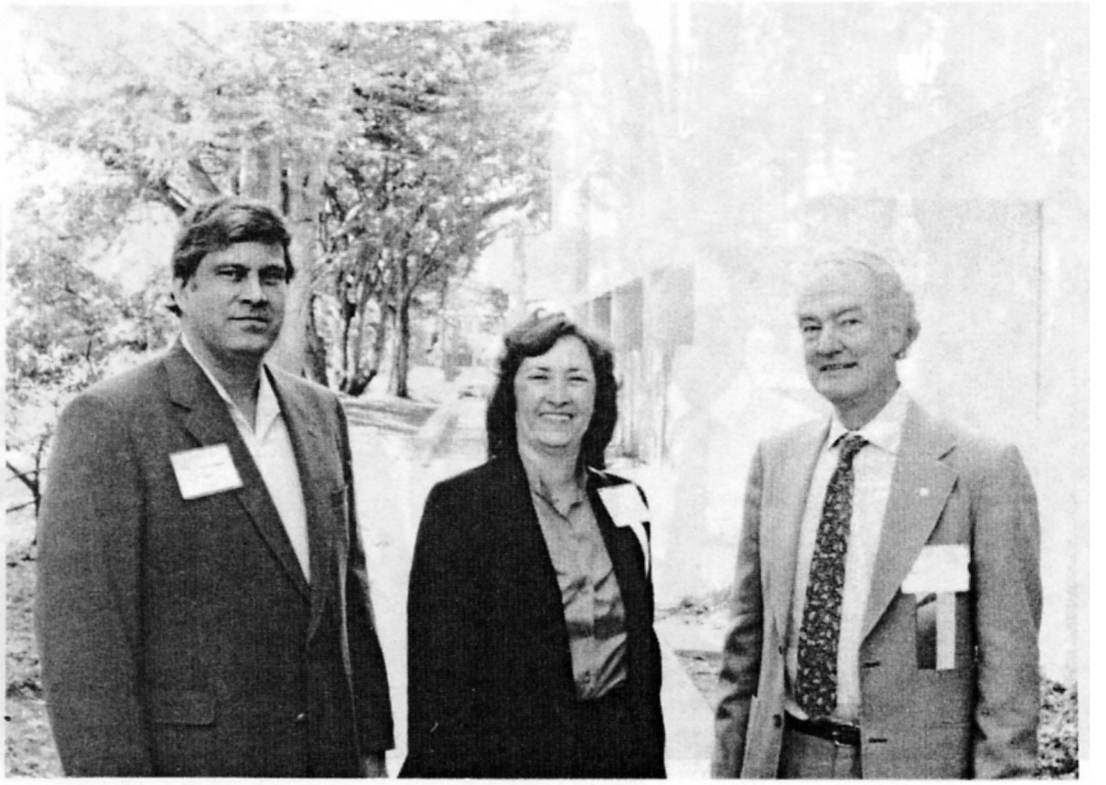

Pete Cunningham Janet McDonald Bob Bevensee

Pete Cunningham - New AdCom member,
3 years until 1989
Janet McDonald - AdCom member 1 year from Mar
1986 to Mar 1987. Currently chairman of
Constitution & By-Laws Comm.
Bob Bevensee - AdCom member 3 yrs,
from Mar 1986 to Mar 1989.
J/NL editor of Nov 86 issue.
Program chairman of 3rd & 4th Annual Review.

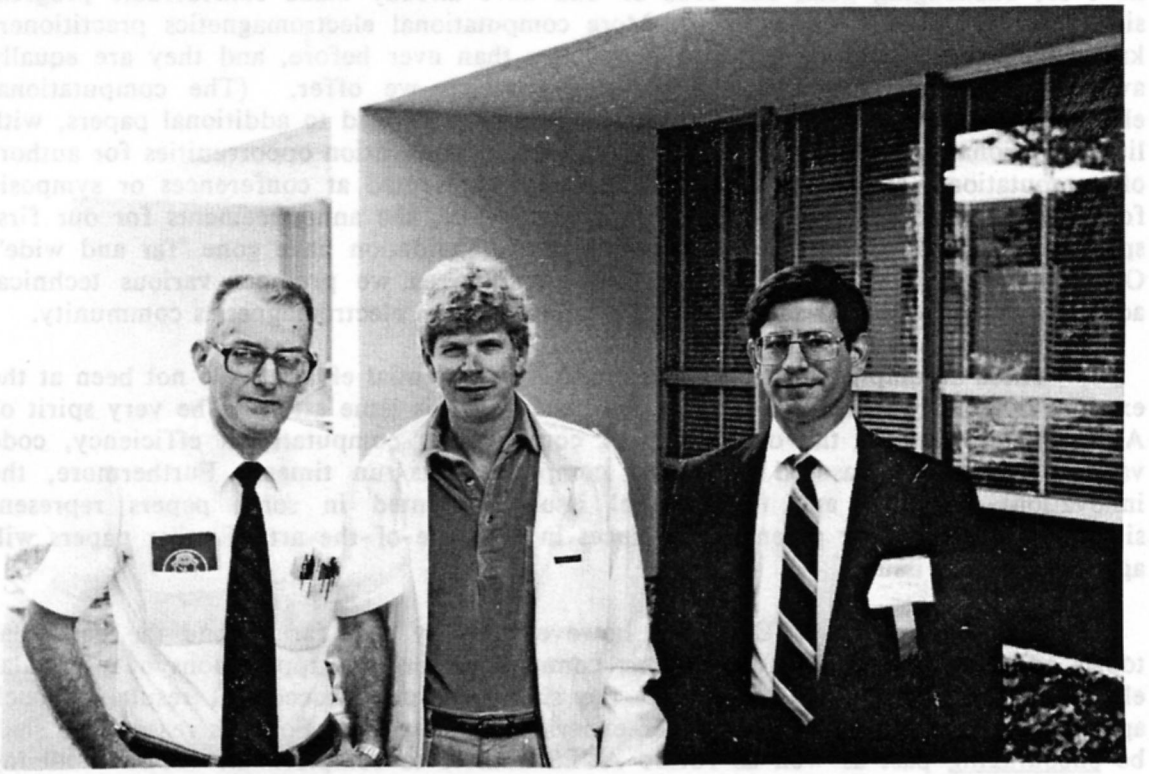

Dick Adler Jim Breakall Dave Stein

Dick Adler - Secretary since Mar 1986.
Jim Breakall - Treasurer since Mar 1986.
Dave Stein - Newsletter Editor

FROM THE EDITOR

With a renewed sense of purpose, our publication moves into its third year. We have set challenging goals for 1988-89 and have already made considerable progress since the March 1988 Conference. More computational electromagnetics practitioners know about the ACES Journal and Newsletter than ever before, and they are equally aware of the new publication opportunities which we offer. (The computational electromagnetics aspects of many research programs can lead to additional papers, with little additional effort). Similarly, we have created publication opportunities for authors of computational electromagnetics-related papers presented at conferences or symposia for which no proceedings are published. Meanwhile, the announcements for our first special issue on Electromagnetics Computer Code Validation have gone "far and wide". Our initiatives in all of these areas will continue as we promote various technical activities and serve larger segments of the computational electromagnetics community.

These accomplishments, though requiring substantial effort, have not been at the expense of quality performance -- as the papers in this issue attest. The very spirit of ACES is reflected in the discussions of convergence, computational efficiency, code validation against measured data, and computer costs/run times. Furthermore, the innovations, insights, and fundamental issues presented in some papers represent significant (achieved or potential) advances in the state-of-the-art. Similar papers will appear in future issues.

The value of an ACES paper, however, usually goes far beyond the particular topics addressed therein. ACES papers commonly represent applications of particular electromagnetics modeling codes, and the successful or unsuccessful results of such application are of interest from a user-experience standpoint. For this reason, we shall be encouraging past as well as future ACES authors to complete the ACES Modeling Short Note form as a supplement to their respective papers. This form, proposed over 1 1/2 years ago, will facilitate the compilation of a user-experience data base. In addition, it will play a role similar to that played by the keywords used by other publications and by literature-search data bases.

Your Editorial Board has included several other proposed projects in a tentative agenda for 1988-89. Some of these projects involve the "Newsletter part", others are more focused toward the "Journal part", while still others are of a general promotional nature. Each ACES member is being provided a copy of this list of "ACES Publications Initiatives", though portions of this list are already familiar to those of you who attended the recent Fourth Annual Review. Of course, most of these initiatives will succeed only with your active support as ACES members. In some cases, success is also contingent upon the efforts of various ACES committees -- for which we were pleased to see a number of recent volunteers.

Although we believe that the agenda reflects your interests and needs, your timely feedback can help us be more responsive to you. Such timely feedback is most critical in a young, rapidly-evolving professional society such as our own. (Unfortunately, in many organizations, there exists at least one member who never responds to solicitations for suggestions or viewpoints -- but who is prompt with complaint after a course of action is selected or after a decision is otherwise reached. This benefits no one).

In the end, the agenda belongs to you.

David E. Stein
Editor-in-Chief

PRESIDENT'S CORNER

James C. Logan

It is an honor to be elected President of ACES and I intend to do my utmost to carry out the duties of this office. To follow in the footsteps of Ed Miller will be no easy task. Under Ed's able leadership over the last few years, ACES has grown to be a viable professional society. The challenge is to continue the growth, filling a niche that serves the professional needs of our members and compliments the activities of other professional societies.

I wish to offer many thanks to all who have served as officers and worked on committees over the past two years to get ACES started up. I especially want to thank Ed Miller, Dick Adler, Bob Bevensee, Mike Thorburn and David Stein for their outstanding contributions. We are fortunate that each of these individuals continue to be very much involved in ACES activities.

With the approval of ADCOM, I have appointed chairman for all standing committees required by the Bylaws as well as the newly created committees. New committees include the Software Performance Standards Committee, the Meetings Committee and the Awards Committee. The Committee on Long Range Planning (or Activities Committee) and the Bylaws Committee have been reactivated. A full list of committees and chairman with addresses and phone numbers appear elsewhere in the Newsletter.

The committee chairman shoulder tough responsibilities that sometimes take a great deal of their personal time. We should all be appreciative of their efforts and do what we can to help them out. I call on my fellow ACES members to volunteer to serve on these committees -- to do so will of course help ACES and it will be an opportunity to work side by side with some top notch people. If you are interested in working on a particular committee, please contact the chairman directly. If you have indicated your interest to volunteer on the questionnaire at the ACES meeting and have not yet been contacted, please call the appropriate chairman -- as we may have unfortunately missed you in summarizing the survey.

We plan to retain current membership and attract new members by offering interesting and useful technical activities. We will continue to expand and develop our software services. But the core of our activities is technical information exchange through our Journal and Newsletter. This year, David Stein is very ambitiously taking on the publication of a special issue of the Journal.

Our goal for the next two years is to double our membership. I believe we can attract many new members through our technical activities. But, everyone can help to achieve this goal by taking every opportunity to spread the word about the advantages of ACES membership. If each member would recruit just one of his colleagues, we could easily achieve this goal.

Our Society is healthy and growing. We have some excellent leadership in our Committee Chairman and together with an active membership, ACES will continue its successful record.

ACES NEWS

1. The 4th Annual Review of Progress in Applied Computational Electromagnetics was a real success. Attendance increased from 125 at the 3rd Annual Review to 166 at this year's meeting. Membership has grown from 189 in 1987 to 453 today.

2. NEEDS 1.0 distribution is at 113 copies. An upgrade will be announced this fall which includes a new antenna matching network code, NEC2-PC compiled for Microsoft Fortran 77 ver. 4.01 and IGUANA 5.1 with surface patch capability.

3. There is a substantial W. German NEEDS User Group operating under IABG, a government-owned non-profit organization which is an active member of the German EMC-Standardization Committee. The committee is considering NEEDS as a reference program for basic EMC numerical work. IABG will work through ACES in updating NEEDS in FRG and will report status to ACES annually, including users' experiences. IABG will act as a German secretary to ACES.

4. A NEC/MININEC User Group is being formed in the UK and has started to distribute an informal newsletter. An ACES connection is being pursued.

5. ACES now has established a co-operative arrangement with several groups. The Nuclear EMP Meeting (NEM), IEEE Antennas and Propagation Society (APS) and IEEE Electromagnetic (EMC) Society. Details will be presented in the Fall J/NL by Ed Miller.

6. The Naval Postgraduate School remains as the site of the 5th Annual Review, in March 1989. Penn State has been proposed as the location of the 1990 6th Annual Review, in May.

7. Printing of the Conference Proceedings of 1988 has been delayed by two factors: Fifteen participants did not submit copies of their presentations on-time, and the NPS Printing Division, who print the Proceedings, had a freeze placed on it until 1 July. The expected date of mailing the Conference Proceedings is 15 Sept.

The Applied Computational Electromagnetics Society announces a

CALL FOR PAPERS

for a Special Issue of the ACES Journal/Newsletter on

Computer Code Validation

Suggested Topics Include:

- Validation of final output with other codes, with analytic solution, or with measurements.
- Identification of suitable test cases/standards.
- Solution convergence, parameter sensitivity, and truncation error.
- Validation of intermediate results.
- Graphical methods in validation.
- Machine dependencies.
- "Basic physics" validation (reciprocity, energy conservation, boundary condition matching).
- Built in diagnostics
- User-option dependencies (mesh size, basis/weight functions)

Applications Include:

Antennas
Radar Cross Section
Shielding
Compatability
RF Networks
Power Transmission
Guided Waves
Basic Physics

DEADLINE IS AUGUST 31, 1988

Send Papers and/or Inquires to:

David Stein
Editor, ACES Journal/Newsletter
Post Office Box 530685
Grand Prairie, TX. 75053-0685
(214) 266-4309

For ACES membership and subscription information contact:

Richard W. Adler
Naval Postgraduate School
Code 62 AB
Monterey, CA. 93943
(408) 646-2352

1989 Symposium

Michael Thorburn
Department of Electrical and Computer Engineering
Oregon State University
Corvallis, Oregon 97331-3202
(503) 754-3617

The 1989 ACES symposium will be held at the Naval Postgraduate School in Monterey from the 21st to the 23rd of March. This may be the last ACES meeting at NPS for a while. With any luck and a little hard work the meeting will be the best we have had yet.

The first CALL FOR PAPERS is being circulated now. Keep an eye out for it. Another announcement will come out in the fall with more information for those who just wish to attend the conference. The deadline for abstract submission has been moved up to January 6, 1989, in order to give the program committee time to review the submissions and reply to all contributors, informing them of their assigned time slot.

Volunteers are needed to serve on the Program Committee. At this time positions are open for:

1. Session Chairmen
   Reviewing abstracts and organizing sessions.

2. Moderator for the Panel Discussion
   Recruit and select the panel, develop the topic and coordinate the discussion.

3. Poster Paper Session Chairman.
   A poster paper session may be held concurrently with the P. C. demonstrations to give the conference attendees something interesting to do while waiting for their turn at the computers. The chairman will organize this effort and establish guidelines for poster papers.

4. Vice Chairmen for the 1989 Symposium (Hosts for future Symposia.)
   ACES is very interested in helping anyone who may be interested in hosting the conference in 1990 or beyond. Such individuals may benefit from being a vice chairperson this year. No specific duties would be required, but vice chairmen would have a voice in all major decisions made.

Suggestions from members are always welcome. Feel free to call me at any time. Let's all participate.

Michael

THE APPLIED COMPUTATIONAL ELECTROMAGNETICS SOCIETY

CALL FOR PAPERS
FOR
THE 5TH ANNUAL REVIEW OF PROGRESS
IN
APPLIED COMPUTATIONAL ELECTROMAGNETICS

March 21-23, 1989 in Monterey, California

- A unique forum for information exchange among practitioners of applied computational electromagnetics.
- Contributions by both users and developers of electromagnetic computer modeling codes are solicited.

SUGGESTED TOPICS INCLUDE:

Codes, Modifications, and Applications
- Moment Methods
- Finite Elements and Finite Differences
- Spectral Domain Techniques
- GTD and Asymptotic Techniques

Graphical Input/Output Issues
Code Validation
New Mathematical Algorithms

APPLICATIONS INCLUDE:

Antenna Analysis
Electromagnetic Compatibility and Interference
Scattering
Microwave Components
MMIC Technology

SEND ABSTRACTS TO:

Michael Thorburn
Dept. of Electrical & Computer Engineering
Oregon State University
Corvallis, OR 97331-3202
(503) 754-3617

Abstracts should be received by January 6, 1989

Camera Ready Summary/Manuscripts will be required later

Benchmark cases are a pet subject of mine, and I welcome a chance to share some ideas with other ACES members.

Comparing numerical results of two or more computer codes is a valuable validation technique. The same is true for experimental data from different antenna ranges, and of course, numerical vs. experimental comparisons.

To facilitate such comparisons, standard benchmark cases are important. The second essential step is to persuade many users to exercise their codes, and antenna ranges, on these cases, and publish their results.

As an attempt to initiate a dialogue on this idea, a strawman set of cases is described below. Obviously more cases are needed to include permeable bodies, etc. It is also desirable to keep the number of cases as small as possible.

Art Ludwig
General Research Corp.
Santa Barbara, CA 93111

Strawman Benchmark cases for perfectly conducting solid bodies

1.0 Body shapes: L=length, D=diameter

- 1.1 Prolate spheroid, L/D=2:1, 4:1, 8:1
- 1.2 Cylinder
  - 1.2.1 Hemisphere-capped L/D=2:1, 5:1
  - 1.2.2 Flat end L/D=5:1, 1-:1
- 1.3 Cube, dimension L
- 1.4 Cone-sphere, Length L, cone half angle 7.5 & 15 degrees

2.0 Frequency: body lengths in wavelengths: 1/2, 1, 5, 10

3.0 Field parameters

- 3.1 Incident field direction: 5-degree increments over interesting region
- 3.2 Incident field polarization: 0 and 90-degree linear
- 3.3 Scattered or radiated field: 1-degree increments over interesting region, relative amplitude and phase of two linear polarizations

4.0 Surface currents in amps/meter along surface of body in 0.1 wavelength increments, for 1-volt/meter incident field

5.0 Other data

- 5.1 Input impedance real and imaginary parts in ohms
- 5.2 Peak gain in dB, or peak RCS in dB relative to one square wavelength

AVAILABLE SOFTWARE

By Charles H. Vandament

The Software Exchange Committee has decided to attempt compilation of a thorough catalog of electromagnetics types of programs. It is our goal to collect and distribute programs to ACES members if the authors authorize such activity, but we also want to list descriptions of programs that are more closely held for one reason or another. In addition to descriptions, we solicit independent opinions on how well programs work compared to other programs.

The catagory is intended to include almost all computational tools used by people engaged in antenna / antenna-field design and research. We might even include propagation programs.

Two programs have been submited by Dr. Darko Kajfez of the University of Mississippi, and two by David J. Pinion of Los Angeles. They are described on the ACES Software Forms in this issue.

Software Distribution Committee
Chuck Vandament, Chairman
802 Brentwood
Richardson, TX 75080

--30--

ACES LIBRARY - UPDATE

CURRENT INDEX OF ITEMS IN LIBRARY:

Item#	Description	Computer
002	MININEC2F frequency sweep	IBM-PC
003	ENHANCED MININEC2 double ARRAY size to 20 wires, etc.	IBM-PC
004	ENHANCED MININEC2	IBM-PC
005	THIN WIRE MININEC2	IBM-PC
006	NEC2	DEC VAX
007	NEC3	DEC VAX
008	NEEDS MININEC3, NEC-PC, IGUANA, GRAPS	IBM-PC/XT or AT
009	MININEC3/GRAPS	IBM-PC/XT or AT
011	NAC-3 ver. 1.3 Updated version (see this issue)	IBM-PC/AT or XT
012	SIGDEMO	IBM-PC
013	Misc BASIC programs RF Designers Toolbox	IBM-PC
014	AT-ESP	IBM-PC/XT or AT

The following items have been added since the Fall 87 J/NL

015	VMAP 2-D vector field plot	IBM-PC
016	DRESP,DRESV2 Dielectric resonators, field distribution plots	IBM-PC
017	NEC-AM AM Broadcast array design	IBM-PC/XT or AT
018	RF65FT v2.0 RF power density for FM/TV via FCC OST BULL.65	IBM-PC/XT or AT

ACES SOFTWARE FORM

Software Number: 011 NAC-3 Vers. 1.30

Machine: IBM PC-AT/XT

Directory Listing:

NAC3.BAT	NAC3IAC.EXE	Library of input files
NAC3.INF	NAC3COR.EXE	

Description: NAC-3 performs a frequency domain analysis of thin wire antenna and scatterers of arbitrary geometry in isotropic but otherwise lossy propagation media. The MoM Code utilizes the point matching technique with collocation and is based on 3-term hyperbolic basis functions of arbitrary complex arguments. NAC-3 is highly modular and consists of a pre-processor, core (may be moved to mainframes or minis for extensive number crunching) and a post-processor. NAC-3 has been optimized for efficiency, numerical stability and accuracy as well as fast execution on PCs, minis and mainframes. VLF limits for dipoles are at L/Wl=1.E-7 single precision and at 1.E-17 double precision, while the corresponding limits for loops are at C/Wl=1.E-3 and 1.E-7 respectively.

a) Features:

1) 800 Segments std. (adjustable)

2) Max size of matrix (adjustable)
   a) 230 Unknowns (in-core)
   b) 800 Unknowns (off-core)
   c) unrestricted symmetry handling

3) 3-D Geometry creation modules

4) Multiple loads (3 modes) and excitations (m modes, mixable)

5) Perfect and finite ground (RCA, and NORTON approximation)

6) Frequency sweeping. Start, stop, linear and user definable f-steps, increments not array limited.

7) Interactive mode (I-NAC-3)
   a) Softkey driven menus
   b) Immediate and extensive input data testing and error analysis

8) Graphics
   a) 3-D geometry views, with optional markers
   b) Display of current/charge
   c) Polar and rectangular far-field plots, lin/log scale
   d) Smith chart, VSWR plot

9) Disk file save and recall of
   a) Geometry
   b) Current and impedance
   c) Far-fields

b) Configuration:

512K RAM (matrix size 195x195 in-core)
640K RAM (matrix size 230x230 in-core)
Add on RAM as VDISK suggested to speed up overlay loading

8087 co-processor required
HERCULES card for graphics
Dot matrix IDS - or Epson compatible printer

c) Software Language:

STAND ALONE versions for either 512K or 640K RAM options, IBM PROFESSIONAL FORTRAN 77 compiler Version 1.00 required if array dimensions need to be adjusted to fit the available RAM

d) Formatted: one 5.25" floppy 1.2M 2HD DOS 2.1

e) Available from:

Dr. Roger Anders
Applied Electromagnetics Engineering
Vorder Halden II
D-7777 Salem 1, West Germany
Ph: ___49 (7553) 7349

f) Access:

no restriction

g) Documentation:

Provided with purchase

h) Cost:

US$ 1,780.00

ACES SOFTWARE FORM

Software Number: 015 VMAP

Machine: IBM PC

Directory Listing:

EXAMPLE1.DAT	EXAMPLE4.DAT
EXAMPLE2.DAT	VMAP.EXE
EXAMPLE3.DAT	VMAP.INI

Description: The interactive graphics program converts the file of data into a 2-dimensional vector field plot. The program drives an x-y plotter and/or a dot matrix graphics printer.

a) Features:

1) Interactive graphic display
2) x-y plotter hard copy
3) graphic printer hard copy

b) Configuration:

EXE file	IBM PC, XT, AT or compatible
Demo data files	Math Coprocessor recommended
256 K bytes min	HP 7475A plotter or equivalent

c) Software Language Required:

DOS 2.1 or later

d) Formatted:

DOS 2.1 or later
5 1/4" diskette

e) Available from:

Dept of Electr. Engr.
U of Mississippi
University, MS 38677

f) Access:

None

g) Documentation:

13 pages and 13 figures

h) Cost:

$25.00

ACES SOFTWARE FORM

Software Number: 016 DRESP,DRESV2

Machine: IBM PC

Directory Listing:

DRESP.BAS DRESV2.ASC
DRESV2.BAS
DRESP.ASC

Description: DRESP: Approximate computation of res. freq. and energy distribution
DRESV2:Approximate computation of res. freq. and a factor both for TE01 mode only

a) Features:

1) Shielded dielectric resonator on a substrate
2) DRESP plots the field distribution

b) Configuration:

BASICA language

c) Software Language Required:

DOS 2.1 or later IBM PC, XT, AT or compatible
128 K bytes min

d) Formatted:

DOS 2.1 or later
5 1/4" diskette

e) Available from:

Dept of Electr. Engr.
U of Mississippi
University, MS 38677

f) Access:

None

g) Documentation:

User's instructions and listings have been published in Dielectric Resonators, Kajfez and Guillon (eds), Artech House 1986.

h) Cost:

$15.00

ACES SOFTWARE FORM

Software Number: 017 NEC-AM v1.0

Machine: IBM-PC/XT or AT

Directory Listing:

NEC-AM.EXE	Data Files for
SOMNEC.EXE	sample I/O

Description:

Enhanced PC implementation of NEC2 program which can be used to analyze AM broadcast antenna arrays. NEC-AM will accept FCC-type array excitation parameters (i.e. the field magnitude and phase for each radiator) and calculate feed point impedances, voltages and currents. NEC-AM retains all the capabilities of NEC2.

a) Features:

1) 300 segments, enough for more than 20 90 degree radiators.
2) 90 X 90 matrix in-core solution with 640K of RAM.
3) Models finitely conducting radiators and ground plane.
4) User can add lumped-circuit networks and transmission lines.

b) Configuration:

IBM PC/XT or AT
640K RAM
Math co-processor required

c) Software Language Required:

DOS 2.1 or later

d) Formatted:

2) 360 K DSDD 5 1/4" diskettes

e) Available from:

David J. Pinion, P.E.
P.O. Box 35492
Los Angeles, CA 90035
(213) 653-8054

f) Access:

unlimited

g) Documentation:

Enhanced features documentation provided with software. Purchaser should obtain most recent NEC User's Manual for general program information.

h) Cost:

$595.00

ACES SOFTWARE FORM

Software Number: 018 RF65FT

Machine: IBM-PC/XT or AT

Directory Listing:

RF65FT.EXE — Data Files for sample I/O

Description:

Program calculates the RF power density near ground level produced by a single or multiple FM and TV broadcast stations. All calculations are based on the EPA computer model described in the FCC OST Bulletin No. 65.

a) Features:

1) 50 stations max per run
2) Includes EPA antenna patterns
3) 12 bay max FM antennas
4) Includes standard pattern for VHF and UHF TV stations
5) Simple input file format
6) Output is grid of field values
7) Works with any printer, no plotter required

b) Configuration:

IBM PC/XT or AT
128 K RAM
Math co-processor recommended

c) Software Language Required:

DOS 2.1 or later

d) Formatted:

1) 360K DSDD 5 1/4" diskette

e) Available from:

David J. Pinion, P.E.
P.O. Box 35492
Los Angeles, CA 90035
(213) 653-8054

f) Access:

unlimited

g) Documentation:

Provided with software.

h) Cost:

$295.00

ELECTROMAGNETIC MODELING SOFTWARE COMMITTEE

E.K. MILLER
Rockwell International Science Center
1049 Camino Dos Rios
Thousand Oaks, CA 91360
(805) 373-4297

This discussion is included to solicit suggestions and comments concerning a new EM Modeling Software Committee that AP-S is initiating and which it is expected will be working collaboratively with the new committee formed at the March ACES meeting. Although written for the AP-S Newsletter, it is included here essentially unchanged because of the parallel interests developing concerning this general topic by ACES and AP-S. The major impetus for this committee comes from increasing recognition of the need to do something about model validation, there are several other areas to which such a committee could direct attention. In what follows, I first provide some background from a special session on validation at the Syracuse meeting and related AdCom discussion. Then I elaborate on possible specific topics for which this new committee could be assigned responsibility. Finally, I suggest one particular activity that might be undertaken at the San Jose 1989 meeting for which I would especially appreciate your feedback. You can look for a continuation of this discussion in the October AP-S Newsletter.

SPECIAL SESSION ON SOFTWARE VALIDATION AT THE SYRACUSE MEETING

At least two events occurred at the recent record-setting Syracuse meeting (~730 scheduled papers and ~ 1100 attendees!) that bear on the general problem of EM modeling software. First, there was a special session "Software Validation" organized by yours truly in which eight other invited presenters addressed various aspects of this increasingly important topic. For those of you who were not able to attend the meeting or perhaps have not seen the digest or program, the session included the following presentations and authors:

Development of EM Modeling Software Performance Standards, E. K. MILLER, ROCKWELL SCIENCE CENTER

Benchmarks: An Option for Quality Assessment, L. B. FELSEN, POLYTECHNIC UNIVERSITY

Workshops and Benchmark Problems to, Validate Eddy Current Computer Codes, L. TURNER, ARGONNE NATIONAL LABORATORY

Some Practical Considerations in the Validation of EM Modelling Codes, S. J. KUBINA, C. W. TRUEMAN, CONCORDIA UNIVERSITY

Progress Toward a Benchmark Solution for 3D, Perfectly Conducting Scatterers with Edges and Corners, A. D. YAGHJIAN, M. G. COTE, M. B. WOODWORTH, RADC, HANSCOM AFB

Validating Scattering Calculations Using Boundary Value and Internal Field Checks, A. C.

Ludwig, General Research Corporation

Reflector Antenna Distortion Compensation by Array Feeds, Y. RAHMAT-SAMII, J. MUMFORD, R. THOMAS, CALIFORNIA INSTITUTE OF TECHNOLOGY

A Model of Ferrite-Core Probes Over Composite Workpieces, H. A. SABBAGH, L. D. SABBAGH, J. R. BOWLER, SABBAGH ASSOCIATES

What Do You Mean by a Solution to an Operator Equation?, T. K. SARKAR, E. ARVAS, SYRACUSE UNIVERSITY

A basic thrust of these presentations as well as much hallway discussion and liberal sprinklings throughout the rest of the meeting, is that it's high time we EMer's begin to get serious about the question of how to assess the numerical and physical relevance of the proliferating amount of numerical results that we are generating. With the increasing preponderance of computation in analysis (few theoretical results are now obtained without computers), measurement (data acquisition and processing), and of course computer modeling itself, the sheer volume of numbers with which we must contend emphasizes the necessity of "separating the wheat from the chaff" in a computational sense. Although routine mention is made of validating numerical results, we have no systematic means of doing this within one even one class of computer codes, let alone intercomparing different kinds of models and formulations.

NEW AP-S COMMITTEE ON EM MODELING SOFTWARE

The other event that bears on this discussion is that the AP-S AdCom gave initial approval to form a new committee to deal with computational issues. As outgoing chairman of the Education Committee of AP-S, I had proposed that a new committee with the provisional name "Software Performance Standards Committee" be setup to develop a strategy for addressing the problem of model validation. The Applied Computational Electromagnetics Society had approved forming such a committee at its March 1988 meeting, and I thought that ACES and AP-S could work together in this area. I also thought that we might approach other IEEE societies such as MTT, EMC, etc. to invite their participation.

In a subsequent presentation by Allen Schell, chairman of the AP-S Long-Range Planning Committee, the independent proposal was made that an "EM Modeling Software Committee" be formed, suggesting me as a possible chairman. The eventual outcome was that I was asked to consider developing a broader charter for this new committee to deal with not only model validation, but software distribution, the role of personal computers, I/O including graphics, etc. Since AdCom also objected to use of the word "standards" in the name I proposed for this committee, because that word can have legal implications from the viewpoint of the IEEE and might bog us down in diversionary rigamarole, the proposed new committee will likely have the name proposed by Allan, but that remains to be settled. The basic focus of the committee in any case would be collection and distribution of information concerning EM modeling software together with developing procedures for how this should be done.

In any case, because only two newsletters will appear (the August and

October issues) in time to affect paper submittals for the 1989 meeting in San Jose, we felt that an initial report of this still-evolving activity should be included in the August newsletter. I want to give you my "zeroeth-order" thoughts about some general possibilities that might be considered, along with some proposals for specific actions to be taken in time to affect the San Jose meeting.

SUGGESTED TOPICS/ACTIVITIES FOR EM MODELING SOFTWARE COMMITTEE

Among the kinds of activities that the new committee might undertake, the following come readily to mind:

Model performance and validation
Software acquisition
Input/Output options
Computing environments, e.g., parallel/array processors, PCs, etc.

each of which itself includes a number of different, but related, components. Each of these major areas is discussed briefly below.

Model Performance and Validation

It would be agreed I think, that the most important single issue of those listed above is that of model validation. The value of a given code is first of all directly determined by the numerical accuracy and physical relevancy of the results it produces. Fancy user interfaces and graphical displays are irrelevant when the model produces misleading or wrong results. On the other hand, a model that satisfies all accuracy requirements but which requires so much computer time and/or storage that its routine use is inhibited, may be similarly devalued. That is why the most meaningful comparison of alternate models for solving the same problem is probably from the viewpoint of comparing the solution accuracy provided as a function of the associated computer cost, which is why this category includes both performance and validation.

If we are in agreement that validation is a key attribute of modeling, then we must develop systematic and consistent ways of quantifying what we mean by validation. I won't attempt doing that in this brief discussion, but do expect that our new committee will need to do some hard and thoughtful work on this topic. The outcome would be, I hope, an "experimental protocol" for guiding how models are validated, by comparison with other models, by using experimental measurements, or by analytical requirements.

Among the other issues this process should raise are identification and development of "benchmark" problems and solutions which could provide physically meaningful tests of any applicable model. Most important I think, is that model performance and validation be done from an applications viewpoint, since it is the end user who most needs help in model selection and application. That's not to say that this area is not of interest to model developers also, as any deficiencies identified by a validation exercise should help guide future needs and research. However, the end user has different interests, revolving not around selection of basis and testing functions, iteration versus inversion of model matrices,etc. but rather: for what problems can the model be used, at what cost, and to provide what accuracy?

An additional component of model performance and validation would be to develop a library of solved problems. I have used the term

"user-experience data base" in the past to describe this library. The goal would be to collect information helpful to others in modeling the same or similar kinds of problems with respect both to what was found to work as well as what difficulties were encountered. By including negative as well as positive results, this data base would be much more useful than would be the case were it to contain only successes. If the problems could be organized into various categories and into some logical progression of increasing complexity in each, the collection would eventually become a "modeling handbook" which could give guidance to the experienced and novice modeler alike. Results presented in the modeling handbook could be "keyed" to the codes included in the catalog described below. It should be observed that handbook results as well as those for benchmark solutions should be available in hard copy as well as in electronic form.

Software Acquisition

For the same reason that an accurate but computationally unaffordable model may be largely of only academic value, an otherwise useful model that is unknown beyond its developer(s) or unavailable for whatever reason, is of similarly limited value. As a minimum first step, there is needed a computer-code catalog in which modeling software can be described in some consistent, uniform fashion. This would then provide prospective users with the the information necessary for making informed comparisons and code selections, as well as directions on how to acquire software of interest.

The catalog might have software of the following three (at least) types:

Public domain--available to anyone for at most a nominal charge;

Limited distribution--available to contractors and others approved by the sponsor, usually the US government;

Vendor--available for purchase or lease from the developer/marketer.

While these various types of codes might naturally be distributed in different ways, it would be desirable for those in the public domain to be made available via electronic mail. Possibly *netlib* at Argonne National Laboratory (see December 1987 PCs for AP) would provide a way to do this, but other outlets might also be developed.

Input/Output Options

Probably the most labor-intensive part of modeling, especially as problems become electrically larger and geometrically more complex, is that of model description (input) and results presentation (output). The efficiency of both input and output can be immeasurably increased by use of computer graphics, interactive digitizers, automatic mesh generators, etc. Decisions by users about which code is most appropriate for a given application will increasingly be driven by the user interface provided by the various alternatives available. As a matter of fact, the overall efficiency of the modeling process has an often-overlooked component whose cost can greatly exceed that of the computer resources themselves, this being of course the cost of the human resources incurred in exercising the model.

This activity would deal with the general problem of workstation environments designed for running EM computer models. It would involve collecting information about software available for this purpose in any of the three categories mentioned above. In addition, we could

expect to consider the problem of validating the input data needed for model description and whether some standards for model description would be appropriate. Another area of concern would be graphics packages for displaying not only the input, but especially the output as the amount of EM data produced for a given problem can greatly exceed that needed to describe the problem itself. We need to explore unconventional ways of presenting model-related data and results for improving our interpretation and understanding of what is being computed.

Computer Hardware

As the bottleneck imposed by raw component speed is approaching, it is becoming apparent that alternate architectures will be needed to continue the past exponential growth of computer throughput into the future. Parallel and array processing offers some hope that the number of unknowns solvable per unit clock time will continue to increase at least as fast as it has over the past 30 years if not more so. At the same time, PCs, workstations, and minicomputers have greatly increased the scope of problems that can be solved outside the mainframe environment. These are topics of general interest to users and developers alike and therefore appropriate as well as one activity for our new committee.

Particular areas of interest in this activity would include the various parallel architectures that are becoming available and whether they might be better suited for one kind of model/formulation than another. These designs include those like the Hypercube, the Connection Machine, and possibly even neural nets as well as array processors and special parallel/parallelable microprocessors like the INMOS Transputer. If it happens that such designs are significantly better suited for one kind of model than another, this could be significant in determining where the greatest modeling improvements will be realized.

A PROPOSAL FOR YOUR CONSIDERATION

We learned in the special session on software validation that both the Acoustical Society and the eddy-current community have already initiated some activities to develop benchmark solutions and intercompare models and codes. This seems like an appropriate kind of thing for the EM modeling community to undertake. One possibility would be to develop a list of test problems for which solutions would be solicited and presented at a special session in San Jose 1989. It would be necessary to specify parameters to be used, observables to be computed, and how the results are to be presented to ensure that convenient comparison could be made.

As a specific example, suppose that we consider the modeling of wire objects. Among the list of geometries that could be considered are the linear dipole and circular loop, collinear and coplanar arrays, conical spirals, and other more complex shapes, possibly including wire-mesh models of surfaces. Results could be obtained for excitation as antennas or scatterers over some size-to-wavelength range in a free-space as well as a half-space environment. Scattering and radiation patterns, near fields, and current and charge distributions (including input impedance for the antenna) could be the observables chosen for comparison. How this might be done and what is intended to be demonstrated are aspects of the "experimental protocol" to which I referred above.

Similar sets of problems could be developed for 2D and 3D surface and volumetric problems involving perfect conductors, and dielectric and lossy objects. In any case, the emphasis should not be on how the answer is obtained, but on quantitatively determining how well it compares with other model results, exhibits analytically required behavior, or agrees with physical reality. If you think that this would be a worthwhile exercise, and if you would be willing to participate, please let me know.

In order to help structure the many responses that will be forthcoming (I am an optimist), I request your input be provided via completing either, or both, of the sections below and mailing to the address above.

SUGGESTED TEST PROBLEM(S)

I suggest that that the following problem(s) would be appropriate for use in developing a set of test results for model validation--

TEST-PROBLEM GEOMETRY (e.g, a straight wire of specified length-to-diameter ratio; provide the information needed to define the geometry):

_____

_____

_____

ELECTROMAGNETIC PROPERTIES (e.g., length-to-wavelength range of straight wire, impedance value(s) and location(s) if discretely loaded, impedance/unit length if distributed loading, etc.):

_____

_____

_____

EXCITATION (e.g., if straight wire as scatterer, angles of incidence, or if straight wire as antenna, source location):

_____

_____

_____

OBSERVABLES TO BE USED (e.g., current and charge distributions, near fields, far fields, integrated far-field power, etc., in order of their importance as a validating test relevant to a particular application):

_____

_____

_____

INTENTION TO PARTICIPATE IN PRESENTATION OF TEST-PROBLEM RESULTS AT 1989 MEETING

Yes, I would like to present results for one or more test problems (to be determined based in part on input received) at a special function at the 1989 meeting--

NAME _____

ORGANIZATION _____

ADDRESS _____

_____

_____

TELEPHONE _____

COMMENTS _____

_____

_____

PANDORA'S BOX

by Dawson Coblin

According to Greek mythology, Pandora opened her box only long enough for evil to escape and roam the world. By closing it, she trapped hope in the box. So man is doomed to live in an evil world without hope. In their less sanguine moments, code users feel the same way; lost, abandoned and despairing. It is intended that in this column Pandora's box can be opened again and hope allowed to excape.

Lhe purpose of this column is to concentrate on unsuccessful applications of commonly used codes. The goal will be to determine areas where the application may have forced the code to break down and make suggestions for improving the results. The success of this approach depends on the responsiveness of the ACES members to share their less successful attempts and quandaries.

The membership is therefore solicited to send their problem cases to me for review. Please include the name of the code used (and version, if applicable), the specifics of the test case, examples of the output, a list of the problems and contradictions observed, and your name, address, and telephone number. Please respond to the following address:

R.Dawson Coblin
O/62-42 B/o76
Lockheed Missiles & Space Co.
111 Lockheed Way
Sunnyvale, CA 94089-3504

MODELING NOTES

The Primary purpose of ACES and the Journal/Newsletter is to foster information exchange among workers involved in developing and applying computer codes to model electromagnetic problems.

This section features short articles about particular aspects of the more popular codes and short notes which summarize user experience with specific codes. To facilitate the submission of short notes in a standard form which can be easily referenced later, we include the ACES MODELING SHORT-NOTES form for 1-3 page submittals.

Readers are encouraged to report their code experiences in these ACES MODELING SHORT-NOTE forms and send them to the ACES Secretary, whose address is listed in the FRONTISPIECE. Camera-ready SHORT-NOTE forms are preferred.

EM Modeling Notes *

Gerald Burke
Lawrence Livermore National Laboratory
Livermore, CA 94550

As in previous Newsletters, this column will summarize developments on the NEC Method of Moments code. The subjects discussed this time are the NEC model for insulated wires which was completed in December 1987 and the status of improvements in NEC for modeling wires with discontinuous radii and tightly coupled junctions. Also, there are code bugs to report involving NECVLF and an earlier version of the insulated wire code. As I was writing this I received a report from a user pointing out a serious error in the double precision version of NEC–2 for VAX computers. Hence users of these codes should check the last section here for corrections.

Considering the topics covered to date, NEC News would be a more appropriate title for this column. However, there are probably enough NEC users in ACES to justify a dedicated column. With regard to error reports, particularly the NEC–2D case, I hope that people who have passed the code along to others can forward the correction as well. We try to notify users who are known to have a particular code, but due to lack of person-power here and the extent that code distribution has spread it is impossible to notify everyone.

The NEC Model for Insulated Wires

Development of the insulated-wire code, NEC–3I, was started in 1985 and has been sponsored by the U. S. Air Force, RADC/EECT and RADC/DCCL. The code is an extension of NEC–3 to model an insulating sheath on wires in air or buried in a lossy half space including, if desired, the effect of the air-ground interface. Insulating sheaths are sometimes used in air to protect wires from the environment, to modify the electrical characteristics of an antenna or simply because the available wire is insulated. Also, the sheath formed by ice accumulation on antenna wires can sometimes affect the antenna performance. The effect of a thin sheath on an antenna in air is generally relatively small, while for a wire buried in a lossy medium, such as earth or water, an insulating sheath can greatly reduce the electrical length and attenuation.

An initial version of the NEC–3I code was released in 1986. We have now completed this code and a report including validation and documentation of the model [1].

* Work performed under the auspices of the U. S. Department of Energy by the Lawrence Livermore National Laboratory under Contract W-7405-Eng-48.

This report is summarized below. The earlier version of NEC–3I was found to have errors in the Sommerfeld ground model for a buried insulated wire. Hence anyone having this code who has not received a copy of the report and code update should contact LLNL.

The effect of a sheath is modeled in NEC–3I by including the field due to radial polarization currents in the sheath in enforcing the boundary condition on the wire. This approach, first described by Richmond and Newman in [2], is suited to modeling sheaths that are electrically thin relative to the wave number in the medium external to the sheath. For a wire with radius a and sheath radius b, as shown in Fig. 1, the insulating sheath with complex relative permittivity $\tilde{\epsilon}_2 = \epsilon_2 - j\sigma_2/\omega\epsilon_0$ in a medium with $\tilde{\epsilon}_1 = \epsilon_1 - j\sigma_1/\omega\epsilon_0$, can be replaced by an equivalent polarization current for $a \le \rho \le b$ of

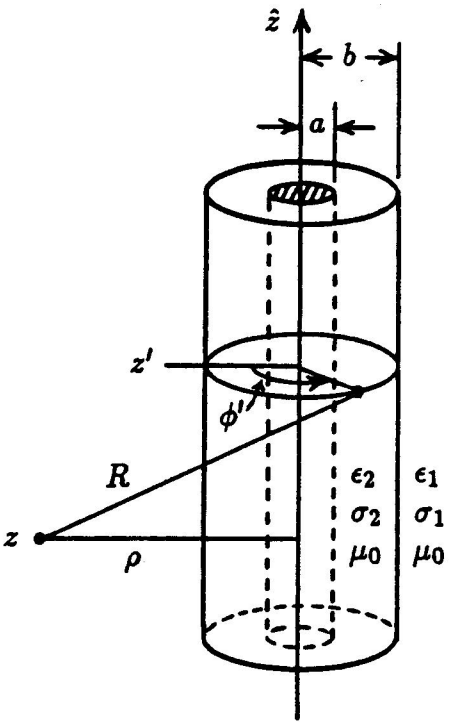

Fig. 1. Coordinates for evaluation of the field due to polarization currents in an insulating sheath on a wire.

$$\vec{J}_s(\rho,z,\phi) = j\omega\epsilon_0(\tilde{\epsilon}_2 - \tilde{\epsilon}_1)[\vec{E}^S(\rho,z,\phi) + \vec{E}^I(\rho,z,\phi)]$$

radiating in medium 1. $\vec{E}^S$ is the electric field due both to currents on the wire and to $\vec{J}_s$ itself, and $\vec{E}^I$ is the excitation field. To retain a one dimensional integral equation for the axial wire current, the sheath is assumed to be electrically thin, and the total field in the sheath is assumed to be dominated by the radial field due to charge on the wire. The equivalent current is then

$$\vec{J}_s(\rho,z,\phi) \approx \frac{-(\tilde{\epsilon}_2 - \tilde{\epsilon}_1)}{2\pi\tilde{\epsilon}_2\rho} I'(z)\hat{\rho}$$

for $a \le \rho \le b$. In the thin wire approximation of the electric field integral equation, the field due to $\vec{J}_s$ is needed on the wire axis. For a straight segment of insulated wire with $|k_1 b| \ll 1$ the field on the axis due to $\vec{J}_s$ can be approximated, as shown in [1], in terms of the second derivative of the axial current as

$$\hat{z} \cdot \vec{E}_s^S(z) \approx \frac{j(\tilde{\epsilon}_2 - \tilde{\epsilon}_1)}{2\pi\omega\epsilon_0\tilde{\epsilon}_1\tilde{\epsilon}_2} I''(z)\ln(b/a).$$

Then with the current on segment i represented in the form

$$I_i(z) = A_i + B_i \sin[k_s(z - z_i)] + C_i \cos[k_s(z - z_i)] \qquad (1)$$

the field at the match point at the center of segment i is

$$\hat{z} \cdot \vec{E}_s^S(z_i) \approx \frac{-jk_s^2(\tilde{\epsilon}_2 - \tilde{\epsilon}_1)}{2\pi\omega\epsilon_0\tilde{\epsilon}_1\tilde{\epsilon}_2} C_i \ln(b/a).$$

This field is included in the total, axial electric field in the thin-wire integral equation.

The field on the outside of the sheath due to the polarization currents in the sheath is shown in [1] to be less than this axial field by a factor of about $k_1^2(b^2 - a^2)/4$. Hence this field can be neglected relative to the axial field for thin wires, so that the mutual interaction of segments involves only the field due to the axial wire current. The model for the sheath thus reduces to a simple form comparable in complexity to the model for a wire with finite conductivity, in that the sheath modifies the field only on its own segment. This result is particularly convenient in the case of a wire near the air-ground interface since no addition is needed to the present evaluation of the effect of the interface on the field due to the axial wire current.

One other change was needed in NEC to model insulated wires embedded in earth or water. In this case the current tends to have a sinusoidal form as for a bare wire, but the propagation constant may be orders of magnitude less than for a bare wire in the medium. Use of k_s in Eq. (1) equal to the wave number in the surrounding medium can then result in very slow convergence of the solution. Fortunately, a simple approximation for the propagation constant on a buried insulated wire is available from the theory of coaxial transmission lines [3]. For a perfectly conducting wire, this solution predicts a propagation constant of

$$k_L \approx k_2 \left[1 + \frac{H_0^{(2)}(k_1 b)}{k_1 b \ln(b/a) H_1^{(2)}(k_1 b)} \right]^{1/2} \tag{2}$$

where k_1 is the wave number in the infinite medium and k_2 is the wave number in the insulating material. $H_0^{(2)}$ and $H_1^{(2)}$ are Hankel functions of order 0 and 1. This approximation should be valid for $|k_1| \gg |k_2|$. Hence, in the NEC solution, k_s is set equal to k_L when $|k_1/k_2|$ is greater than 2. For smaller $|k_1/k_2|$, k_s is set equal to k_1. The accuracy of this estimate of k_s, within a factor of 2 or so, is not important since the solution is relatively insensitive to k_s. With a dense outer medium, the use of k_L in the current expansion greatly improves the convergence of the solution.

Allowing k_s different from k_1 increases the complexity of the field equations, however. The fields due to $\sin k_s s$ and $\cos k_s s$ current distributions, which are given by simple closed-form expressions when $k_s = k_1$, involve additional exponential integrals when $k_s \neq k_1$. The integrals were evaluated in NEC–3I by numerical integration after subtracting integrable functions to remove the peaked behavior of the integrand. Evaluation of these integrals can be difficult since, while $k_s\delta$ must be small, $k_1\delta$ may be large when $|k_1| \gg |k_2|$. The present evaluation appears to be accurate, but more work in this area could reduce the computation time.

To validate the insulated wire model in NEC, results were compared with published measurements for insulated antennas in air and water and with the solution for the propagation constant on an infinite insulated wire. Also, the total radiated power of an insulated dipole was compared with the input power less the power dissipated in the sheath as a self-consistency check on the solution.

The measured input admittance of a dipole antenna with dielectric insulation in air was included in [2]. NEC results are compared with these measurements and with the results of Richmond and Newman's code in Fig. 2. The two computer codes are in close agreement for the dipole antenna, with a difference evident only toward antiresonance as often occurs with method of moments codes. Comparison with NEC results for a bare dipole showed that the resonant length was reduced from $0.47\lambda_0$ to $0.42\lambda_0$ by addition of the sheath. A similar comparison for a square loop is included in [1].

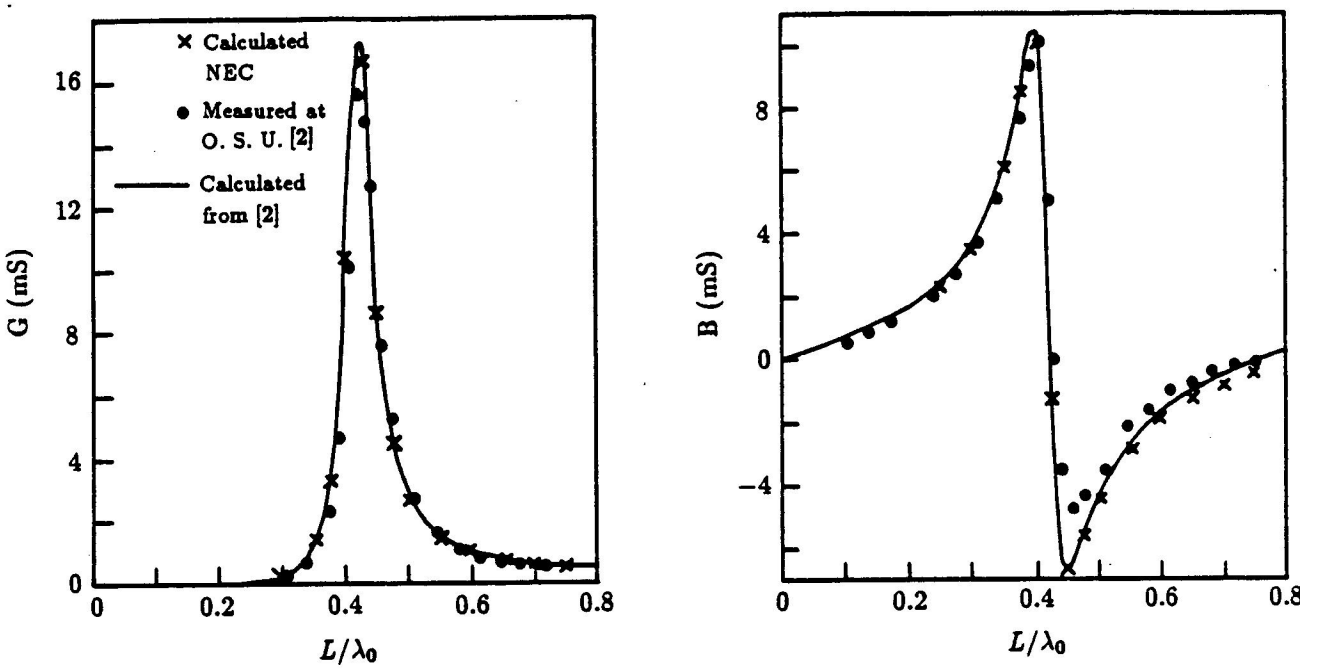

Fig. 2. Input admittance of an insulated dipole antenna in air with length L, radius $a = L/640$ and sheath radius $b = 5.84a$. The relative permittivity of the sheath is 2.3 and the conductivity is zero.

A self-consistency check on the solution for an insulated wire in air can be obtained from the balance of input power, radiated power and power dissipated in the sheath. This check was implemented by computing the efficiency of an insulated dipole antenna as

$$e_1 = 100(P_{in} - P_{loss})/P_{in}$$

and comparing with the integral of radiated power as

$$e_2 = \frac{100}{2\eta P_{in}} \int_{4\pi} \vec{E}_{rad} \cdot \vec{E}^*_{rad}\, d\Omega$$

which is obtained from the average gain printed by NEC. P_{in} is the input power computed from the voltage and current at the source. The power loss in the sheath P_{loss} is computed by NEC–3I and is included in the power budget in the output. These quantities are compared in Table 1 for a dipole with $b/a = 2$ and $\tilde{\epsilon}_2 = 3 - j3$. The loss tangent equal to one results in the maximum dissipation of power in the sheath. The results for e_1 and e_2 are seen to be in good agreement except for small dipole lengths for which the accuracy of e_1 is limited by cancellation.

Table 1. Radiation efficiency of an insulated dipole in percent. The complex relative permittivity of the sheath material is $\tilde{\epsilon}_2 = 3 - j3$ and $b/a = 2$. The upper entry in each box is e_1 and the lower entry is e_2.

	Dipole length / λ_0									
a/λ_0	0.01	0.02	0.05	0.1	0.2	0.3	0.4	0.5	0.6	0.8
10^{-8}	5.65	1.89	2.37	6.09	28.92	58.34	77.53	87.14	91.51	93.27
	0.005	0.04	0.57	4.44	27.83	57.75	77.15	86.78	91.09	92.65
10^{-6}	6.45	2.11	2.53	6.19	28.94	58.43	77.62	87.14	91.38	92.86
	0.005	0.04	0.57	4.41	27.79	57.82	77.24	86.78	90.95	92.21
10^{-4}	17.99	4.53	3.65	6.74	29.07	58.68	77.84	87.07	90.94	91.64
	0.004	0.03	0.54	4.30	27.64	58.01	77.43	86.67	90.45	90.88
10^{-3}				10.52	29.98	59.40	78.21	86.78	89.97	89.44
				3.82	27.19	58.27	77.61	86.23	90.31	88.45
10^{-2}					20.23	47.18	69.40	76.98	78.39	75.35
					9.07	41.44	61.03	71.52	74.10	71.72

A valuable check on the NEC results is provided by the analytic solution for the propagation constant on an infinite insulated wire. A rigorous solution to this problem was developed by J. R. Wait [4] who solved the boundary value problem for a horizontal insulated wire buried in the ground below an interface with air. The wire is at depth d below the air-ground interface in a medium where the wave number is k_1 in the present notation. Assuming a current $I_0 \exp(-\Gamma x)$, Wait matched boundary conditions at the air-ground interface, the outer boundary of the sheath and on the wire, assuming that $d \gg b$ so that azimuthal variation of the field around the wire can be neglected, to derive an equation for Γ. An explicit solution for Γ is obtained in [4] when $|k_1| \gg |k_2|$. We chose here to solve Eq. (11) in [4] with a numerical root finder to ensure good accuracy over a wide range of parameters.

The transmission line model used in [3] provides another solution for the propagation constant on a buried insulated wire, which is repeated here as Eq. (2). An extension of this model to include an interface was proposed in [5] assuming an image of the wire reflected

in the interface with a reflection coefficient of one. The result for a wire at depth d is

$$k_L \approx k_2 \left[1 + \frac{H_0^{(2)}(k_1 b) + H_0^{(2)}(2k_1 d)}{k_1 b \ln(b/a) H_1^{(2)}(k_1 b)} \right]^{1/2} \tag{3}$$

As with Eq. (2) it is required that $|k_1| \gg |k_2|$ in this model.

To determine the propagation constant from the NEC solution, an insulated wire several wavelengths long was modeled with a source approximately $\lambda/4$ from one end and a load approximately $\lambda/4$ from the other end, where λ should be the wavelength of the propagating wave on the wire. The position and size of the terminating load were adjusted to achieve a reasonably small standing wave. This required some trial and error since the value of λ and the optimum load value were not known in advance. The phase constant β_L for the current was then determined from the phase shift divided by distance and the attenuation constant α_L was determined from a linear match to the log of the magnitude of current. The source and termination regions were excluded in these calculations.

The propagation constants determined from the NEC–3I solution, Eq. (2) or Eq. (3) and the solution from [4] are compared for a number of cases in [1]. For an infinite medium the wire radius a was varied with b/a fixed. A typical result for a wire with air insulation in conducting water is shown in Fig. 3. Wait's solution from [4] should be the most accurate of these results over the entire range of a/λ_0. The NEC solution is seen to be in good agreement with the result from [4] for small a/λ_0, diverging for larger values. The result of Eq. (2) is more accurate for large a/λ_0. Other results showed, as expected, that Eq. (2) becomes more accurate with increasing $|\tilde{\epsilon}_1|$. It is less accurate for small b/a and small $k_1 b$. Hence the NEC solution and Eq. (2) are often complementary in their ranges of accuracy. The value of α_L is more difficult to determine accurately than that of β_L for either Eq. (2) or NEC.

The input admittance computed by NEC–3I for an insulated monopole in conducting water with $\tilde{\epsilon}_1 = 80 - j0.197$ is compared in Fig. 4 with measurements made by S. Mishra and included in [3] and [6]. As described in [6], the monopoles were constructed from coaxial cable and were measured in lake water at 300 MHz. Agreement is generally good in this case, with the NEC–3I results differing mainly in the height of the peak at resonance. Other cases included in [1] show increasing error in the peak heights for NEC–3I as b/a is increased but good agreement in the resonant frequency. This observation confirms the results for the propagation constant on this monopole, for which $a = 3.175(10^{-3})\lambda_0$ and $k_1 b = 0.45$, since α_L from the NEC–3I solution is starting to diverge to large values while β_L is still reasonably accurate. Eq. (2) is accurate in this case but loses accuracy for smaller a/λ_0. Hence for smaller wire and sheath radii the NEC–3I solution should become more accurate and the the transmission line model less accurate.

For an insulated wire near an interface the propagation constant determined from NEC–3I was compared with that predicted by J. R. Wait's solution in [4] and with Eq. (3). Results from NEC–3I using the Sommerfeld integral option are compared in Fig. 5 with the solution from [4]. The latter, since boundary conditions are accurately satisfied at the

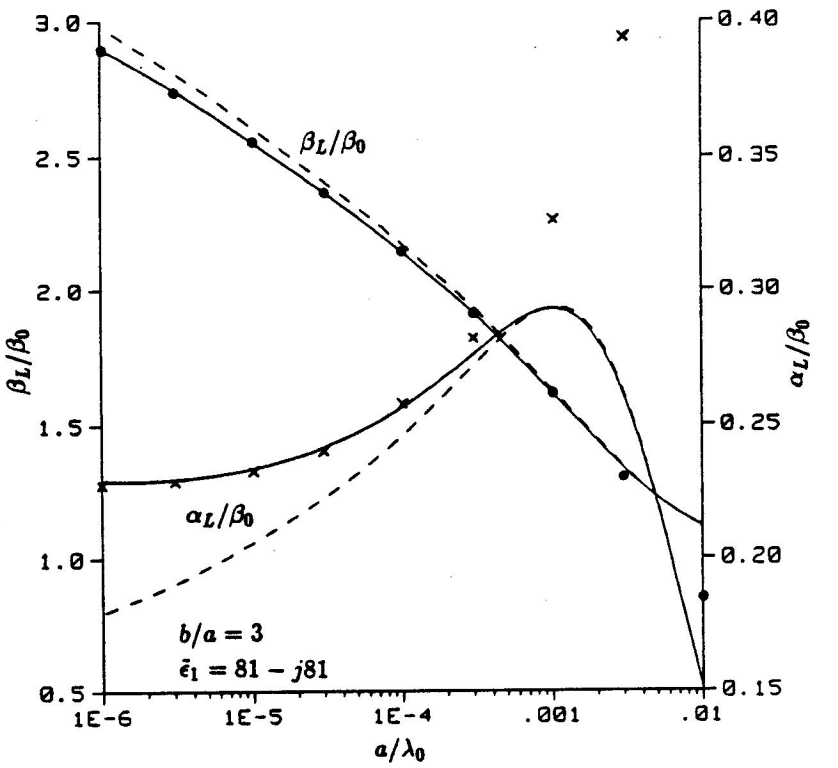

Fig. 3. Propagation constant $\Gamma = \alpha_L + j\beta_L$ versus wire radius a on a wire with air insulation in water with complex relative permittivity $\bar{\epsilon}_1$ for $b/a = 3$ and $\beta_0 = 2\pi/\lambda_0$. Results of the NEC model (• ×) and Eq. (2) (- - - - - -) are compared with the more accurate solution from ref. [4] (————).

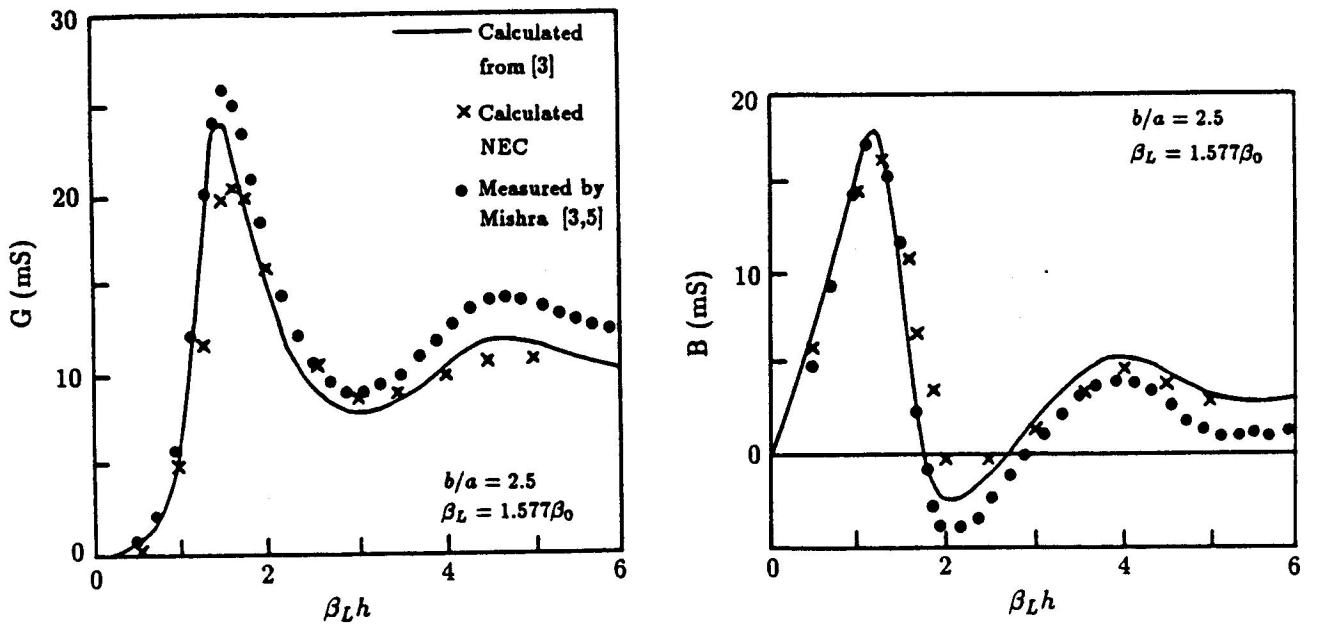

Fig. 4. Input admittance of a monopole antenna with air insulation in water with $\bar{\epsilon}_1 = 80 - j0.197$ and $a = 3.175(10^{-3})\lambda_0$. The monopole length is h and β_L is the real part of k_L from Eq. (2).

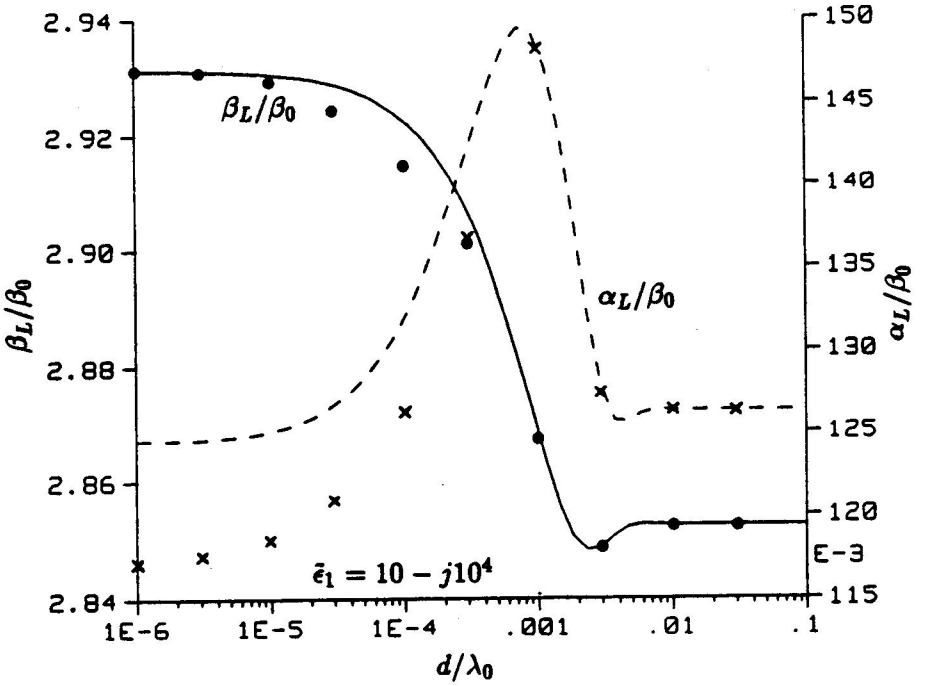

Fig. 5. Propagation constant on an insulated wire at depth d below an interface computed with the Sommerfeld integral option in NEC (• , ×) and solution of Eq. (11) from [4] (———,- - - -). The upper half space is air, the complex relative permittivity of the medium surrounding the wire is $\tilde{\epsilon}_1$ and the insulation is air. Wire radius is $a = 2.38(10^{-7})\lambda_0$ with $b/a = 3$ and $\beta_0 = 2\pi/\lambda_0$.

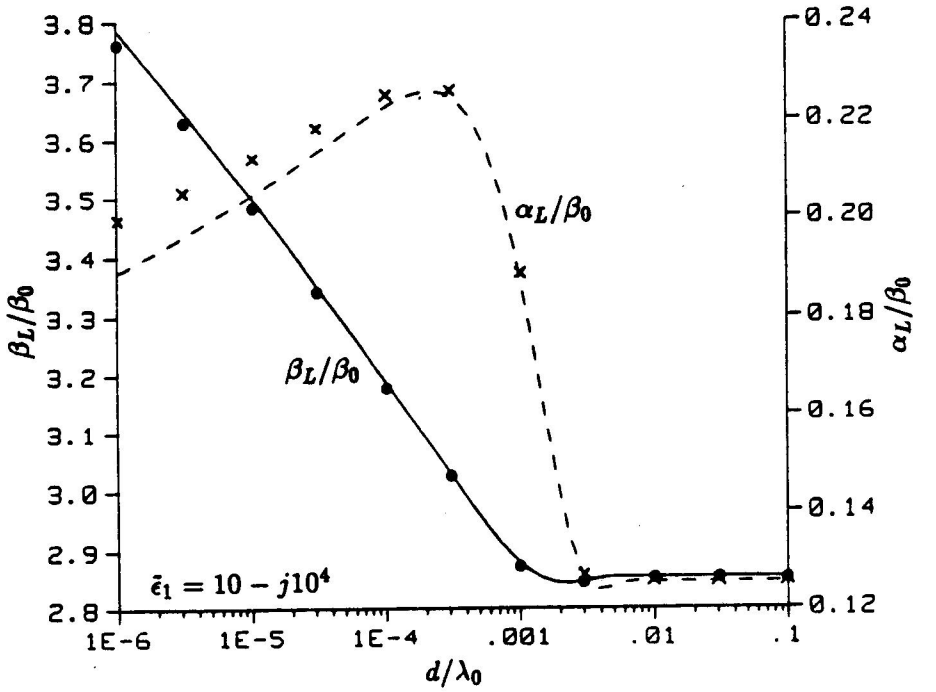

Fig. 6. Propagation constant on an insulated wire at depth d below an interface computed with the reflection coefficient option in NEC (• , ×) and Eq. (3) (———,- - - -). Both results are incorrect as a result of using the reflection coefficient for the interface. Model parameters are the same as for Fig. 5.

interface, should be equivalent to the Sommerfeld integral solution. The solutions for β_L are seen to be in very good agreement, while α_L shows some difference for small d but generally good agreement. The maximum error in α_L is about 5 percent.

NEC–3I results using the reflection coefficient approximation are compared in Fig. 6 with the results of Eq. 3 which also is based on a reflection coefficient treatment of the interface. The two results are in reasonably good agreement but differ substantially from the presumably accurate results in Fig. 5. Hence it appears that the plane-wave reflection coefficient is not suitable for modeling a buried wire. Although the reflection coefficient is close to one for a dense ground, the cancellation in the integral for the field appears to require a more accurate treatment.

The comparisons with measurements and other analytic results indicate that the accuracy of the NEC model for an insulated wire in a conducting medium is mainly dependent on $|k_1 b|$. The error in α_L determined by NEC reaches ten percent when $|k_1 b|$ is approximately 0.15, while the solution for β_L, reaches ten percent error at about $|k_1 b| = 0.7$.

Instructions for using NEC–3I are contained in [1]. The code will allow modeling of a discontinuous sheath, but the results for such a model may be less accurate than when the sheath covers the entire wire. A number of complicated situations can occur with insulated wires, such as a change in wire radius within the sheath, a junction of several insulated wires or an insulated wire penetrating an interface with the sheath continuous or vanishing on either side. These are difficult problems and could not be considered here. Such models may be entered into the code, but the accuracy of the results is unpredictable.

The transmission line model from [3] provides a fast, simple alternative to the method of moments model in NEC for straight buried dipoles when the restriction that $k_1 \gg k_2$ is satisfied. In a project separate from the NEC development, we have developed a code combining this transmission line model with a numerical evaluation of the field of a source in a stratified medium [7]. This model may be preferable to NEC for a deeply buried dipole antenna. The effect of the interface on the current distribution is not considered in the transmission line model, but as was seen in Fig. 5 this effect is negligible unless the wire is very close to the interface.

Modeling Discontinuous Wire Radii and Junctions

Work has been under way for about the past year, sponsored by the U. S. Army, Ft. Huachuca, ISEC, to improve the treatment of wires with discontinuous radii and tightly coupled junctions in NEC. A study of the stepped-radius problem in [8] has shown the accurate solution of this problem and the limitations of the NEC model. A previous ACES Newsletter [9] contained a demonstration that a discontinuity in wire radius by as little as a factor of two can lead to inaccurate results. Hopefully we will soon have a new version of NEC with much improved accuracy for discontinuous radius or tightly coupled junctions.

Two basic changes in the NEC model for wires were found to be necessary. One was to locate the match points on the wire axis with the current on the surface. In the present NEC the current is treated as a filament on the wire axis and the match points are on the surface. This was originally done to avoid any discontinuity in the current at bends or changes in radius, since such discontinuities introduce point or ring charges that cause problems in the solution. However, as part of the NECVLF development [10] we realized that, since continuity of current is enforced in the current expansion, we could simply drop the field due to point or ring charges from the field evaluation. With the current located on the wire surface, the wire ends and the annular surface at a radius change can be closed by including the field due to charge on these surfaces. Closing these annular surfaces improves the accuracy when the segment length to radius ratio is small, but is not critical as long as it is recognized that there are no ring charges at these points.

When the current was located on the surface and the match points on the axis it was found that the solution converged to the correct behavior of charge at a step in radius, agreeing with results in [8]. With the current on the axis and match points on the surface the solution converged to an incorrect result with continuous charge at a step in radius. The reason for this difference is not obvious, although the former convention is justified by the Extended Boundary Condition [11]. In a Galerkin Method of Moments solution there should be no difference when the locations of the current and field evaluation are interchanged. With the point-matched solution in NEC, however, it appears to be an important factor. Hence the new code will locate the current on the surface and will close annular surfaces with caps.

The other change needed in NEC is the condition imposed in the basis functions on charge at a junction or step in radius. The present code relates the charge on a wire to a function of the log of wire radius. This condition comes from a solution for a continuously tapered wire [12]. The same condition was derived in [13] by enforcing continuity of scalar potential across a junction. However, the potential was computed by treating each wire as infinite in length and isolated from other wires, and the result was restricted to "loosely coupled junctions." It is shown in [8] that the proximity of the junction and other wires has a significant effect on the charge over distances comparable to the segment length. Also, the NEC solution is quite sensitive to this charge condition. Hence a more accurate treatment of charge is needed.

One approach would be to leave the ratios of charges on wires at a junction as unknowns. Additional match points are then needed on wires at the junction to determine the charge. However, for a junction of N wires, this would introduce $N-1$ new equations in the structure impedance matrix. An alternative that does not increase the size of the matrix is to consider the junction removed from the rest of the structure and solve for the charge to produce equal scalar potentials. A small method of moments solution was developed using triangular basis functions for the charge, along with one constant, semi-infinite basis function on each wire. A half triangle and the semi-infinite basis function on each wire appears to be sufficient to determine appropriate charge ratios for the NEC basis functions.

A new version of NEC with these changes should be ready for testing in a few months. The code will combine the improvements of precision in NECVLF with the new treatment for discontinuous radii and junctions. The new code will require a check-out period, as demonstrated by the section below, but is expected to eventually replace NEC–3.

Code Error Reports

There are three errors to report in NEC codes. One, as mentioned above, is in the version of NEC–3I released before November 1987. This error involves modeling buried insulated wires. The changes to the Sommerfeld ground model to allow for a current expansion with wave number different from that in the surrounding medium had not been made in this code. Since several changes are needed and the code distribution has been limited, persons having an early version of NEC–3I should contact LLNL for corrections.

The code NECVLF [10] has an error that results in incorrect values for the radial electric field when the evaluation point is along side of a segment within a radial distance of 0.01 of the segment length. The corrections are shown below. Line 50 of subroutine EKSCEX was:

```
IF(RHO.GT..01*AMIN1(R1,R2))THEN
```

It should be:

```
IF(RHO.GT..01*AMIN1(R1,R2).OR.(Z2.GT.0..AND.Z1.LT.0.))THEN
```

Also, line 85 of subroutine EKSMR was:

```
IF(RHO.GT..04*AMIN1(R1,R2))THEN
```

and should be changed to:

```
IF(RHO.GT..04*AMIN1(R1,R2).OR.(S1.LT.0.AND.S2.GT.0.))THEN
```

The error that could have the most wide spread effects involves NEC–2D, the double precision version of NEC–2 for VAX computers, and was reported to us by Dr. J. G. Morgan at Culham Laboratory in England. A comma was lost in this code from the end of the COMPLEX statement in subroutine EKSCX. The statement was:

```
 COMPLEX*16 CON,GZ1,GZ2,GZP1,GZP2,GR1,GR2,GRP1,GRP2,EZS,EZC,ERS,ERC EX    5
1GRK1,GRK2,EZK,ERK,GZZ1,GZZ2                                       EX    6
```

and should be:

```
 COMPLEX*16 CON,GZ1,GZ2,GZP1,GZP2,GR1,GR2,GRP1,GRP2,EZS,EZC,ERS,ERC EX    5
1,GRK1,GRK2,EZK,ERK,GZZ1,GZZ2                                      EX    6
```

This error causes an incorrect evaluation of the radial component of electric field due to the $\cos ks$ component of current when the extended thin-wire kernel option is used. It does not have any effect in the example cases provided with NEC–2, since the extended thin-wire kernel is only used on a straight wire which does not involve the radial field. On a bent wire, however, this error can lead to completely wrong results. I will try to send notices of this error to people to whom we have sent NEC–2, since there are a reasonable number of people forced to use NEC–2 because they do not meet the DoD requirements for receiving NEC–3.

In conclusion, there are a number of extensions and upgrades to NEC that are completed or under development. In addition to those discussed above there is also a version of NEC–3 with restructured Fortran code known as NEC–R. These new developments should eventually be combined into a new code, perhaps NEC–4.

REFERENCES

[1] G. J. Burke, *A Model for Insulated Wires in the Method of Moments Code NEC*, Lawrence Livermore National Laboratory, Report UCID–21301, January 1988.

[2] J. H. Richmond and E. H. Newman, "Dielectric Coated Wire Antennas," *Radio Science*, vol. 11, no. 1, pp. 13–20, Jan. 1976.

[3] R. W. P. King and G. S. Smith, *Antennas in Matter*, The MIT Press, Cambridge, MA, 1981.

[4] J. R. Wait, "Electromagnetic Wave Propagation Along a Buried Insulated Wire," *Canadian J. of Phys.*, vol. 50, pp. 2402-2409, 1972.

[5] R. W. P. King, "Antennas in Material Media Near Boundaries with Application to Communication and Geophysical Exploration, Part II: The Terminated Insulated Antenna," *IEEE Trans. Antennas and Propagation*, vol. AP-34, no. 4, pp. 490–496, April 1986.

[6] R. W. P. King, S. R. Mishra, K. M. Lee and G. S. Smith, "The Insulated Monopole: Admittance and Junction Effects", *IEEE Trans. Antennas and Propagation*, vol. AP-23, no. 2, pp. 172–177, March 1975.

[7] G. J. Burke, C. G. Dease, E. M. Didwall and R. J. Lytle, *Numerical Modeling of Subsurface Communication*, Lawrence Livermore National Laboratory, Report UCID–20439 Rev. 1, August 1985.

[8] A. W. Glisson and D. R. Wilton, *Numerical Procedures for Handling Stepped-Radius Wire Junctions*, Department of Electrical Engineering, University of Mississippi, March 1979.

[9] J. K. Breakall and R. W. Adler, "A comparison of NEC and MININEC on the Stepped radius Problem", *Applied Computational Electromagnetics Newsletter*, Vol. 2, No. 2, Fall 1987.

[10] G. J. Burke, "EM Modeling Notes", *Applied Computational Electromagnetics Newsletter*, Vol. 1, No. 2, November 1986.

[11] P. C. Waterman, "Matrix Formulation of Electromagnetic Scattering", *Proceedings of the IEEE*, vol. 53, pp. 805-812, August 1965.

[12] T. T. Wu and R. W. P. King, "The Tapered Antenna and Its Application to the Junction Problem for Thin Wires," *IEEE Trans. Ant. and Prop.*, AP-24, No. 1, pp. 42-45, January 1976.

[13] S. A. Schelkunoff and H. T. Friis, *Antennas, Theory and Practice*, John Wiley & Sons, Inc., New York, 1952.

CIRCUMFERENTIAL CURRENT VARIATION ON THIN WIRES

A.C. Ludwig

ABSTRACT

It is shown that wires 1/100 of a wavelength in circumference can have a significant circumferential current variation when scattering an incident plane wave. This variation typically has a very small effect on far-field scattering, but can have a large effect on near-fields very close to the wire. Since the method-of-moments wire technique typically assumes no circumferential variation, this is a potential source of error in some problems.

1 INTRODUCTION

When the method-of-moments is applied to thin wires, the usual assumptions are (1) current flows only parallel to the wire axis, and (2) current is independent of circumferential position on the wire [1,2]. It seems intuitively obvious that if the wire diameter is small compared to a wavelength, these assumptions will be valid. Surprisingly, it turns out that even a wire 1/100 of a wavelength in circumference can have a significant circumferential current variation! A circumference of 1/100 wavelength is actually borderline in terms of satisfying the thin wire approximateion [4]. However, if a wire grid is used to represent a surface, and the wire diameter is chosen to satisfy the "equal-area" criterion [3], then much thicker wires are in fact typically used. For example, if the grid wires are spaced 1/10 wavelength apart, then the wire must be 1/10 wavelength in circumference. An extended kernel solution also assumes no circumferential current variation, so although it improves the thin wire approximations in some respects, it does not affect the problem addressed here.

For the author, this question arose when scattering from a wire dipole 0.075 wavelengths in diameter was computed, and it was found that there was almost a 2:1 circumferential variation in current amplitude [3]. If the circumferential variation is expressed as $\cos m\phi$, the usual assumption is that only the $m = 0$ term is significant. It was in fact necessary to include both the $m = 1$ and $m = 2$ terms to satisfy the boundary condition with high precision (circumferential currents were also present). The $m > 0$ terms have a relatively small effect on the far field pattern, since radiation from these currents tends to cancel; however, in the near-field very close to the wire, $m > 0$ terms can be very significant. The purpose of this communication is to present numerical results for the exact solution of plane wave scattering by a infinite cylinder, which can be used to indicate when circumferential variation may be significant. Results will also be given for a small sphere as an interesting comparison.

2 PLANE WAVE SCATTERING BY AN INFINITE PERFECTLY CONDUCTING CYLINDER

Consider the case of an infinite cylinder of radius a, and define the cylinder axis to be the z-axis of a standard cylindrical coordinate system. A incident plane wave is assumed to be polarized parallel to the cylinder axis and traveling in the x-direction

$$\bar{E}_i = e^{-jkx}\hat{i}_z \tag{2.1}$$

$$\bar{H}_i = -\frac{1}{Z_o} e^{-jkx}\hat{i}_y \tag{2.2}$$

The exponential term can be expanded in cylindrical harmonics [5]

$$e^{-jkx} = \sum_{m=o}^{\infty} a_m J_m(kr) \cos m\phi \tag{2.3}$$

where

$$a_o = 1$$

$$a_m = 2(-j)^m \quad \text{for} \quad m > 0 \tag{2.4}$$

To match the boundary condition at the surface, and the radiation condition, the scattered field tangent to the surface must then be[1]

$$\bar{E}_s = -\hat{i}_z \sum_{m=o}^{\infty} a_m \frac{J_m(ka)}{H_m^{(2)}(ka)} H_m^{(2)}(kr) \cos m\phi \tag{2.5}$$

[1] The $\bar{H}$ field also has a radial component which does not contribute to the currents.

$$\bar{H}_s = \hat{i}_\phi \frac{j}{Z_o} \sum_{m=o}^{\infty} a_m \frac{J_m(ka)}{H_m^{(2)}(ka)} H_m^{(2)'}(kr) \cos m\phi \qquad (2.6)$$

Surface currents on the cylinder may be obtained by numerically evaluating, on the cylinder surface,

$$\bar{J} = \hat{n} \times (\bar{H}_i + \bar{H}_s) \qquad (2.7)$$

where $\hat{n}$ is a unit vector normal to the surface. The "far-field" scattered pattern is obtained from Eqs. 2.5 or 2.6 using the asymptotic form for the Hankel functions.

3 RESULTS FOR ka << 1 AND COMPARISON WITH SCATTERING BY A SPHERE

An analogous solution can be obtained for scattering by a sphere, using spherical harmonics [5]. For this case, the sphere radius is also a , but a wave propagating in the z-direction of a standard spherical coordinate system was assumed for simplicity. Results for the dominant terms, as $ka \to 0$, for both the sphere and cylinder are shown in Table 3.1.

The surface currents for the cylinder include a slowly diverging logarithmic term which, in the limit, produces a dominant $m = 0$ current. However, as shown in Fig. 3.1, the currents on the leading edge ($\phi = 180°$) and trailing edge ($\phi = 0°$) have a significant amplitude and phase difference for a cylinder circumference as small as 0.01 wavelength.

The sphere currents are interesting because the contribution of the scattered field is exactly 1/2 of the contribution of the incident field. In the E-plane ($\phi = 0$), the currents are in fact uniform around the circumference of the sphere; in the H-plane, there is a null at $\theta = 90°$.

Table 3.1. Scattering of a plane wave incident on body of dimension $a \to 0$.

	Sphere Radius a	Cylinder Radius a, axis = z-axis
Incident field	$\bar{E}_i = -\hat{i}_x e^{-jkz}$ $\quad \bar{H}_i = -\frac{\hat{i}_y}{Z_o} e^{-jkz}$	$\bar{E}_i = \hat{i}_z e^{-jkx}$ $\quad \bar{H}_i = -\frac{\hat{i}_y}{Z_o} e^{-jkx}$
Far-Field	$\bar{E}_s = \frac{(ka)^3}{2}\left[(1 - 2\cos\theta)\cos\phi\hat{i}_\theta + (2 - \cos\theta)\sin\phi\hat{i}_\phi\right]\frac{e^{-jkr}}{kr}$ 3:1 ratio back to forward scatter in the limit $ka \to 0$	$\bar{E}_s = -\hat{i}_z\left[\frac{1}{1 + j\frac{2}{\pi}\ln\frac{1.1229}{ka}} - j\pi\frac{(ka)^2}{2}\cos\phi\right]\sqrt{\frac{2}{\pi kr}}\, e^{-j(kr-\pi/4)}$ Isotropic scattering in the limit $ka \to 0$
Surface Currents	$\hat{n} \times \bar{H}_s = -\frac{1}{2Z_o}\left[\cos\theta\sin\phi\hat{i}_\phi - \cos\phi\hat{i}_\theta\right]$ $\hat{n} \times \bar{H}_i = -\frac{1}{Z_o}\left[\cos\theta\sin\phi\hat{i}_\phi - \cos\phi\hat{i}_\theta\right]$	$\hat{n} \times \bar{H}_s = -\frac{\hat{i}_z}{Z_o}\left\{\frac{-1}{ka\left[\frac{\pi}{2} + j\ln\frac{1.1229}{ka}\right]} + \cos\phi - j\frac{ka}{2}\cos 2\phi + \ldots\right\}$ $\hat{n} \times \bar{H}_i = -\frac{\hat{i}_z}{Z_o}\left\{\cos\phi - jka\cos^2\phi - \frac{(ka)^2}{2}\cos^3\phi \ldots\right\}$

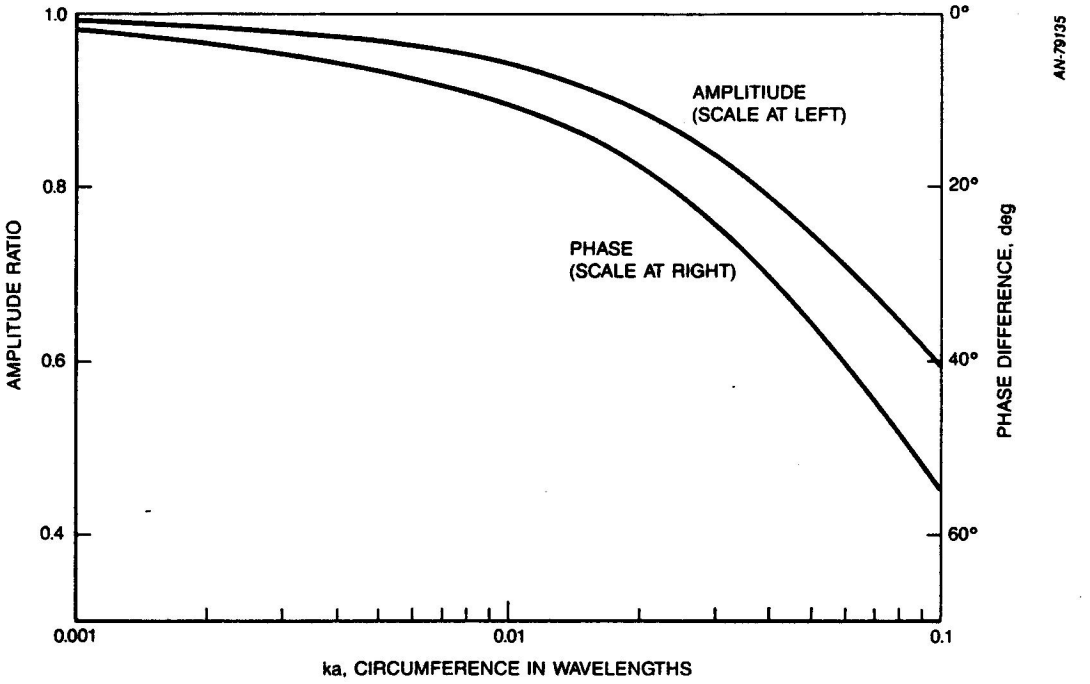

Figure 3.1. Plane wave incident on a cylinder; currents on trailing edge relative to leading edge.

The far-field scattering of the cylinder also contains a slowly diverging term which in the limit produces a $m = o$ (isotropic) scattered pattern. The second term, which varies like $\cos \phi$, is proportional to $(ka)^2$, so it converges to zero much faster than the equivalent surface current term, which is independent of ka. For $ka = 0.1$, the far-field forward-scattering is only 0.415 dB higher than the back-scattering, and for $ka = 0.01$, the difference is 0.008 dB. In contrast, the far-field scattering of the sphere does not approach isotropic; in the limit as $ka \to 0$ the back-scattering is 9.54 dB higher than the forward scattering.

4 CONCLUSIONS

Wires and spheres which have a small diameter in wavelengths still exhibit significant variations in surface currents and, for a sphere, far-field scattering also varies significantly. Whether or not these

variations will be important in a given problem must be determined on a case-by-case basis, but clearly the variations themselves cannot be dismissed.

REFERENCES

1. J. Moore and R. Pizer, Moment Methods in Electromagnetics, Research Studies Press, 1984.

2. R. Mittra (Ed.), Numerical and Asymptotic Techniques in Electromagnetics, Springer-Verlag, 1975.

3. A.C. Ludwig, "A Comparison of Spherical Wave Boundary Value Matching Versus Integral Equation Scattering Solutions for a Perfectly Conducting Body," IEEE Trans., AP-34, No. 7, July 1986, pp. 857-865.

4. J. Logan and J. Rockway, The New MININEC (Version 3): A Mini-Numerical Electromagnetic Code, NOSC TD 938, September 1986.

5. J.A. Stratton, Electromagnetic Theory, McGraw Hill, 1941, Sect. 6.10.

EFFICIENT SOLUTION OF LARGE MOMENTS PROBLEMS:

WIRE GRID MODELING CRITERIA AND CONVERSION TO SURFACE CURRENTS

Thomas R. Ferguson

Robert J. Balestri

This work was supported by the Rome Air Development Center Contract F30602-74-C-0182. Portions of this paper were presented at the 1976 EMP Interaction and Coupling Analysis and Validation Seminar, USAF Academy, July 20-22, and at the IEEE 1976 International Symposium on Electromagnetic Compatibility, Washington, D.C., July 13-15.

Thomas Ferguson is currently with the AFWL, Kirtland AFB, NM. Robert Balestri is currently with Booz•Allen & Hamilton, 4330 East West Highway, Bethesda, MD 20814.

ABSTRACT

A banded matrix iterative solution method for linear simultaneous equations arising from thin wire moments problems has been applied to a variety of problems of intermediate electrical size with the number of unknowns ranging up to 1000. Using a convergence criterion of 1 percent, solution efficiencies varied from 2.5 for short, fat objects up to 35 for long, thin objects. Application of the method requires some expertise. Approximate guidelines for wire grid modeling of surfaces have been developed for the moments formalism used. A new method for computing surface currents from grid currents is discussed.

AUTHOR'S NOTE

This article was originally submitted to IEEE-AP in 1977 for publication. As received, it was turned down due to emphases on the computational aspects. The computational techniques have been incorporated into the GEMACS computer code.

Since this work, there has been much activity related to modeling large structures. While GEMACS is not capable of exploiting computer architecture to reduce computational cost, this work clearly demonstrates that large problems can be solved efficiently using peripheral processors and asynchronous input/output operations.

A brief addendum is provided which to some degree substantiates the rather surprising modeling guidelines of length to radius ratios of 5 for square grid representations of solid surfaces.

This paper is being printed in the ACES Journal and Newsletter in order that the results may be available to individuals to whom the computational and modeling aspects of wire grid or patch models are more significant.

1. INTRODUCTION

The BMI (banded matrix iterative) solution method was developed to reduce the cost of solving the linear simultaneous equations arising from the thin wire method of moments formalism. The results have been reported in detail.[1] A summary of the theory and results for small problems has been published.[2] This paper is a summary of the study of intermediate to large size problems (100 to 1000 unknowns). The majority of the problems investigated are wire grid models of objects with surface areas ranging up to 10 square wavelengths. Intermediate sized problems of this type were investigated to establish wire grid modeling criteria.[1d] These criteria were used in larger problems to investigate the solution efficiency of the BMI method.[1e] The reported formula for converting grid currents to surface currents was established in retrospect.

2. THEORY

The equations to be solved are written

$$AX = b, \tag{1}$$

where A is a full complex nonsymmetric N x N matrix usually called the impedance matrix, X is a column vector of N unknowns related to the coefficients in the current expansion, and b is the excitation column vector. The least expensive general method for solving these equations is by triangular decomposition of A using Gaussian elimination, which requires about $N^3/3$ complex multiplicative operations (MOs). An approximate solution with an accuracy of about 1 percent can be obtained at less expense by making use of knowledge about the elements of A. The wire segment self impedances (principal diagonal elements of A) are always large. The relative size of segment interactions (off-diagonal elements) decreases with increasing separation. Near neighbor interactions can be as large as the self terms.

Suppose the wire segments are numbered in the following manner. The object model is sliced into parallel sections across the most narrow dimension. All wire segments in an extreme slice are numbered first. All

segments are then numbered in the adjacent slice, and the process is repeated to the opposite extremity of the object. The slices are kept thin so that numbering proceeds across the object within a slice. As a result, the difference in segment numbers between segments in neighboring slices is always much less then N, the total number of segments. For problems of significant electrical size, the large off-diagonal matrix elements are the interactions between segments with separations much less than the object length. These matrix elements can be grouped within a small bandwidth about the principal diagonal using this numbering scheme.

The BMI solution method takes advantage of these characteristics by partitioning the matrix as

$$A = L + B + U, \tag{2}$$

where B is a banded matrix of equal upper and lower bandwidths M, and L and U are the strictly lower and upper triangular matrices below and above B in A. Then (1) can be written as

$$BX = b - (L + U)X. \tag{3}$$

The banded matrix is decomposed into a product of a banded lower triangulation matrix B_L and a banded upper matrix B_U by pivoting on the principal diagonal elements. An iterative sequence is then defined by the solutions of

$$B_L B_U X_{i+1} = b - (L + U)X_i. \tag{4}$$

Forward elimination and back substitution are required for each iteration. Assuming that the decomposition of B does not lead to large rounding errors, the sequence $\{X_i\}$ will converge to a solution of (1) if the spectral radius of $B^{-1}(L + U)$ is less than one. Pivoting on the principal diagonal elements theoretically could lead to large rounding errors, especially in ill-conditioned problems. Monitoring of the pivot ratio and comparisons to solutions of canonical problems have provided confidence in this method when used on computers with high precision.

In terms of MOs, the cost of decomposing B is $NM^2 - 2M^3/3$. The cost of each iteration is N^2. Assuming K iterations are required to reach the criterion for convergence, the solution efficiency of the BMI method relative to triangular decomposition of the full matrix is

$$g = N^3\left[3(NM^2 - \frac{2M^3}{3} + KN^2)\right]^{-1}. \quad (5)$$

Termination of the iteration is achieved by imposing a numerical criterion on some measure of convergence. In the early study of small problems, the exact solution x_e was available for comparison. The RE (relative-error) at the j-th iteration was defined by

$$RE_j = \left[\frac{(x_j - x_e)^\dagger(x_j - x_e)}{x_e^\dagger x_e}\right]^{1/2} \quad (6)$$

where (†) denotes the complex conjugate transpose. Because the exact solution is normally not known, some alternative measure is required. One candidate is the BCRE (boundary condition relative error) defined by

$$BCRE_j = \left[\frac{(AX_j - b)^\dagger(AX_j - b)}{b^\dagger b}\right]^{1/2} \quad (7)$$

Unfortunately, the ratio of the RE to the BCRE is bounded between the condition number of A and its reciprocal. This number can be computed at a cost of about N MOs at each iteration, however, and provides useful information about convergence. In particular, an increase in the BCRE has always been found to be a forecast of divergence.

An adequate measure of convergence is the IRE (iterative relative error) defined by

$$IRE_j = \left[\frac{(x_j - x_{j-1})^\dagger(x_j - x_{j-1})}{x_j^\dagger x_j}\right]^{1/2}. \quad (8)$$

For cases of rapid convergence, the sequence of values of both the RE and the IRE can be approximated by an exponential function.[1c] As a result, the value of the IRE at the next iteration can be predicted as

$$IREj+1 \simeq \frac{IRE_j^2}{IRE_{j-1}}. \quad (9)$$

This quantity is called the PRE (predicted relative error). The iteration for large problems was terminated when the PRE was less than 1 percent.

In all calculations, the starting value for x_0 was zero. Once B is decomposed, the cost in MOs for obtaining x_1 is less than N^2 because the operation $(L + U)x_0$ need not be performed. Experience shows that x_1 is a reasonable approximation to the solution in all cases of rapid convergence.

Hence no physical arguments or complicated problem-dependent calculations are required to start the iteration.

If the spectral radius of B^{-1} (L + U) is greater than 1, the sequence $\{x_1\}$ must eventually diverge. However, the sequence may initially converge and then diverge. This behavior is called pseudoconvergence. It has been observed in this study, and the best solution obtained may be of useful accuracy.

3. COMPUTER PROGRAM

The computer program used to investigate the capabilities and limitations of the BMI solution technique for large problems was a modified version of the Antenna Modeling Program.[3] This program is based on the Pocklington integral equation, with pulse plus sine plus cosine expansion functions, point matching, and a charge redistribution scheme at multiple wire junctions that accounts for differing segment lengths. The BMI solution method was incorporated using machine dependent programming techniques peculiar to the CDC computers (flip-flopping of storage areas and simultaneous buffering of data) to reduce costs and turnaround times. Different sections of code were used in the solution process depending on N, M, and a core size allocation parameter to take advantage of cases where A, B, B_L, B_U, or L + U fit entirely in core. This procedure does not affect the computer CP (central processor) time, which depends only in the number of MOs, but reduces the peripheral processor costs for problems of moderate size. Other portions of the program were not optimized, and segmentation was not used to further reduce core requirements. This program will not be disseminated. However, a general modeling program that includes an ANSI FORTRAN version of the BMI solution technique may be available.[4]

4. RESULTS FOR LARGE PROBLEMS

For the segment numbering scheme used, a bandwidth M corresponds to a distance R_M within which all interactions are kept in the banded matrix. During the research phase on small problems, each problem was investigated at several bandwidths to determine the value of M

for peak efficiency using a convergence criterion of 1 percent. The resulting guideline was that R_M should be about 1/7 of the object length. Cost limitations in the study of large problems prohibited varying the bandwidth for each problem. Calendar restrictions together with early convergence difficulties for models of spheres resulted in conservative choices of M for some large problems.

Eleven example problems are briefly described below and in Table 1. Geometric symmetries in these problems were not used to reduce solution costs.

(1) One straight wire, $L/\lambda = 100$.

(2) Four parallel wires, $L/\lambda = 25$.

(3) 10 by 10 array of half wavelength dipoles.

(4) Rectangular plate grid, 2.77 by 3.18 λ.

(5) Rectangular plate grid, 3.0 by 0.637 λ.

(6) Square plate grid, 2.0 by 2.0 λ.

(7) Parabolic cylinder reflector grid with array feed, 2.0 by 2.0 λ.

(8) Cylindrical grid, $L/\lambda = 3.0$, $ka = 1$.

(9) Cylindrical grid, $L/\lambda = 2.8$, $ka = 3.4$.

(10) Cylindrical grid, $L/\lambda = 2.8$, $ka = 3.4$, 24 wires.

(11) Gridded cylinder with axial stubs, $L/\lambda = 2.0$, $ka = 2.1$.

TABLE 1. Efficiency of Solution for Example Large Problems

PROBLEM NUMBER	N	M	K	g
1	1000	150	3	14.3
2	1000	60	6	35.3
3	500	70	1	16.9
4	963	236	3	6.2
5	396	65	4	9.8
6	544	132	2	6.3
7	860	120	1	17.7
8	392	64	3	10.6
9	984	336	9	3.4
10	480	168	11	2.9
11	822	240	7	4.3

These examples include both antennas and scatterers. The above-mentioned guideline for choice of M was used in examples 1,3,5,7, and 8. Convergence was rapid for these problems and the average efficiency was about 14. For example 2, a relatively small bandwidth resulted in high efficiency. Although this result could be problem dependent, the BMI solution method may prove to be more efficient than expected for long, thin objects. For examples 4 and 6, conservative choices for M resulted in rapid convergence. Higher efficiencies would probably be found by using the guideline for these examples. Good efficiencies were obtained for all objects with planar or near-planar geometries. Results for some of these examples using other lengths or wavelengths were comparable, but are not shown in Table 1.

To further exhibit the iteration characteristics for problems with rapid convergence, example 4 is described in greater detail. The grid mesh is square. There are 23 wire segments along one edge and 20 along the other. Numbering is along one edge, then along the adjacent segments perpendicular to the edge, then along the segments parallel to the edge, etc. The excitation is a plane wave with E-polarization and a 45° angle of incidence. The convergence data are shown in Table 2. The efficiency is computed at each iteration from (5) with K as the current number of iterations. As is evident, most of the solution time for this example was spent in decomposing B, and the rapid convergence points to better efficiency at smaller M. The PRE is a fair predictor of the IRE at the next iteration, which is characteristic of cases with rapid convergence. Note that the BCRE is about 1/5 of the IRE at each iteration, which shows that the BCRE is not an adequate measure of convergence. (The pivot ratio for decomposing B was only 53 for this example, indicating that the small values of the BCRE are not due to an ill-conditioned problem.)

TABLE 2. Convergence Data for Example 4; N=963, M=236

ITERATION	EFFICIENCY	BCRE	IRE	PRE
1	6.6	16.9	100.0	—
2	6.5	4.0	19.1	3.6
3	6.4	1.1	4.9	1.3
4	6.2		1.5	.4

The efficiency of the BMI solution method is considerably lower for short, fat objects. The performance for spheres will be discussed later. For a cylinder with length and circumference approximately equal, the guideline for M generally results in divergence or pseudoconvergence. Larger bandwidths yield convergence as shown by examples 9-11, but with lower efficiencies than for planar or long objects. Example 9 exhibits several details of interest. The cylindrical grid has 24 wire segments in a circumference and 20 along a length. Numbering is helix-like, which is a special choice of numbering within each slice across the cylinder. The guideline for M suggests a value of about 144 for this problem. Actual values used were 336, as shown in Table 1, and 195. For a plane wave excitation with E-polarization, the convergence data are shown in Table 3 at a bandwidth of 336. Note again that the BCRE is not a reliable measure of convergence. The PRE is an excellent predictor of the IRE at the next iteration in this example.

TABLE 3. Convergence Data for Example 9; N=984, M=336

ITERATION	EFFICIENCY	BCRE	IRE	PRE
1	3.7	11.93	100.00	—
2	3.7	4.62	45.81	20.98
3	3.6	2.66	20.84	9.48
4	3.6	1.76	13.54	8.80
5	3.5	1.20	9.30	6.39
6	3.5	.81	6.29	4.25
7	3.5	.55	4.30	2.95
8	3.4	.38	2.93	1.99
9	3.4	.26	2.00	1.37
10	3.4		1.36	.93

At a bandwidth of 195, example 9 was studied for E-polarization, H-polarization, and also for an annular gap voltage impressed on longitudinal segments at one cross section of the cylinder. For E-polarization, pseudoconvergence occurred. The best solution was at the fourth or fifth iteration, with an IRE of 26 percent and a BCRE of 6 percent. Compared to the solution obtained at a bandwidth of 336, this solution showed differences ranging up to 30 percent. (Far fields computed from this solution agreed with those from the accurate solution to within about 3

percent.) For H-polarization, the solution diverged after the first iteration. For the gap excitation, pseudoconvergence occurred. The best solution was obtained at the fifth or sixth iteration, with an IRE of 8 percent and a BCRE of 3 percent. These results emphasize the following characteristics of the iterative process. Whether the sequence converges depends on the spectral radius of B^{-1} (L + U) and not on the excitation. The number of iterations required for convergence depends on the spectral radius, the excitation, the starting point, and the convergence criterion.

Several wire grid models of spheres were investigated. Each model was constructed with a finite degree of rotational symmetry. The models generally had wire segments along lines of latitude or longitude, with occasional tapering at moderate latitudes to prevent extreme differences in segment length at junctions near the poles. Solutions were sought with the BMI method without making use of symmetries. Solutions were obtained with the use of symmetries for comparisons in some cases. In the iterative method, segment numbering spirals outward from one pole to helix-like numbering at the equator, and then spirals inward at the other pole.

For a sphere with ka equal to 4.7, a model using 996 segments was used. The excitation was a plane wave, incident normal to the polar axis. The wave had E (case 1) or H (case 2) lying in the equatorial plane. In the first case, pseudoconvergence occurred at bandwidths of 220 and 360. The best solutions obtained were poor. In the second case, at a bandwidth of 220, 33 iterations reduced the IRE to 2.7 percent and the BCRE to 2 percent. Termination was due to an independently set default. No sign of divergence was present. The distribution of current on wires normal to the H plane at the equator was in full agreement with known surface currents. Because pseudoconvergence occurred at a bandwidth of 220 for E-polarization, it must also eventually occur for H-polarization. This example shows that even a fairly small convergence criterion could be satisfied in an iterative sequence eventually destined for divergence.

It is possible that interior mode contributions affect the iterative solution for wire grid models of fat objects. Little is known about such modes. For the spherical cavity, the mode of lowest frequency occurs at ka equal to 2.744. A grid model for this sphere with 552 segments was

subjected to a plane wave excitation. With M equal to 192, pseudoconvergence occurred. The IRE and BCRE were reduced to less than 20 percent at the sixth iteration. The corresponding current distribution and resulting scattering cross section showed fair agreement with known behavior for the sphere external problem.

Additional studies of short, fat objects will be required to establish adequate guidelines for choice of M.

5. COMPUTER COSTS

All of the example problems were run on a CDC 6600 computer. For those examples resulting in convergence, the CP times required for solution are plotted in Figure 1 versus the number of MOs. The CP time is almost entirely due to performing the multiplicative operations, as expected. Time requirements on other machines may be approximated by comparing times required for one multiplication.

The PP (peripheral processor) times for full program execution are plotted in Figure 2 versus the number of MOs. Almost all of the PP time is used during the decomposition of B. The PP time required for performing iterations is quite small. The one point in Figure 2 well below the line is for the sphere problem with 33 iterations mentioned earlier. The large value for K raises the number of MOs considerably without much effect on the PP time. The PP time is dependent on the machine and the operating system, and on the amount of fast access core available for matrix operations. The latter factor determines whether all of A, B, B_L, B_U, or L + U can reside entirely in core. The most significant savings in PP time occur when B will reside in core, which requires about N(2M+1) complex words of storage. None of the large problems satisfied this requirement. Projections of PP time for other computers would be difficult. If M<<N, the PP time for the BMI solution method should be far less than for full decomposition of A. No numerical comparisons were available. The dollar cost for computing was dominated by the PP time.

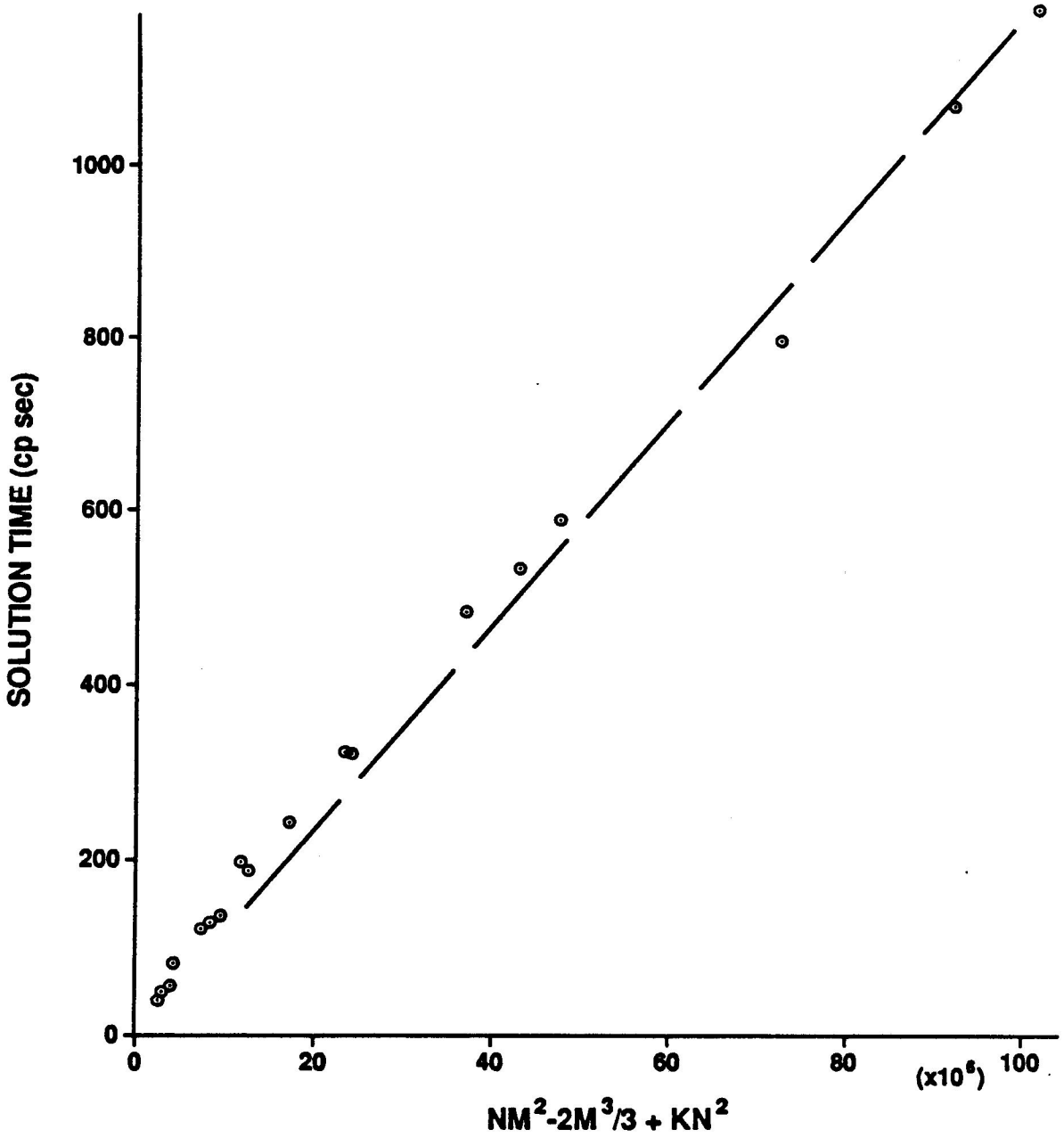

Figure 1. Equation Solution Time Versus Number of Complex Multiplicative Operations

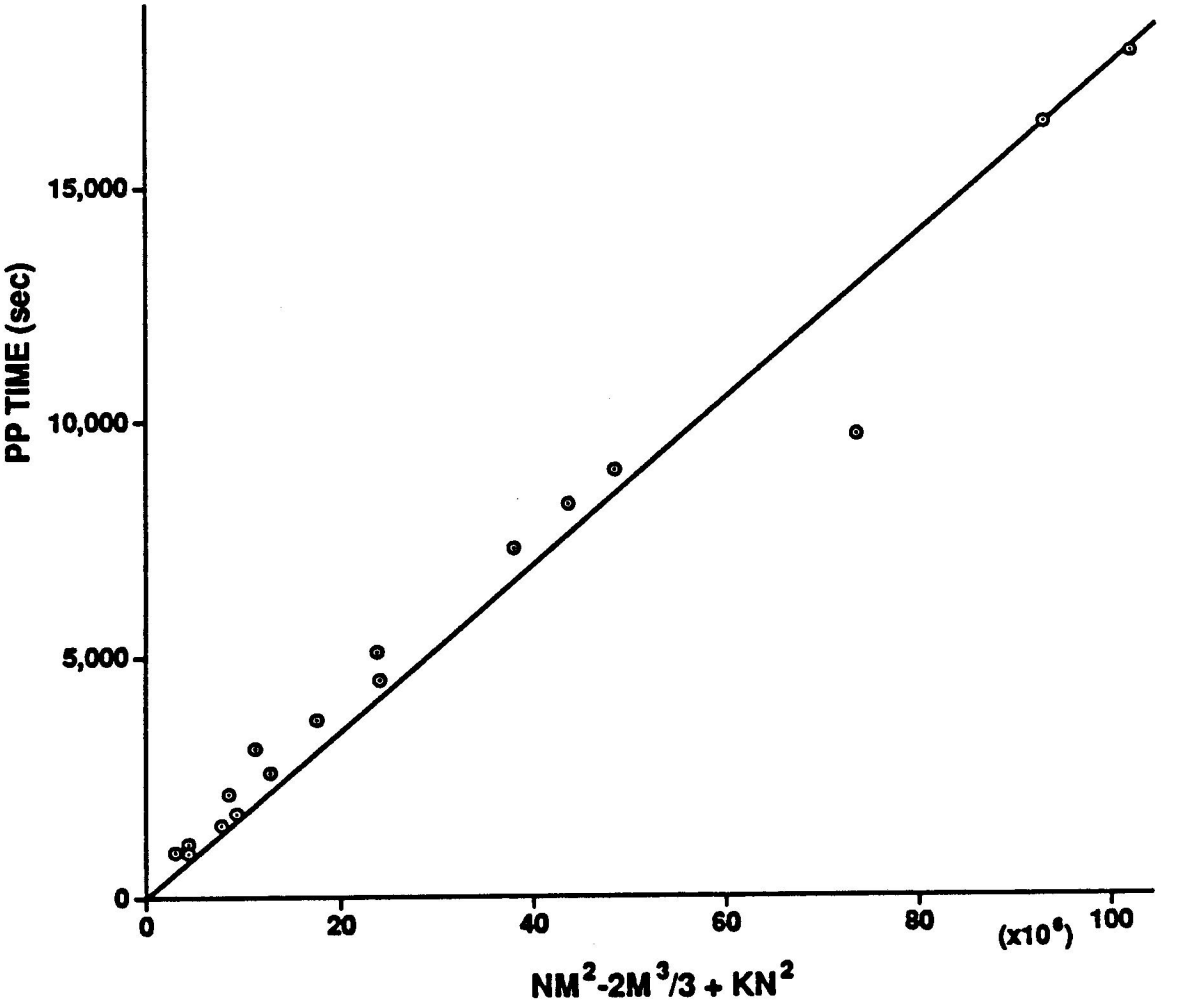

Figure 2. Peripheral Processor Time Versus Number of Multiplicative Operations

6. SURFACE MODELING WITH GRIDS

Early experience with the BMI solution method showed that the convergence properties for wire grid models of conducting surfaces should be based on models that are known to adequately represent the surfaces. Hence a limited modeling study was undertaken. Several objects of moderate size and rotational symmetry were modeled by wire grids with finite degrees of rotational symmetry. Symmetry was used in the solution process to reduce costs.[1d]

Wire grid modeling guidelines are not well defined in the literature. Mesh circumferences must be appreciably less than a wavelength to prevent mesh loop resonance phenomena. The maximum segment length depends on the details of the moments formalism in use, but must be restricted to about one-fifth of a wavelength even for single straight wire problems solved with sophisticated expansion functions. One guideline for the wire radius suggests that the wire surface area be about equal to the area of the modeled surface. Thinner wires have been used. For models with varying mesh shape and size, most studies have used the same wire radius for all segments. This practice was followed here.

No method for accurate conversion of wire grid currents to equivalent surface currents was available during this study. As a consequence. radiation patterns and bistatic scattering cross sections available from the literature for canonical objects were used for comparison to model results. These attributes are not as sensitive as current distributions for comparison purposes. After a conversion method was developed, current comparisons were made in a few cases.

Far field calculations from sphere models were compared to graphed results for radiation patterns of spherical antennas[5] and to bistatic scattering cross sections.[6] The models used wire segments along lines of latitude and longitude, yielding nearly rectangular mesh shapes at the equator.

For a spherical antenna with an equatorial gap and ka equal to 2, the power radiation pattern is shown in Figure 3 as a solid line. The other lines

were computed from the model, with the average ratio of segment length to wire radius at the equator denoted by d. Good agreement was obtained for ka equal to 3. Agreement deteriorated rapidly for ka equal to 4 and 5. Corresponding mesh circumference for the larger mesh area near the equator were 0.35, 0.52, 0.70, and 0.87 wavelengths respectively.

For plane wave scattering by a sphere, the bistatic scattering cross section in the E plane for ka equal to 2.3 is shown by the line in Figure 4. The points were computed from the model. Reasonable values were obtained for d equal to 5. Wire radii were fixed at this value and the frequency was varied. Good agreement was found at lower frequencies. At ka equal to 4.7, corresponding to mesh circumferences of about one wavelength, cross section errors of a factor of 2 were found.

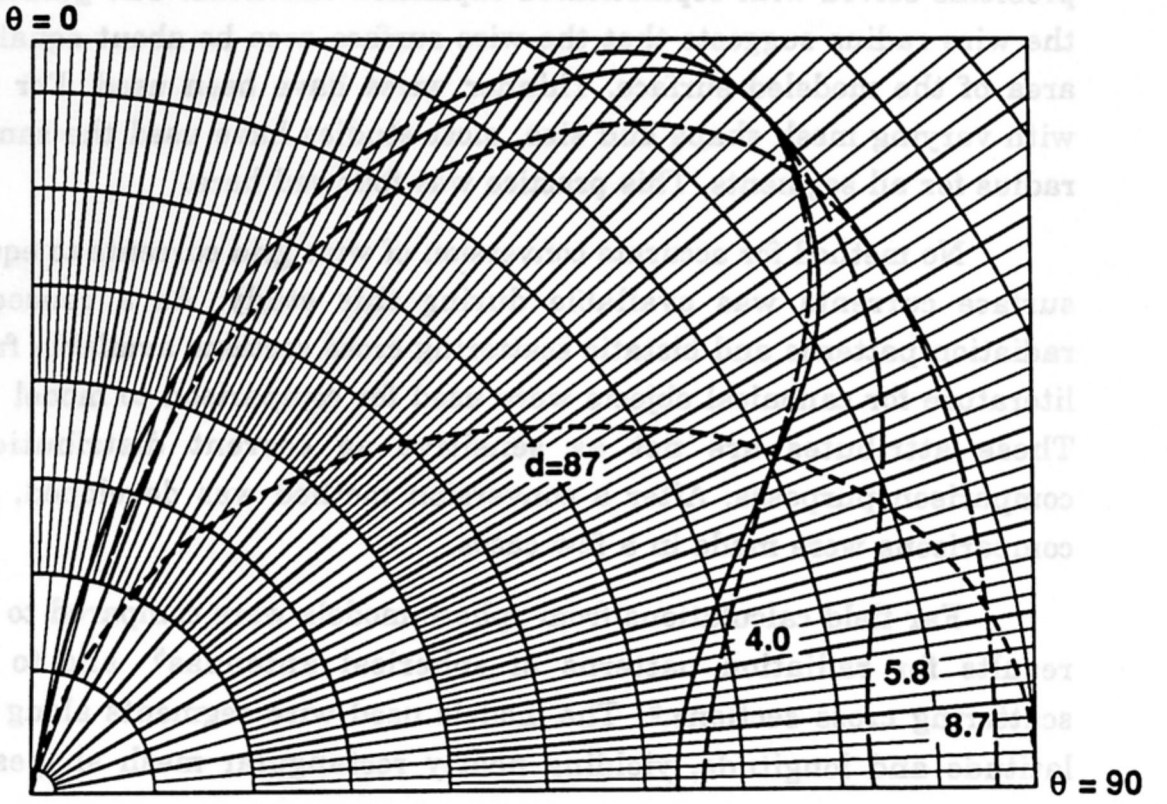

Figure 3. Power Radiation Pattern of a Sphere Excited Across an Annular Gap at the Equator, ka=2. (Solid Line After [5], Others from Model.)

Guidelines suggested by these comparisons are that the largest mesh circumference should not greatly exceed one half wavelength and the ratio of segment length to wire radius in regions of square mesh should be about five. Models of other objects (disk, toroid, cylinder, cone-sphere, etc.) were constructed using these approximate guidelines. Consistently good agreement with other theoretical results were obtained.[1d,e]

The guideline suggests a relatively fat wire for grid models in view of the thin wire assumptions common to all wire moments formalisms. It is likely that the best choice of radius depends not only on the choice of integral equations, expansion functions, weighting functions, and methods of treating junctions, but also on the type of kernel approximations used in computing segment interactions and self terms. Consequently, guidelines should be investigated for each choice of formalism.

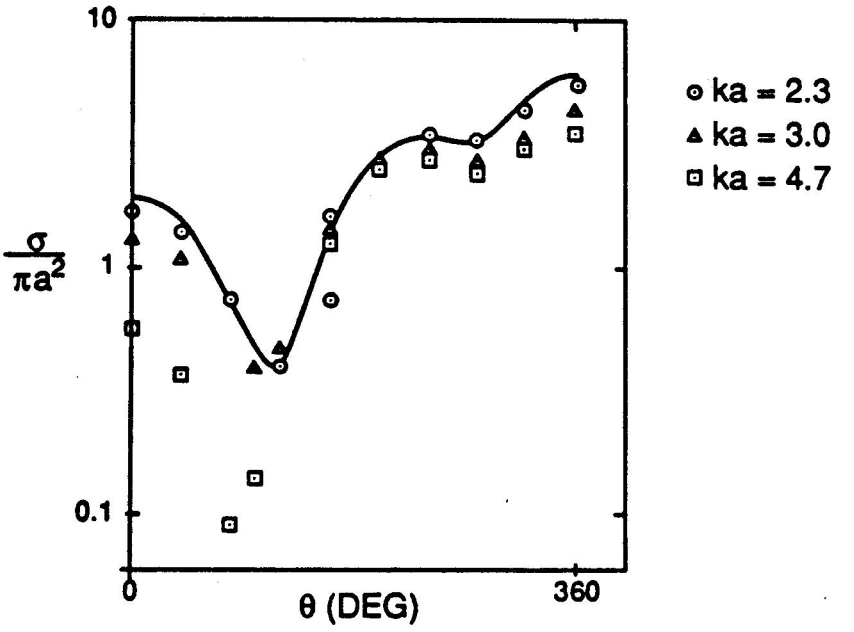

Figure 4. E-Plane Bistatic Scattering Cross Section For a Sphere with ka=2.3. (Line After King and Wu, Points From Model

7. CONVERSION TO SURFACE CURRENTS

Direct comparisons of shapes of wire grid current distributions and surface current distributions are possible in some cases. Surface current distributions for canonical problems are usually plotted as a function of one natural geometrical coordinate, with the current component either along or normal to the coordinate. If the wire segments in the grid lie along the natural coordinates and the grid is highly regular (mesh shapes repeated along the coordinate), excellent comparisons are possible.[10,7] In such cases, the equivalent local component of the surface current density is approximately equal to the wire current divided by the distance between wires carrying the current. This fact is closely related to the assumptions inherent in wire grid modeling and in the thin wire moments formalism. It is assumed that the current is slowly varying over a region small compared to a wavelength. The wire current is assumed to be uniformly distributed around the wire. This information can be used to redistribute the grid currents on the modeled surface for grids of arbitrary shape.

Figure 5 shows a portion of a planar wire grid around the j-th surface subdomain, which has an area equal to A_j. This area is bounded by wire segments with lengths L_i which carry midpoint currents $\vec{I}_i$. The currents are complex and are spatial vectors. The magnitudes of the complex currents are spatial vectors denoted by $|\vec{I}_i|$. The surface subdomains bounding A_j and sharing common wire segments are shaded in Figure 5, and their areas are denoted by A_{ji} (not to be confused with matrix elements). The magnitude of the complex surface current density is a spatial vector denoted by $|\vec{J}_j|$. An approximate formula for this quantity is

$$|\vec{J}_j| = \sum_{\substack{i \\ \text{loop}}} \left(\frac{L_i}{A_j + A_{ji}} \right) |\vec{I}_i| \,. \tag{10}$$

The vector sum is over all segments bounding A_j. The coefficient in brackets is the reciprocal of an average width of the two areas joined by wire i, in the direction normal to the wire. For a square mesh, this formula reduces to the simple result mentioned earlier.

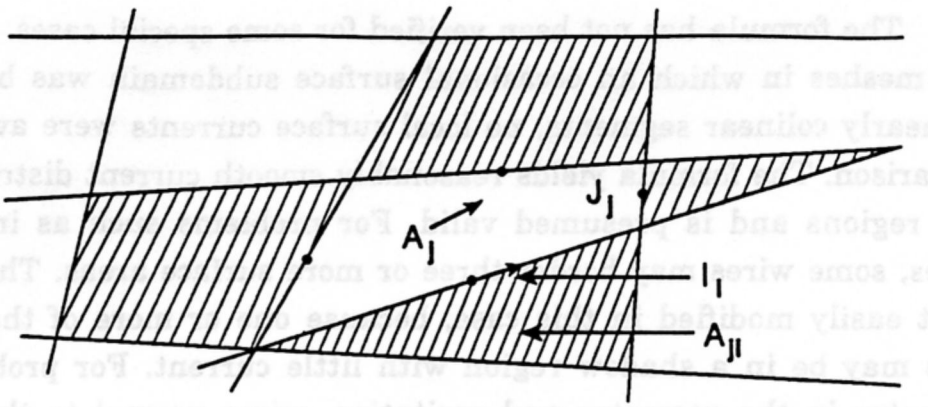

Figure 5. Equivalent Surface Currents From Wires

Several special cases must be considered. If one of the bounding wires is an edge wire, the corresponding value of A_{ji} is zero. The phases of all complex currents bounding A_j should be about the same.* The predicted surface current is the sum of currents from both sides of the modeled surface. If the surface is not closed, the predicted current cannot be uniquely separated into currents for each side. The formula gave reliable prediction for the sum of the two surface currents for example problems.

The formula was spot verified for square, rectangular, trapezoidal, and triangular mesh shapes in models of disks, spheres, and cylinders. For all meshes with four bounding wires, all wires were coplanar. For objects of arbitrary curvature, this may not always be possible. Slight deviations from planarity in a mesh should have little effect, and (10) should still be adequate. Large deviations result from poor modeling, since sharp bends should be modeled with wires along the bend.

---

* This should always be the case for regions small compared to a wavelength. The current phase and the interpretation of vector direction are interrelated, and are affected by the order in which segment ends are defined. It has been suggested[8] that the absolute value restrictions in (10) be removed. A paucity of surface current phase comparisons prevented verification of this suggestion.

The formula has not been verified for some special cases. For models with meshes in which an occasional surface subdomain was bounded by two nearly colinear segments, no local surface currents were available for comparison. The formula yields reasonably smooth current distributions in such regions and is presumed valid. For problems such as intersecting planes, some wires may border three or more surface areas. The formulas is not easily modified in this case, because one or more of the bordered areas may be in a shadow region with little current. For problems with symmetry in the geometry and excitation, wires normal to the expected direction of current flow are sometimes omitted even though the resulting mesh circumferences are greater than one wavelength. The formula is not appropriate for such models.

A more sophisticated formula could be generated using complicated interpolation methods. However, (10) is probably as accurate as is justified by wire grid modeling. If a poor model is used, no formula will give accurate surface currents.

8. SUMMARY AND PROSPECTUS

The banded matrix iterative method for solving linear simultaneous equations is useful for thin wire moments problems of intermediate electrical size. Compared to full matrix decomposition, the efficiency based on computer central processing time (or MOs) ranged from 35 for long, thin objects to about 10 for flat objects of significant width. Efficiencies of about 3 were found for fatter cylinders, and poor results were found for spheres. For flat objects, the guideline for bandwidth selection corresponding to about one-seventh of the object length resulted in reasonable convergence rates. Smaller bandwidths may be appropriate for long, thin objects. Larger bandwidths are required for short, fat objects. More examples might yield better guidelines. Even with use of the iterative method, the cost of solving large problems may be prohibitive for academic studies. Use of the method on machines of limited precision may lead to large rounding errors in the decomposition of the banded matrix. Partial pivoting may alleviate this problem, but at the expense of lower efficiency and increased storage requirements.

The computer program was recently converted to the CDC 7600 computer with no attempt at optimization for that machine. Up to 1250 unknowns have been used. Larger problems can be solved with minor code modifications. Optimization could greatly reduce the peripheral processor times, which currently dominate the dollar costs.

A limited study of wire grid modeling of surfaces established approximate guidelines for the specific moments formalism in use. The mesh circumference should not greatly exceed one-half wavelength. The segment length to wire radius ratio should be about 5 in regions of square mesh. Consistently good results were obtained, but no overall statement of accuracy was developed. The wire radius was constant for all segments in a single model, even though much smaller mesh sizes occurred near such regions as sphere poles. No deleterious effects of this practice were observed, which may indicate that further increases in wire radius would produce little change in currents.

The formula for converting grid currents to equivalent surface currents is useful for arbitrary mesh shapes. The accuracy of the computed surface currents is probably limited more by the accuracy of wire grid modeling than any other factor. The question concerning the phase of the predicted surface current should be investigated.

ADDENDUM

Since this work was originally performed, some additional insights into wire grid modeling have been developed. There follows a discussion of the wire length to radius ratios, wire grid models using regular polygons, and, finally, a different view of impedance matrices.

A.1 Wire Length/Radius Ratios

Conventional guidelines recommend that there be 10 wire segments per wavelength and that the wire segment length/radius ratio be 10 or greater. During investigations of the BMI solution technique, very good results were obtained with 5-6 wire segments per wavelength when the length/radius ratio was 5 to 6. This agreement held for both field values and surface current density when compared to analytical results.

While these were empirical results, their general validity has been substantiated in the open literature.[9,10] In these references, the EFIE MoM formalism is represented as:

$$(\mathbf{L}_o - \mathbf{L}) \cdot \underline{J} = - \underline{\ell} \cdot \mathbf{E}_{inc}$$

where $\mathbf{L}_o$ is the usual electric field linear operator and $\mathbf{L}$ is a perturbation operator induced by representing a continuous surface by a wire grid. $\mathbf{L}$ is explicitly given by:

$$\mathbf{L} = jf\mu_o \, \underline{\ell} \cdot \ln\left(\frac{\ell}{2\pi r_o}\right)\left[\mathbf{I} - \frac{j\nabla\nabla}{k^2}\right]$$

where ℓ is the grid segment length, μ_o is the free space permeability ($4\pi 10^{-7}$), f is the frequency, k is the wave number, and r_o is the wire element radius. The perturbation term can be made to vanish using a length to radius ratio of 2π, which explains the empirical results obtained in the early GEMACS work of Ferguson and Balestri in which the ratio of 5 was used. Rewriting the segment length as a fraction of wavelength $\ell = \alpha\lambda$, the perturbation term $\mathbf{L}$ becomes:

$$\mathbf{L} = j\alpha 120\pi \ln\left(\frac{\ell}{2\pi r_o}\right)[\ldots]$$

which is recognizable as a fraction of the free space impedance of 377Ω. In the GEMACS, and also most other formulations, the self terms are dominated by the complex part of the interaction, and the terms are on the order of 10^3. We can that see the trade-off between the segment length and the length to radius ratio can alter the diagonal element of the structure matrix appreciably.

A.2 Wire Surface Grid Models

Another general rule is to attempt to have as much wire segment surface area as the actual surface being modeled. This rule has never been substantiated in the literature, however, there appears to be a conflict with the previous requirements. Consider a square mesh with each element having sides of length ℓ. If each wire element contributes 1/2 of its area to the interior (the other 1/2 contributes to the adjacent mesh) then we have:

$$\ell^2 = \frac{1}{2}[(8\pi r_o \ \ell\ )]$$

for the mesh area in terms of the wire segment parameters. This results in a length to radius ratio of 4π or approximately 10 which is where we started using the conventional modeling lore.

It would appear that the correct wire grid representations of surfaces lies somewhere in between, and the user should always make the ultimate decisions. It is natural to ask if there is a grid representation which supports a length to radius ratio of 2π and at the same time preserves the total surface area. In general the answer is no since there is no regular polygon for which this condition holds. The area of a regular polygon of n sides of length ℓ is:

$$A = \tfrac{1}{4} n \ell^2 \bullet \cot\left(\frac{\pi}{n}\right)$$

and the area of the n wire segments each of length ℓ is:

$$A_W = n \bullet 2\pi r_o \ \ell$$

Setting $A = \frac{1}{2} A_W$ leads to :

$$\cot\left(\frac{\pi}{n}\right) = \frac{4\pi r_o}{\ell}$$

or:

$$\frac{\ell}{r_o} = 4\pi\tan\left(\frac{\pi}{n}\right)$$

Setting n to 3, ..., 10 yields $\frac{\ell}{r_o}$ ratios and perturbation factors of:

n	$\frac{\ell}{r_o}$	$\ln\left(\frac{\ell}{2\pi r_o}\right)$
3	21.76	1.25
4	12.56	.69
5	9.13	.37
6	7.25	.14
7	6.05	-.04
8	5.20	-.18
9	4.57	-.31
10	4.08	-.43

for surface area modeling. It is seen that the $\frac{\ell}{r_o}$ ratio of 2π requires a seven-sided polygon, whereas the ratio of 4π requires 4-sided polygons which are typical planar surfaces. It is interesting to note that modeling surfaces with triangular meshes (n = 3) requires an extremely thin wire which will have a perturbation factor twice that of 4-sided polygons.

A.3 A Different View of Impedance Matrices

The banding scheme presented in the earlier work has since been referred to as the Principle Axis Slicing System or PASS. The problem with such a system is the fact that the interaction "strength" is assumed to be dependent on relative separation. It is possible for model elements to be quite far apart and still interact strongly to produce a scattered field when the elements are in phase. Figure A-3 is a magnitude plot of an impedance matrix. While there is a strong diagonal band, off band elements are clearly seen. Based on magnitude, a band-width can easily be selected as illustrated. Figure A-3 was originally displayed in color, and by using color graphics a different perspective of the "electromagnetics" of the model may

be obtained. Also, by assigning a reference phase, plotting the relative phases of the impedance matrix elements may indicate when certain regions of the model can interact coherently to produce large effects. I haven't attempted this since I think it will require more than the three colors available to me at present.

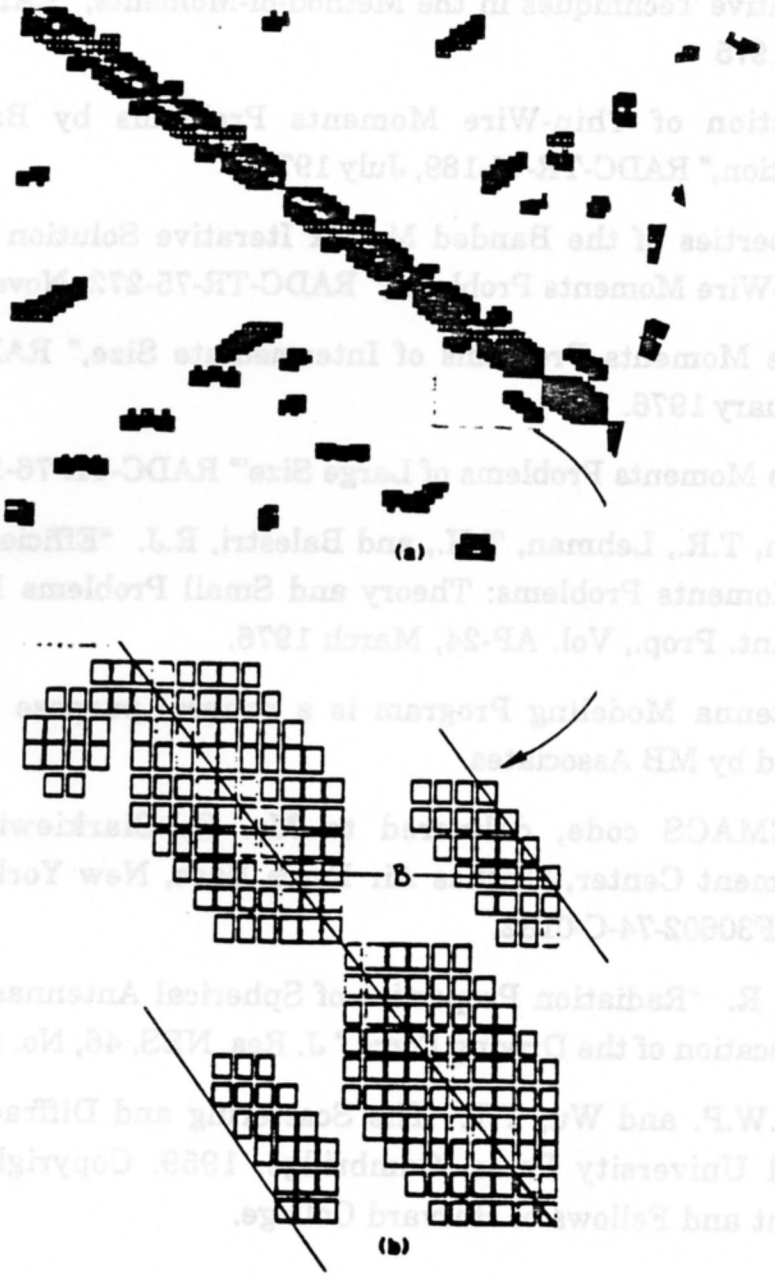

Figure A.3 (a,b) Impedance Matrix and Bandwidth Display

REFERENCES

1 Ferguson, T.R. The EMCAP (Electromagnetic Compatibility Analysis Program) Quarterly Reports, the BDM Corporation:

a. "Iterative Techniques in the Method-of-Moments," RADC-TR-75_121, May 1975

b. "Solution of Thin-Wire Moments Problems by Banded Matrix Iteration," RADC-TR-75-189, July 1975.

c. "Properties of the Banded Matrix Iterative Solution Technique for Thin-Wire Moments Problems," RADC-TR-75-272, November 1975.

d. "Wire Moments Problems of Intermediate Size," RADC-TR-76-148, February 1976.

e. "Wire Moments Problems of Large Size'" RADC-TR-76-122, May 1976.

2 Ferguson, T.R., Lehman, T.H., and Balestri, R.J. "Efficient Solutions of Large Moments Problems: Theory and Small Problems Results'" IEEE Trans. Ant. Prop., Vol. AP-24, March 1976.

3 The Antenna Modeling Program is a general purpose thin-wire code developed by MB Associates.

4 The GEMACS code, delivered to Mr. K. Siarkiewicz, Rome Air Development Center, Griffiss Air Force Base, New York 13440, under contract F30602-74-C-0182.

5 Karr, P. R. "Radiation Properties of Spherical Antennas as a Function of the Location of the Driving Force," J. Res. NBS, 46, No. 5, May 1951.

6 King, R.W.P. and Wu, T.T. The Scattering and Diffraction of Waves, Harvard University Press, Cambridge, 1959. Copyright 1959 by the President and Fellows of Harvard College.

7 Ferguson, T.R. and Balestri, R.J. "Solution of Large Wire Grid Moments Problems," IEEE International Symposium on Electromagnetic Compatibility, July 1976.

8 In conversation with Carl E. Baum

9 Kontorovich, N.I., "Averaged Boundary Conditions at the Surface of a Grating with Squaremesh," Rad. Eng. Electron, Phys., Vol 8, No. 9, 1963.

10 Lee, K.S.H., et al., "Limitations of Wire-Grid Modeling of a Closed Surface," IEEE-EMC-18, No. 3, Aug. 1976.

Scattering Error in a Radio Interferometer Located on a Finite Length Conducting Cylinder

by

R. J. Luebbers
Communications and Space Sciences Laboratory
The Pennsylvania State University
University Park, PA 16802

and

V. P. Cable
Lockhead Aeronautical Systems Co.
Burbank, CA 91520

Abstract

A modified general purpose plate/wire analysis computer program is used to predict the performance of a four-element interferometer mounted on the end cap of a finite length conducting cylinder. The analysis method includes effects of scattering from the cylinder and the antennas. Due to limitations of the computer program a square cylinder is modeled, and the antennas "float" above the end cap. Measurements made of a circular cylinder physical model generally confirm the computer results and show that good performance can be obtained with loop antennas provided that the cylinder exceeds a critical size.

Introduction

Accurate measurement of relative phase at radio frequencies using small and lightweight electronics has been made possible by recent advances in Surface Acoustic Wave discriminators. This, in turn, has made possible the use of very closely spaced (in terms of wavelengths) interferometer antennas. In some applications the antennas may be located on a structure which itself has a size of the same order of magnitude as the wavelength, and thus the currents excited on the supporting structure may cause severe errors in the bearing computed from the antenna current phases. This is in addition to the errors caused by reradiation from the antenna elements themselves, which was investigated by Harrison [1].

Harrison's work involved using numerical methods to evaluate the currents induced on four half-wave dipoles in free space due to both an incident plane wave and the currents on the other dipoles. He then compared the bearing angle computed from the relative phase of the induced currents with the actual bearing. Our approach is generally the same, in that numerical methods are be used. However, we consider the more practical problem of interferometer antennas located on the end cap of a finite length conducting cylinder and will include the effects of the currents induced on the cylinder as well as the reradiation from the antennas themselves.

Problem and Approach

The problem is to determine the performance of a four-element interferometer mounted on the end cap of a finite length circular conducting cylinder. Due to time limitations, rather than develop a special purpose computer model for analyzing a circular cylinder, an available general purpose wire-plate moment method code (known as ESP) was used.[2] Since this code was not capable of modeling curved surfaces, a square cylinder with sides equal in length to the circular cylinder geometry was made. The geometry considered by the computer model is shown in Fig. 1. This figure shows half-loop antennas, and dipole antennas were considered as well. Connected flat conducting plates were used to model the sides and end cap, and wire and lumped loads for the receiving antennas. Each antenna modeled included an impedance load, located for the antennas shown in Fig. 1 at the peak of the triangular loop and marked by a dot.

During the early phases of the computer analysis and design it was found that due to approximations made in computing the impedance matrix in ESP the currents in the interferometer antennas were not in phase even when the incident wave was on boresight, i.e., incident theta of zero degrees. These approximations involved an automatic reduction in the number of Simpson's rule integration intervals used to compute mutual impedances between current modes as a function of the distance between the modes. After modifying ESP so that the number of integration intervals remained constant for all mutual impedance calculations [3] this problem was removed, at the expense of increased running time. (This problem does not seem to be present in newer versions of ESP).

By using the computer model, the currents induced in the receiving interferometer antennas due to an incident plane wave, including reradiation from the cylinder and antenna currents, were calculated as a function of antenna type position (antennas arranged in a "cross" shape performed better than when arranged in a "square" shape with the dipoles parallel to the nearest edge of the square cylinder end), load resistance, and incidence angles of the plane wave (θ and ϕ). Variation in performance was investigated. The most important performance parameter was the relative phase of a pair of antennas as a function of the bearing angle of the incident plane wave. The goal was to have this variation be as close as possible to that which would ideally occur in free space without the disturbing effects of the currents induced on the cylinder and the other antennas.

The other performance parameter considered was antenna gain. It was desired to have the antenna gain be as high as possible subject to the constraint that higher gain would tend to increase errors due to mutual coupling effects between the antennas (since the antenna currents would be larger) and would require matching circuitry which would make the measurement of relative phase at the antenna terminals more difficult. For these reasons the load impedance was chosen to be 50 ohms.

The radially symmetric antenna configuration of Fig. 1 was obtained after investigation of several other configurations using the computer model. The computer results predicted higher gain for loop antennas then dipole, and to confirm these predictions it was decided to include both types of antennas in the experimental measurements. The square cylinder computer design, including the dimensions of the

cylinder, are shown in Fig. 2 for both antenna types. The frequency range considered in the design was 200 to 800 MHz. Over this range of frequencies the cylinder length varies from 0.8 λ to 3.2 λ, the width (diameter) from 0.1 λ to 0.4 λ, and the antenna center-to-center spacing from 0.06 λ to 0.25 λ. Thus the cylinder is in the resonance region, and the induced currents on the cylinder will be relatively large. For the frequencies and cylinder size shown the computer model was not capable of including wires that were connected to the end cap since ESP requires an "attachment" current disk at least 0.1 wavelength in radius, so both types of antennas "float" above the end cap.

The corresponding physical model is shown in Fig. 3. There are two obvious and important limitations of the computer model. First, the square cylinder has been changed into a circular cylinder, since this was the actual shape of interest. Second, the physical antennas cannot actually "float" above the end cap but must be fed using transmission lines and physically connected to the end cap.

Results

The physical model was built, and extensive measurements were made. Both the dipole and half-loop antenna systems were measured for gain, amplitude versus bearing angle, and relative phase versus bearing using a commercial (Scientific Atlantic) receiver. Frequencies of 200, 300, 400, 500, 600, and 800 MHz were covered. Referring to Fig. 1 and considering the pair of antennas which lie along the y-axis to be under test (with all antennas terminated in 50 ohms), pattern cuts were made with ϕ equal to 0°, 45°, and 90° for both ϕ and θ polarizations as a function of θ. Gain measurements were made only for boresight ($\theta = 0$), but were repeated for both vertical and horizontal polarization (with the cylinder rotated by 90° to retain a polarization match) in order to check repeatability and range dependence.

Since relative phase is more important than amplitude in assessing DF antenna system performance, we will be primarily concerned with phase results. However, in general the agreement between calculated and measured received amplitude was as good or better than was the case for the phase measurements.

Regarding the half-loop antenna system, several conclusions can be drawn. First, the measured and computer results agreed well, especially at frequencies above 200 MHz. Even at 200 MHz, the computer results indicated the trend correctly even if they did not agree exactly with the measurements. Second, for frequencies above 200 MHz, both the computer and measured results indicated relative phase reception that was a reasonably good approximation to ideal free-space results for a field of view of approximately ±30°. Third, even for bearing angles not in the principal plane of the antennas, the performance was good for both polarizations.

Figures 4 through 7 contain data that illustrate and quantify the above points. Figure 4 is for a frequency of 200 MHz. Referring to Fig. 1, the active antennas are the pair along the y-axis, and the incident wave direction lies in the y-z plane, i.e., $\phi = 90°$. This is the principal incidence plane for this pair of antennas. The curves in Fig. 4 show the relative phase between the y-axis pair of antennas as calculated using the computer model for θ (principal) polarization

(including effects of induced cylinder currents and mutual antenna coupling), the measured relative phase, and the relative phase for the "ideal" free-space situation with the cylinder absent. The computer predicts less phase variation with incidence angle than ideal, and the measured results show even less. Judging by the measured results, there is not enough phase variation over a ±30° field of view for an interferometer-type direction-finder (DF) processor to function.

The results for the loops for a frequency of 400 MHz contained in Figs. 5 through 7 are much improved. Both the computer predictions and the measured data indicate very nearly ideal performance over a ±30° field of view in the principal plane (Fig. 5). The computer results do not exactly match the measured results, probably due to the previously discussed differences in the physical and computer antenna models. However, the agreement is quite good for the boresight region, which is the area of most interest.

Figures 6 and 7 show the same set of predicted, measured, and ideal relative phase curves, but this time for the 45° plane of incidence and for both polarizations. The computer results agree fairly well with the measurements but not as well as in the principal plane. This is probably due to the square cylinder computer model versus the round cylinder physical model, since in the 45° plane, the computer model corners lie in the plane of incidence. Even so, the computer predictions which indicate a greater deviation from ideal behavior for ϕ-polarized waves as opposed to θ-polarized waves are confirmed by the measurements. The difference between the θ-polarized and ϕ-polarized results as shown in Figs. 6 and 7 is due to the excitation of different currents on the cylinder. At 400 MHz the cylinder is just over one-half wavelength in circumference, and thus the near-resonance circumferential currents excited by the ϕ-polarized incident wave will be stronger than the off-resonance longitudinal currents excited by the θ-polarized wave. For accurate DF performance, both polarizations must give good results in the $\phi = 45°$ incidence plane, since the antennas will receive both equally, and an arbitrarily-polarized incident wave will contain both. Results for higher frequencies are similar to these 400-MHz results.

Before considering the dipole case, let us relate the phase information of the preceding figures to bearing information. An ideal interferometer, given ideal relative phase information, will compute the incident bearing angle θ_b in the principal plane as

$$\theta_b = \sin^{-1}\left(\frac{\lambda \cdot \psi_e}{d \cdot 360}\right) \qquad (1)$$

where ψ_e is the relative antenna current phase, λ is the wavelength, and d is the antenna spacing. Considering, for example, the results of Fig. 5, at an incident θ of 30° the measured result differs from the ideal by about 1° of phase. This value of relative phase would result in an interferometer bearing of approximately 28.5°, which is in error by 1.5°. This error could be reduced by calibration if necessary.

Now let us consider the representative dipole results of Figs. 8 through 10. First, note that the relative phase scale maximum value had to be increased to accommodate the greater variation in dipole phase. Both the measured and calculated results indicate much greater

departure from ideal free-space behavior for the dipole antennas than for the loops. However, the computer results do not accurately follow the phase measurements. Even so, the computer model does predict the trends in the measurements, including the reduced phase change with θ incidence angle evident for the ϕ-polarized case of Fig. 10. Dipole results for other frequencies were either similar or showed even more rapid variations near boresight.

Figure 11 shows a comparison of calculated and measured gain results. For these measurements the gain figure includes the mismatch loss due to terminating the (small, highly reactive) antennas in a 50 ohm load. The gain figures therefore indicate the power these antennas would deliver to a receiver with a 50 ohm input impedance without any impedance matching to compensate for the antenna reactance. The figure contains calculated and measured values of boresight (θ = 0) gain for both antenna types. The measurements were made for both vertical and horizontal polarization with the model rotated 90° to maintain polarization match to the antenna being measured. Thus, for an ideal range both measurements should yield the same result. Unfortunately, this is not the case, especially for the dipole antennas. This is due in part to range reflections and in part, for the dipole case, to the fact that at some frequencies the dipole amplitude pattern had a relative minimum on boresight. This tended to make the gain results for the dipoles more dependent on the precise position of the model. Nevertheless, the measurements do confirm the computer model prediction of higher gain for the half-loop antennas when terminated in 50 ohms. While the gain of both could be improved by impedance matching, the phase measurement would be complicated by the matching network.

Summary and Conclusions

A general purpose moment method computer analysis program capable of modeling wires and plates was modified and used to find the currents induced in four interferometer antennas located on the end cap of a finite length conducting square cylinder. Using this analysis tool, two different antenna configurations were chosen, one utilizing loop antennas and the other dipoles. A physical model based on the computer design was built, but with a circular cylinder and physically realizable antennas. Measurements made of current phase and antenna gain indicated general agreement with the computer predictions. Better agreement was obtained for the loops. Both measured and computer model results indicate that the loop system is capable of providing a good approximation to ideal interferometer performance within ±30° of boresight for a cylinder with length and radius greater than about 1.2 and 0.15 wavelengths, respectively. For a smaller cylinder the relative current phase did not change with bearing angle enough to allow a bearing to be reliably determined.

Acknowledgments

The authors wish to acknowledge the contributions made by Dr. William Ackerknecht and Mr. Sheldon Balk of the Lockheed Palo Alto Research Laboratory. We also wish to thank Dr. Edward Newman of the Ohio State University and Professor E. S. Gillespie of California State University Northridge.

References

1. Harrison, C. W., Jr., "Scattering Error in a Radio Interferometer," IRE Trans. on Antennas and Propagation, vol. AP-10, No. 3, pp. 273-286, May 1962.

2. Newman, E. H., "A User's Manual for Electromagnetic Surface Patch Code (ESP)," The Ohio State University Electro Science Laboratory Report 713402-1, July 1981.

3. Newman, E. H., private communication.

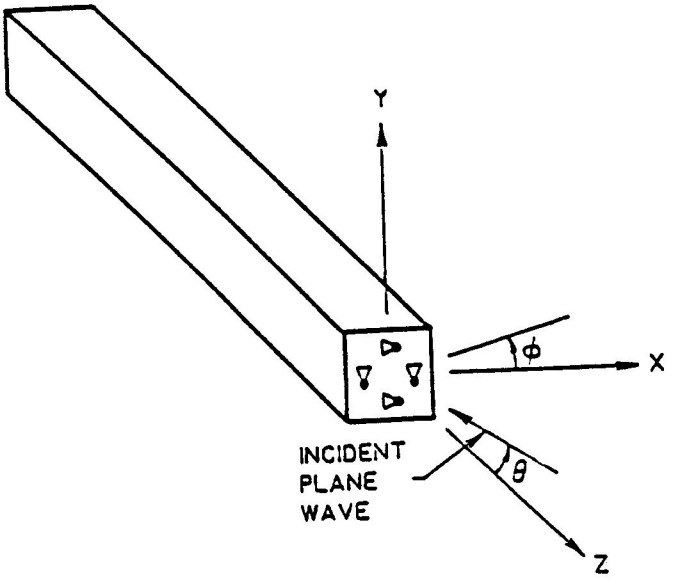

Figure 1 Geometry and coordinate system for computer model of square cylinder with two pairs of interferometer antennas.

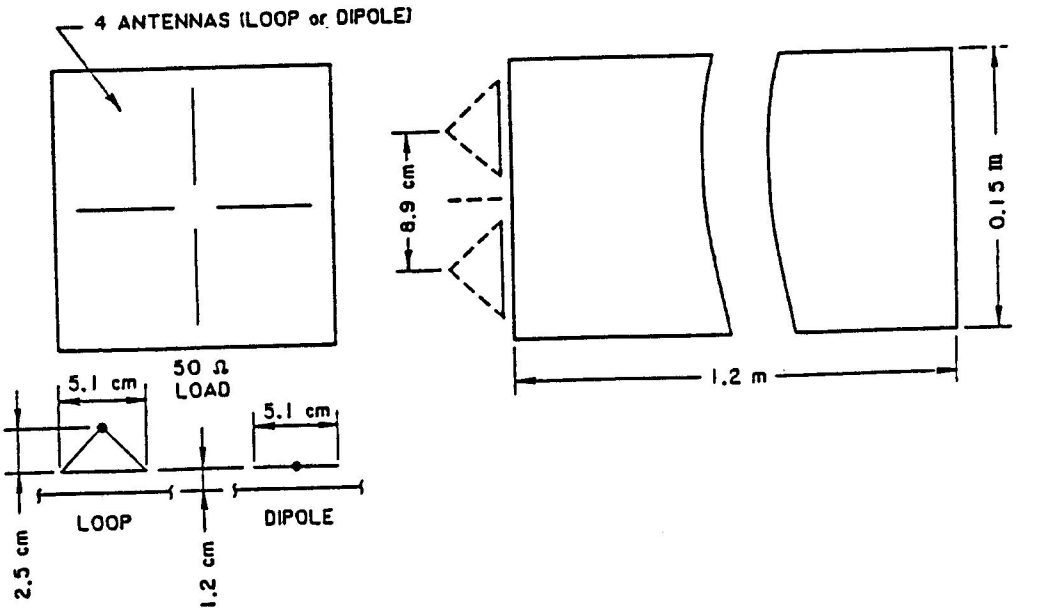

Figure 2 Dimensions of computer model square cylinder and antenna system.

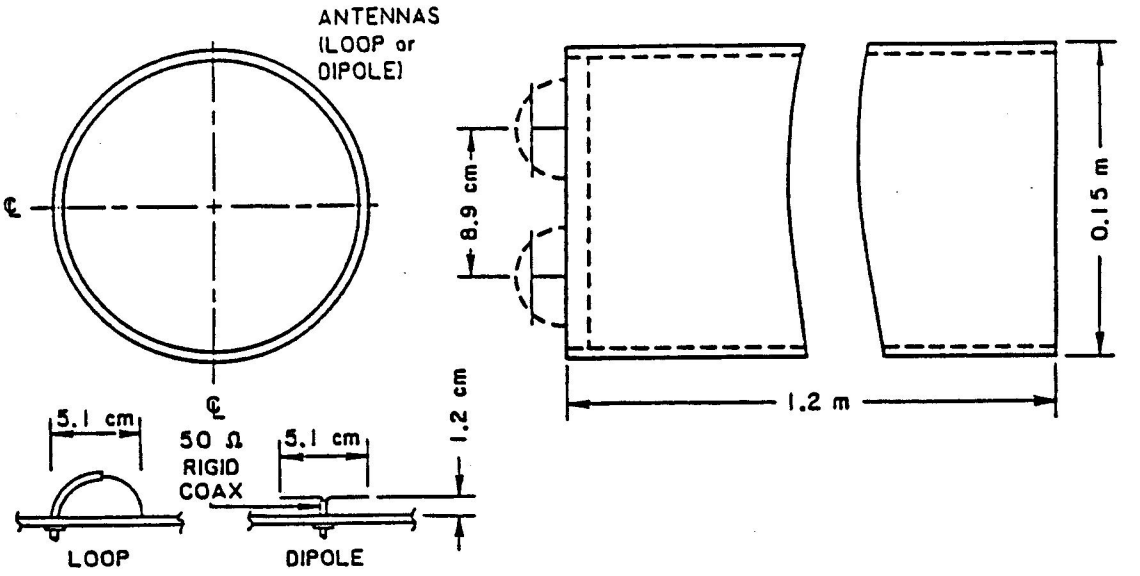

Figure 3 Dimensions of cylinder model actually built and tested, showing details of both the loop and dipole antennas.

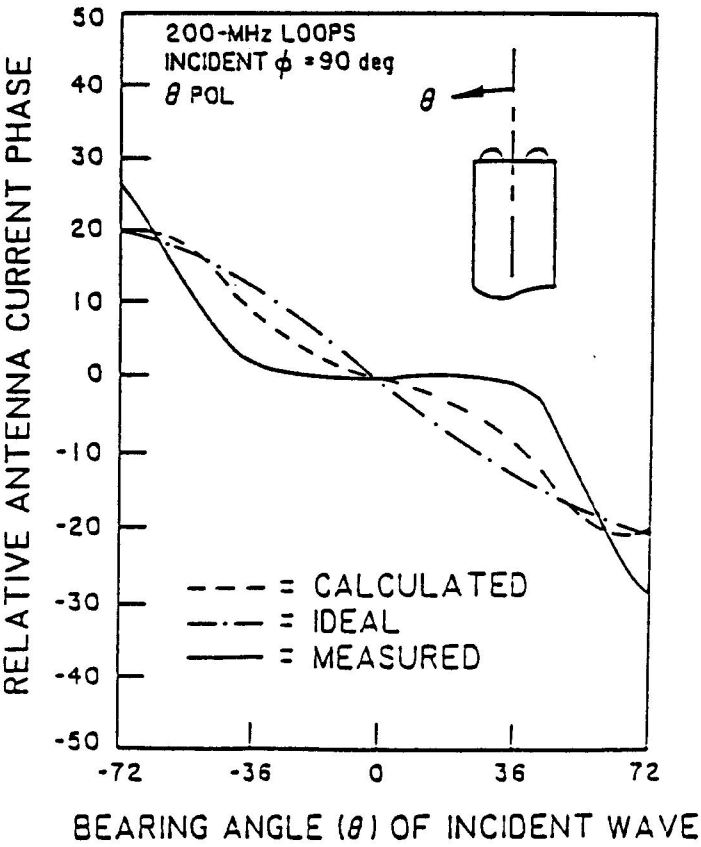

Figure 4 Calculated, measured, and ideal relative phase versus bearing angle for the loop antenna system in the principal plane (ϕ = 90 deg) at 200 MHz.

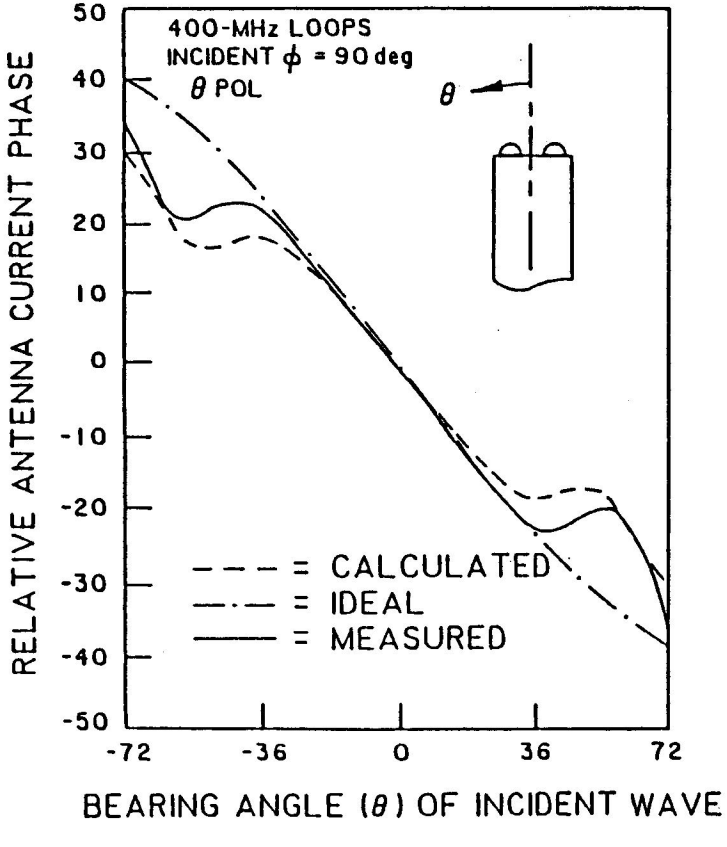

Figure 5 Calculated, measured and ideal relative phase versus bearing angle for the loop antenna system in the principal plane (ϕ = 90 deg) at 400 MHz.

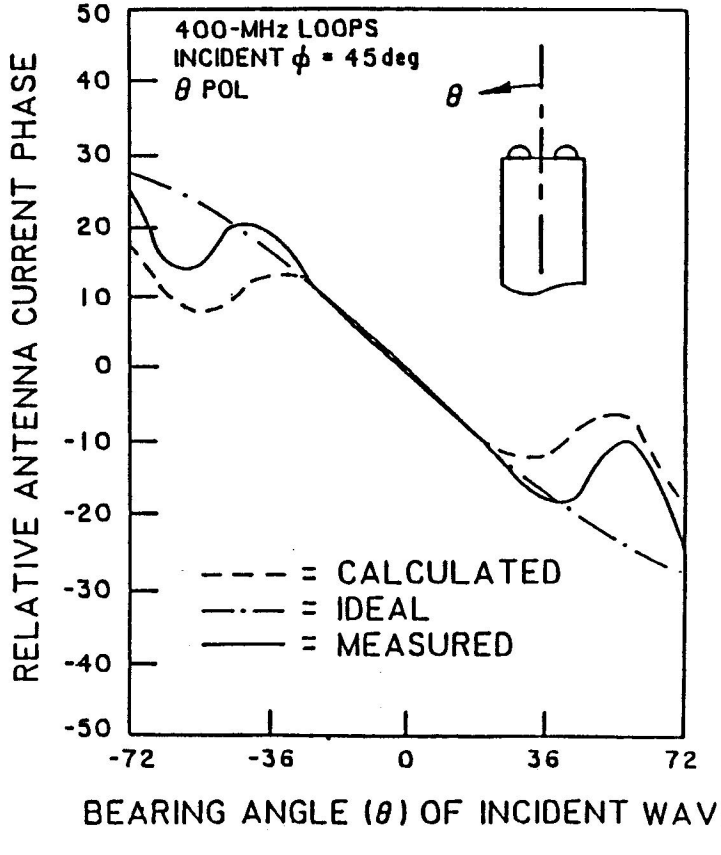

Figure 6 Calculated, measured and ideal relative phase versus bearing angle for the loop antenna system in the ϕ=45 deg plane for θ polarized incident wave at 400 MHz.

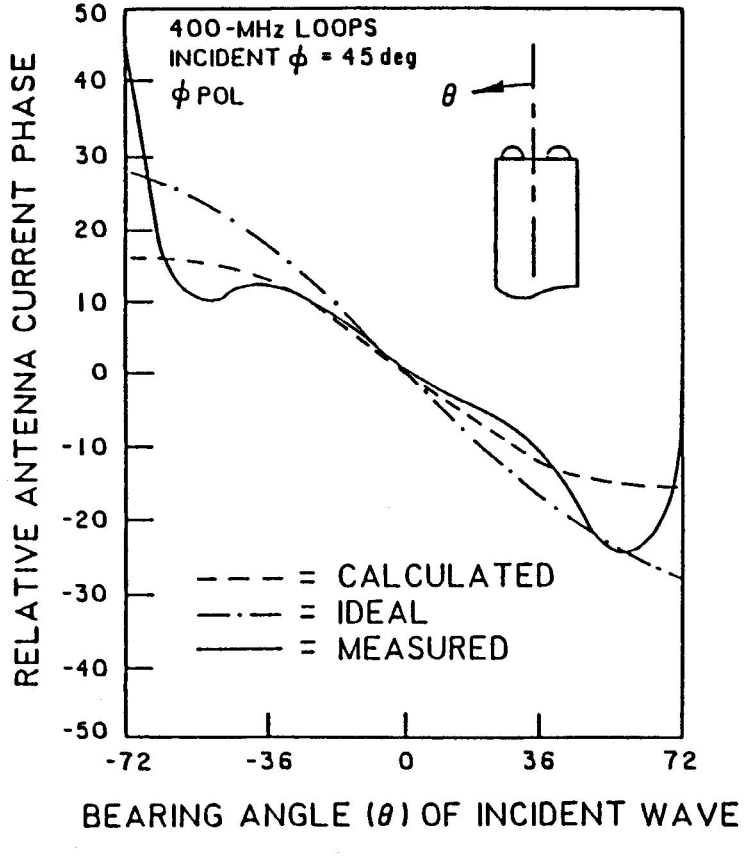

Figure 7 Calculated, measured, and ideal relative phase versus bearing angle for the loop antenna system in the ϕ=45 deg plane for ϕ polarized incident wave at 400 MHz.

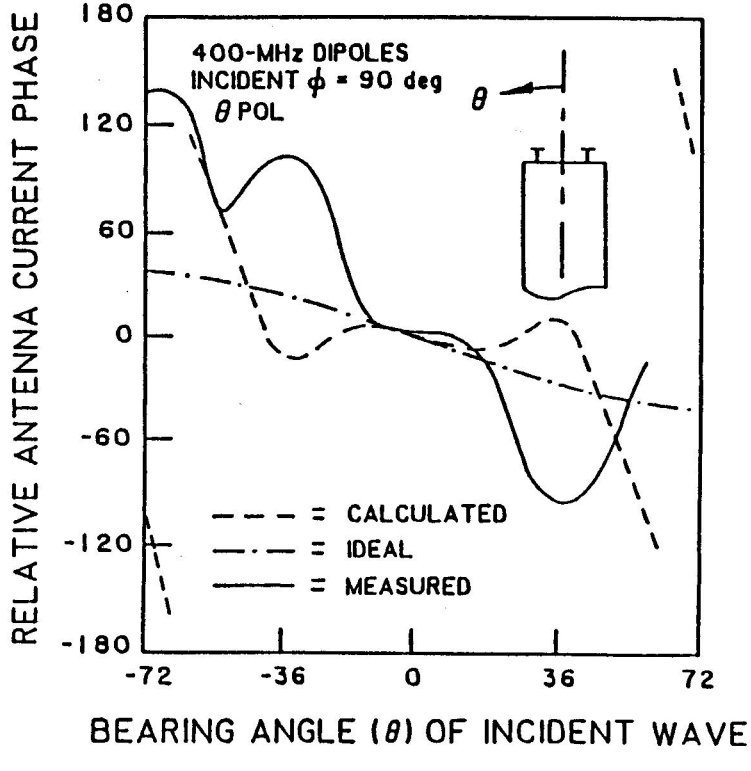

Figure 8 Calculated, measured, and ideal relative phase versus bearing angle for the dipole antenna system in the principal plane (ϕ=90 deg) at 400 MHz.

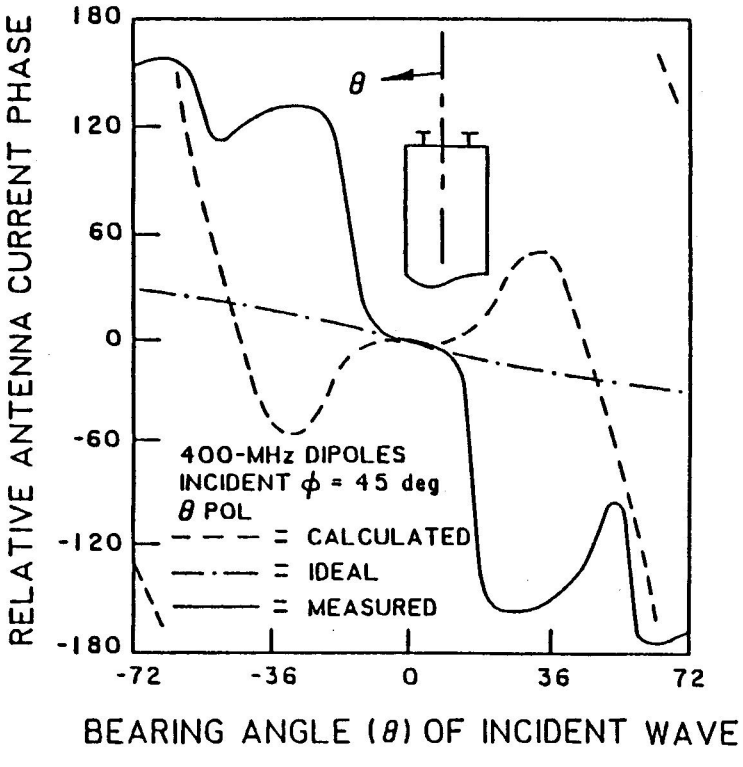

Figure 9 Calculated, measured, and ideal relative phase versus bearing angle for the dipole antenna system in the ϕ=45 deg plane for the θ polarized incident wave at 400 MHz.

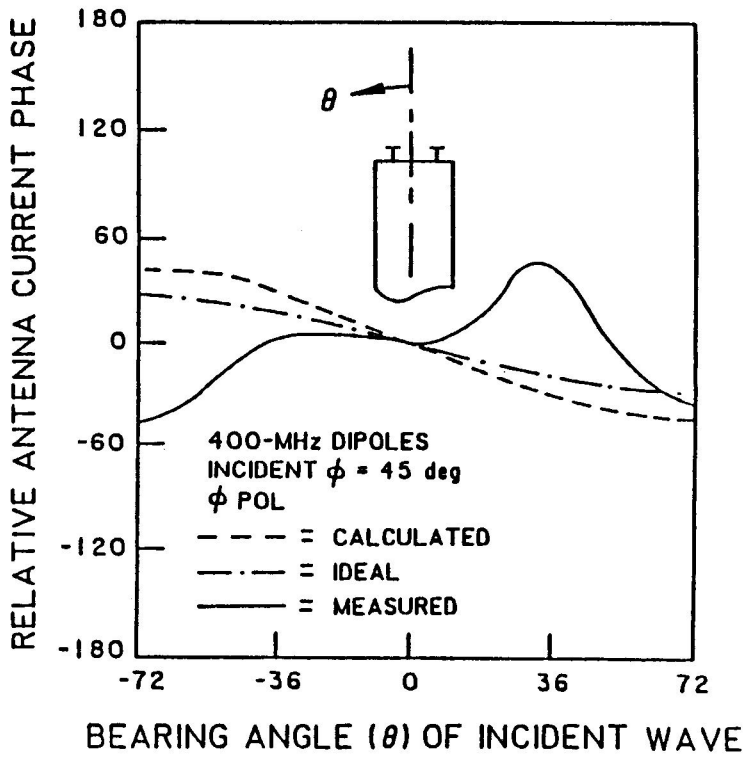

Figure 10 Calculated, measured, and ideal relative phase versus bearing angle for the dipole antenna system in the ϕ=45 deg plane for ϕ polarized incident wave at 400 MHz.

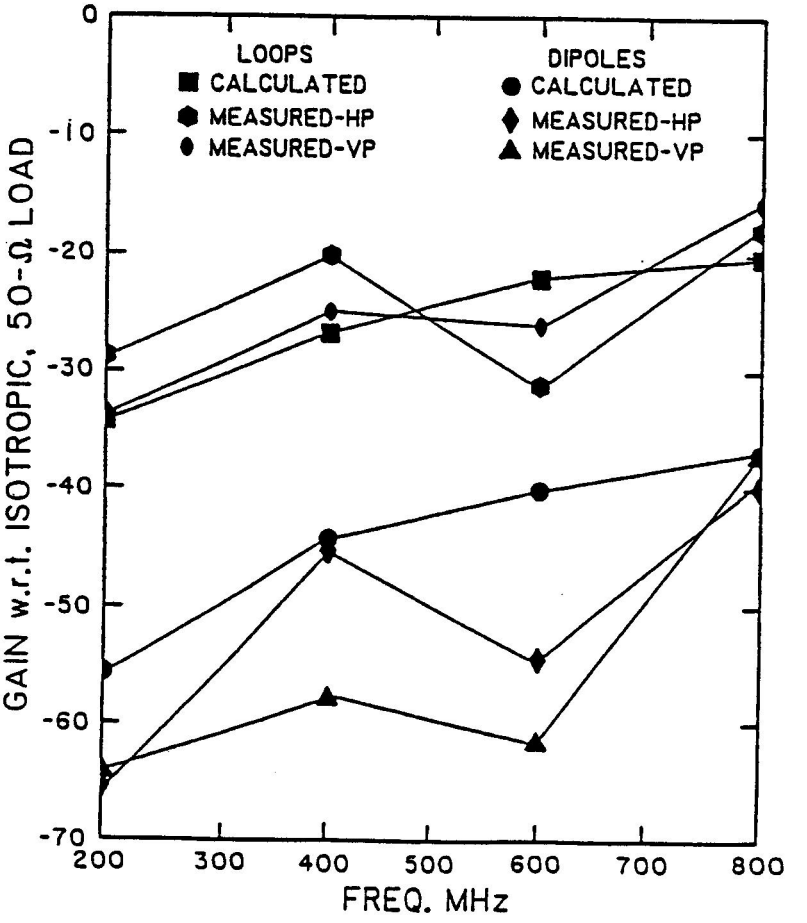

Figure 11 Calculated and measured values of boresight (θ=0 deg) gain versus frequency for both the loop and dipole antennas.

Corrections to the Linvill Normalization Procedure in the NEC Basic Scattering Code

Richard D. Albus

IIT Research Institute

Annapolis, MD, 21401

An error has been found in the Linvill coupling section of the NEC-Basic Scattering Code Version 2.2 (NEC-BSC2.2) [Marhefka, 1982] subroutine OUTPUT. Figure 1 lists the coupling section of subroutine OUTPUT before the error was corrected. On lines 339 and 340 of Figure 1, the short-circuit driving point admittances are incorrectly calculated as the inverse of the open-circuit driving point impedances, i.e., $y_{11} = 1/z_{11}$ and $y_{22} = 1/z_{22}$. The correct expressions for the short-circuit driving point admittances are given in Equation 1.

$$y_{11} = \frac{z_{22}}{z_{11}\ z_{22} - z_{12}\ z_{12}} \tag{1a}$$

$$y_{22} = \frac{z_{11}}{z_{11}\ z_{22} - z_{12}\ z_{12}} \tag{1b}$$

However, the conversion from a z-parameter to a y-parameter representation was unnecessary. An important property of consistent two-port systems is that relationships between variables and parameters in any two-port representation will have the same form as the relationships between the corresponding variables, parameters, and terminations of any other two-port representation [Linvill, 1961]. In other words, power ratios will have the same form regardless of whether one uses the z,y,h or g-parameter representations for the two-port model. Therefore, since the Basic

```
C!!!  ANTENNA TO ANTENNA COUPLING REPRESENTATION
      WRITE(6,300)
      WRITE(6,100)
      WRITE(6,100)
      WRITE(6,821)
821   FORMAT(' ANTENNA COUPLING VIA THE REACTION PRINCIPLE'///)
      WRITE(6,150)
      IF(LRECT.AND..NOT.LFQG) WRITE(6,823)
823   FORMAT(1H ,6X,'X',9X,'Y',9X,'Z',9X,'MAGNITUDE',5X,'PHASE',6X
     2,'MAG.**2',8X,'DB')
      IF(.NOT.LRECT.AND..NOT.LFQG) WRITE(6,824)
824   FORMAT(1H ,6X,'R',7X,'THETA',6X,'PHI',8X,'MAGNITUDE',5X
     2,'PHASE',6X,'MAG.**2',8X,'DB')
      IF(LFQG) WRITE(6,825)
825   FORMAT(1H ,15X,'FREQ.',16X,'MAGNITUDE',5X,'PHASE',6X
     2,'MAG.**2',8X,'DB')
      IF(IPRAD.EQ.4) YR11=REAL(1./Z11)
      IF(IPRAD.EQ.4) YR22=REAL(1./Z22)
      IMAX=10*NSN+1
      DO 820 I=NBN,NEN,NSN
      IM=I-1
      CTM=0.5*BABS(CT(I))
      CTP=DPR*BTAN2(AIMAG(CT(I)),REAL(CT(I)))
      GO TO (815,830,835,840),IPRAD
C!!!  UNNORMALIZED REACTION REPRESENTATION
815   CTM2=CTM*CTM
      CTDB=10.*BLOG10(CTM2)
      GO TO 850
C!!!  IMPEDANCE REPRESENTATION
830   Z12=CT(I)/(CI11*CI22)
      CTM2=BABS(Z12)
      CTDB=DPR*BTAN2(AIMAG(Z12),REAL(Z12))
      GO TO 850
C!!!  MODIFIED FRII'S REPRESENTATION
835   CTM2=0.25*CTM*CTM/(PRAD*PRADR)
      CTDB=10.*BLOG10(CTM2)
      GO TO 850

C!!!  LINVILLE REPRESENTATION
840   Z12=CT(I)/(CI11*CI22)
      Y12=Z12/(Z11*Z22-Z12*Z12)
      YY12=Y12*Y12
      YL=BABS(YY12)/(2.*YR11*YR22-REAL(YY12))
      YYL=YL*YL
      CTM2=0.5*YL*(1.+0.25*YYL)
      IF(YL.LT.0.01) GO TO 845
      YYLS=1.-YYL
      CTM2=(1.-SQRT(YYLS))/YL
845   CTDB=10.*BLOG10(CTM2)
850   CONTINUE
      IF(LFQG) GO TO 818
      RXP=RXS+RXI*IM
      TYP=TYS+TYI*IM
      PZP=PZS+PZI*IM
      WRITE(6,810) RXP,TYP,PZP,CTM,CTP,CTM2,CTDB
      GO TO 819
818   FQG=FQGS+FQGI*IM
      WRITE(6,811) FQG,CTM,CTP,CTM2,CTDB
819   IF(I.GT.IMAX) IMAX=IMAX+10*NSN
      IF(I.EQ.IMAX) WRITE(6,400)
820   CONTINUE
      IF(I.NE.IMAX) WRITE(6,400)
      WRITE(6,100)
      WRITE(6,100)
      RETURN
      END
```

Figure 1. The original listing of the antenna coupling section of subroutine NEC-BSC2.2 OUTPUT.

Scattering Code naturally calculates the open-circuit parameters (z-parameters), it will be more convenient to use these parameters to determine the variables associated with the Linvill coupling method.

In addition to the above calculation error, a labeling error exists. On line 354 of Figure 1 the phase angle of the mutual impedance is calculated. However, in the line-printer output, this phase angle is incorrectly labeled as a dB value as indicated by Format statements 824 and 825. Therefore, the line-printer output should be reformatted to correctly label the mutual impedance phase as an angle.

Figure 2 is a listing of the corrected code for the Linvill coupling method using a z-parameter representation for the two-port model as well as enhanced labeling for the line printer output, as used at the DoD Electromagnetic Compatibility Analysis Center (ECAC).

An example is provided to verify the changes to subroutine OUTPUT. This example consists of a horizontal 0.5 wavelength dipole and a horizontal 0.05 wavelength dipole. Both antennas are situated 0.25 wavelengths above an infinite, perfectly conducting ground plane. The NEC-BSC2.2 input data deck is shown in Figure 3. Figure 4 shows graphs of the outputs from the corrected and uncorrected versions of the NEC-BSC2.2. Also shown, for comparison, are results from the NEC-2 program [Burke and Poggio, 1981] for the same problem. Note that the corrected NEC-BSC2.2 results and the NEC-2 results are in close agreement.

```
      IF(LWRITE)WRITE(6,250) RXP,TYP,PZP,PRXR,PTYR,PPZR,PRXI,PTYI,PPZI
      IF (LPDP) THEN
         IF (LPRR) THEN
            WRITE(22,*)DUMMY, XVARAN, PRXR, PTYR, PPZR
         ELSE
            WRITE(22,*)DUMMY, XVARAN, PRXI, PTYI, PPZI
         END IF
      END IF
      GO TO 259
  258 FQG=FQGS+FQGI*IM
      IF (LWRITE) WRITE(6,251) FQG,PRXR,PTYR,PPZR,PRXI,PTYI,PPZI
      IF (LPDP) THEN
         IF (LPRR) THEN
            WRITE(22,*) DUMMY, FQG, PRXR, PTYR,PPZR
         ELSE
            WRITE(22,*) DUMMY, FQG, PRXI, PTYI,PPZI
         END IF
      END IF
  259 IF(I.GT.IMAX) IMAX=IMAX+10*NSN
      IF (LWRITE) THEN
      IF(I.EQ.IMAX) WRITE(6,400)
      END IF
  260 CONTINUE
      IF (LWRITE) THEN
      IF(I.NE.IMAX) WRITE(6,400)
      WRITE(6,100)
      WRITE(6,100)
      END IF
      RETURN
  800 CONTINUE
C!!!  ANTENNA TO ANTENNA COUPLING REPRESENTATION
      IF (LWRITE) THEN
         WRITE(6,300)
         WRITE(6,100)
         WRITE(6,100)
         WRITE(6,821)
  821 FORMAT(' ANTENNA COUPLING VIA THE REACTION PRINCIPLE'//)
C
C     INITIALIZE THE COLUMN HEADINGS.
C
        MAGVAL = 'MAGNITUDE'
        PHASEV = 'PHASE'
        MAGG2V = '   GAIN  '
        DBVALU = 'GAIN (DB)'
        IF (.NOT. LFQG) THEN
           IF (LRECT) THEN
              VFIRST = 'X'
              VSECND = '  Y  '
              VTHIRD = ' Z '
           ELSE
              VFIRST = 'R'
              VSECND = 'THETA'
              VTHIRD = 'PHI'
           END IF
        END IF
        IF (IPRAD .EQ. 1) THEN
           MAGG2V = ' MAG.**2 '
           DBVALU = '   DB    '
           WRITE(6,1000)
           WRITE(6,150)
```

Figure 2. ECAC's corrected version of the antenna coupling section of NEC-BSC2.2 subroutine OUTPUT.

```
            WRITE(6,2000)
          ELSE IF (IPRAD .EQ. 2) THEN
             MAGG2V = 'MAGNITUDE'
             DBVALU = '  PHASE  '
             WRITE(6,1010)
             WRITE(6,150)
             WRITE(6,2010)
          ELSE IF (IPRAD .EQ. 3) THEN
             WRITE(6,1020)
             WRITE(6,150)
             WRITE(6,2020)
          ELSE
             WRITE(6,1030)
             WRITE(6,150)
             WRITE(6,2020)
          END IF
C
C     WRITE THE HEADINGS FOR EACH COLUMN.
C
          IF (LFQG) THEN
                WRITE(6,2050) MAGVAL, PHASEV, MAGG2V, DBVALU
          ELSE
                WRITE(6,2060) VFIRST, VSECND, VTHIRD, MAGVAL, PHASEV,
     +                         MAGG2V, DBVALU
          END IF
         END IF
         IMAX=10*NSN+1
         DO 320 I=NBN,NEN,NSN
         IM=I-1
         CTM=0.5*BABS(CT(I))
         CTP=DPR*BTAN2(AIMAG(CT(I)),REAL(CT(I)))
         GO TO (815,830,835,840),IPRAD
C!!!     UNNORMALIZED REACTION REPRESENTATION
815      CTM2=CTM*CTM
          CTDB=10.*BLOG10(CTM2)
        GO TO 850
C!!!    IMPEDANCE REPRESENTATION
830     Z12=CT(I)/(CI11*CI22)
        CTM2=BABS(Z12)
        CTDB=DPR*BTAN2(AIMAG(Z12),REAL(Z12))
        GO TO 850
C!!!    MODIFIED FRIIS' REPRESENTATION
835     CTM2=0.25*CTM*CTM/(PRAD*PRADR)
        CTDB=10.*BLOG10(CTM2)
        GO TO 850
C!!!    LINVILL REPRESENTATION
840     Z12=CT(I)/(CI11*CI22)
        ZR11 = REAL( Z11 )
        ZR22 = REAL( Z22 )
        ZZ12=Z12*Z12
        ZL=CABS(ZZ12)/(2.*ZR11*ZR22-REAL(ZZ12))
        ZZL=ZL*ZL
C
        CTM2=0.5*ZL*(1.+0.25*ZZL)
        IF(ZL.LT.0.01) GO TO 845
        ZZLS=1.-ZZL
        CTM2=(1.-SQRT(ZZLS))/ZL
845     CTDB=10.*BLOG10(CTM2)
850     CONTINUE
        IF(LFQG) GO TO 818
        RXP=RXS+RXI*IM
        TYP=TYS+TYI*IM
        PZP=PZS+PZI*IM
        IF ((LPLT) .AND. (.NOT.LFQG)) THEN
```

Figure 2. Continued.

```
            IF(ABS(RXI-TYI).LT.EPSLN) THEN
                IVARAN = 1
            ELSE IF(ABS(TYI-PZI).LT.EPSLN) THEN
                IVARAN = 2
            ELSE
                IVARAN = 3
            END IF
          END IF
          IF (LWRITE) THEN
             WRITE(6,810) RXP,TYP,PZP,CTM,CTP,CTM2,CTDB
          END IF
          IF (LPLT) THEN
              IF (IVARAN .EQ. 1) THEN
                 XVARAN = PZP
              ELSE IF (IVARAN .EQ. 2) THEN
                 XVARAN = RXP
              ELSE
                 XVARAN = TYP
              END IF
              WRITE(19,*)DUMMY,XVARAN,CTDB
          END IF
          GO TO 819
818       FQG=FQGS+FQGI*IM
          IF (LWRITE) THEN
             WRITE(6,811) FQG,CTM,CTP,CTM2,CTDB
          END IF
          IF (LPLT) THEN
             WRITE(19,*) DUMMY,FQG,CTDB
          END IF
819       IF(I.GT.IMAX) IMAX=IMAX+10*NSN
          IF(LWRITE .AND. I.EQ.IMAX) WRITE(6,400)
820       CONTINUE
          IF (LWRITE) THEN
             IF(I.NE.IMAX) WRITE(6,400)
             WRITE(6,100)
             WRITE(6,100)
          END IF
          RETURN
          END
```

Figure 2. Continued.

```
CM:
CM:
CM:
CE: BSC  COUPLING FROM NEC SOURCES
FR:
0,3
US:
1
UN:
1
LP:
T
RG:
0.,0.,.25
90.,0.,90.,90.
-1,.01667,0
.3551E-3,89.984
RG:
-.01667,0.,.25
90.,0.,90.,90.
-1,.01667,0
.1464E-3,89.976
RG:
.01667,0.,.25
90.,0.,90.,90.
-1,.01667,0
.1464E-3,89.976
SG:
-.22222,0.,.25
90.,0.,90.,90.
-1,.05556,0
.2074E-2,-49.546
SG:
-.16667,0.,.25
90.,0.,90.,90.
-1,.05556,0
.4633E-2,-47.518
SG:
-.11111,0.,.25
90.,0.,90.,90.
-1,.05556,0
.6282E-2,-44.915
SG:
-.05556,0.,.25
90.,0.,90.,90.
-1,.05556,0
.7010E-2,-40.997
SG:
.00000,0.,.25
90.,0.,90.,90.
-1,.05556,0
.6863E-2,-35.603
SG:
.05556,0.,.25
90.,0.,90.,90.
-1,.05556,0
.7010E-2,-40.997
SG:
.11111,0.,.25
90.,0.,90.,90.
-1,.05556,0
.6282E-2,-44.915
SG:
.16667,0.,.25
90.,0.,90.,90.
-1,.05556,0
.4633E-2,-47.518
SG:
-.22222,0.,.25
90.,0.,90.,90.
-1,.05556,0
.2074E-2,-49.546
GP:
0
PN:
0.,0.,0.0
0.,0.,90.,0.
T
0.0,0.1,0.25
0.0,0.1,0.0
10
PR:LINVILL
4
(0.55803E-2,-0.39955E-2,(0.10204E-6,0.35507E-3)
(0.11847E+3,0.84823E+2),(0.80936,-0.28163E+4)
XQ:
EN:
```

Figure 3. NEC-BSC2.2 input data.

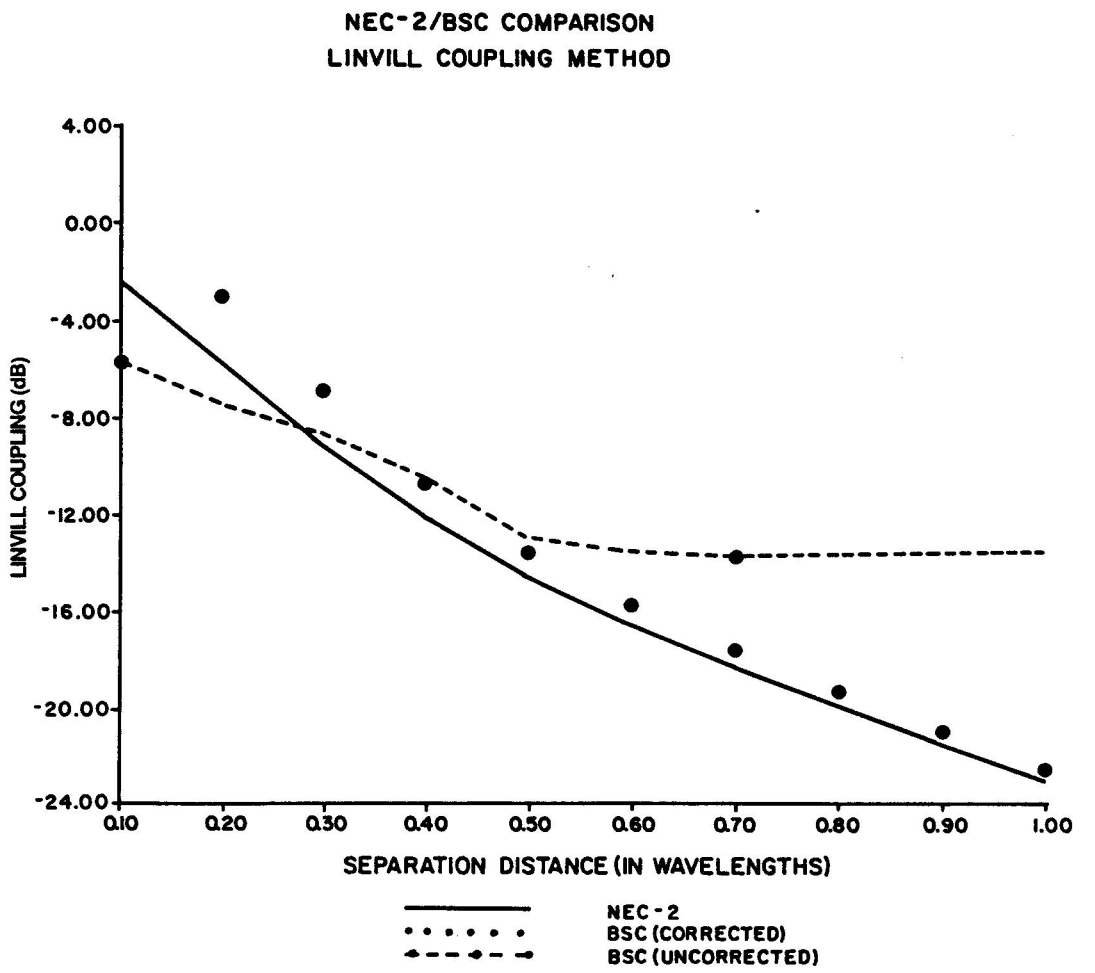

Figure 4. Comparison of corrected and uncorrected BSC coupling outputs with NEC-2 results.

Burke, G. T., and Poggio, A. T., "Numerical Electromagnetics Code (NEC) - Method of Moments", NOSC TD 116 (3 parts), Naval Ocean Systems Center, San Diego, CA, Revised 1980,81.

Linvill, J. G., and Gibbons, J. F., "Transistors and Active Circuits," McGraw-Hill Book Co., New York, NY, 1961.

Marhefka, R. J., "Numerical Electromagnetic Code-Basic Scattering Code NEC-BSC(Version 2) Part II: Code Manual," The Ohio State University ElectroScience Laboratory, Columbus, OH, December 1982.

On the Application of the Secant Method to the Spectral Iterative Approach

C. G. Christodoulou, R. J. Middelveen
University of Central Florida
Orlando, Florida 32816-0993

J. F. Kauffman
North Carolina State University
Department of Electrical and Computer Engineering
Raleigh, North Carolina 27650

ABSTRACT

A new iterative algorithm for calculating the electromagnetic scattering from planar, periodic gratings and grids was developed. Results are compared with the moment method and the Spectral Iteration (S.I.T.) method. The Secant approach is used in conjunction with the Spectral Iteration Approach to achieve convergence. It is shown that the Secant approach, which does not depend on the evaluation of numerical derivatives to achieve convergence like the contraction-corrector S.I.T. method, yields good results. Finally, suggestions for applying this method to two dimensional structures are included and discussed.

1. INTRODUCTION

Over the years, many numerical methods have evolved for solving the problem of electromagnetic scattering from periodic structures. The most popular approach, the method of moments [Harrington, R. F.], usually requires large amounts of computer memory when applied to periodic surfaces, although there are method of moment techniques that use Floquet information which improves this situation [Munk, B. A. and G. A. Burell]. Another technique, the Spectral-Iteration technique (S.I.T.) [Tsao, C. H. and R. Mittra] circumvents this memory requirement, but suffers from convergence problems.

Brand [Brand, J. C. and J. F. Kauffman] applied a corrective scheme that not only solved but accelerated the convergence problem. This method, however, depends on the evaluation of numerical derivatives to generate a series of convergent iterations. In some cases the computation of the derivatives can be so critical that the new corrective scheme fails to converge. This paper offers an improvement over Brand's method by using the Secant method instead of the contraction mapping approach.

The reasons why the contraction corrector-S.I.T. method fails to converge for two dimensional problems are discussed.

Results obtained by this method are compared with other theoretical and experimental data.

2. FORMULATION

It can be shown [Tsao, C. H. and R. Mittra] that the incident $\bar{H}$ field can be expressed in terms of the aperture electric field $\bar{\bar{E}}_a$ as:

$$\bar{H}^{inc} = -2/j\omega\mu \sum \begin{bmatrix} \alpha_{mn}\beta_{mn} & k^2 - \alpha^2_{mn} \\ \beta^2_{mn} - k^2 & -\alpha_{mn}\beta_{mn} \end{bmatrix} \begin{matrix} \cong \cong \\ G\ E_a \end{matrix} \quad (1)$$
$$x\ \exp[j(\alpha_{mn}x+\beta_{mn}y)]$$

where the tilde (~) symbol is used to denote the transformed quantity. The parameters α_{mn} and β_{mn} are the Floquet modes and are given by:

$$\alpha_{mn} = 2\pi m/a - k \sin\theta \cos\phi \quad (2)$$
$$\beta_{mn} = 2\pi n/b \sin\Omega - 2\pi m/a \cot\Omega + k \sin\theta \sin\phi$$

The Fourier transform of Green's function is given by:

$$\overset{\cong}{G} = (-j/2)\ (k^2 - \alpha^2_{mn} - \beta^2_{mn})^{-1/2}\ \overset{=}{I} \quad (3)$$

Equation (1) applies only to the aperture region shown in Figure 1 and in order to include the contribution of the $\bar{H}$ field along the conducting strips, the current densities have to be added to equation (1) to yield:

$$Tcr'(\bar{J}) = \hat{n} \times \bar{H}^{inc} + 2/j\omega\mu \sum \begin{bmatrix} \alpha_{mn}\beta_{mn} & k^2-\alpha^2_{mn} \\ \beta^2_{mn}-k^2 & -\alpha_{mn}\beta_{mn} \end{bmatrix} \begin{matrix} \cong \cong \\ G\ E_a \end{matrix} \quad (4)$$
$$x\ \exp[j(\alpha_{mn}x+\beta_{mn}y)]$$

Because the current density can only be present on the strips, a truncation operator is used which is defined by:

$$Tcr\{X(\bar{r})\} = \begin{cases} X(\bar{r}) & \text{for } \bar{r} \text{ in the aperture} \\ 0 & \text{for } \bar{r} \text{ in the conducting region} \end{cases}$$

$Tcr'\{X(\bar{r})\}$ = the opposite of T_{cr}

For gratings, $\Omega = 90^{o}$, b= ∞, and one ends up with the one dimensional problem.

To solve equation (4), Tsao and Mittra developed an iterative scheme which basically can be expressed in terms of the electric field only as:

$$\bar{E}_t^{(i+1)} = F^{-1}\left[\tilde{\tilde{G}}_0^{-1} F\{(j\omega\mu/2)\left[Tcr'\{\bar{H}_t^{inc} + (2/j\omega\mu) F^{-1}\left[\tilde{\tilde{G}}_0 F\, Tcr(\bar{E}_t^{i})\right]\}\right] - \bar{H}_t^{inc}\}\right] \qquad (5)$$

where:

$$\tilde{\tilde{G}}_0 = \begin{bmatrix} \alpha_{mn}\beta_{mn} & k^2-\alpha_{mn}^2 \\ \beta_{mn}^2-k^2 & -\alpha_{mn}\beta_{mn} \end{bmatrix} \quad \tilde{\tilde{G}} \qquad (6)$$

F stands for the Fourier transform and F^{-1} for its inverse. In this form, equation (5) does not converge for strip spacings of one wavelength or less. Brand imposed a corrective scheme to avoid this convergence problem. An alternative technique was developed, called the Secant Spectral Iterative method [Middelveen, R., C. G. Christodoulou, and J. F. Kauffman]. This method avoids the calculation of numerical derivatives which are required in Brands's technique. To see how the Contraction and Secant methods are used, equation (5) is expressed in an operator form as:

$$\bar{E}_t^{i+1} = L(\bar{E}^i) \tag{7}$$

where L is an operator representing the right hand side of equation (5). For equation (5) to converge the spectral radius of L should be:

$$\rho(L) \leq 1 \tag{8}$$

One way to achieve this is to cast equation (7) as:

$$g(x^i) = x^{i+1} = L(x^i) \tag{9}$$

by letting E = x.

Define a new mapping $G(x^i)$ so that

$$G(x^i) = \theta x^i + (1-\theta) g(x^i) \tag{10}$$

According to the contraction mapping theory [Rus, I.A] the transformation G of a metric space X onto itself is Lipshitz continuous if there exists a ρ, independent of x and y such that

$$d(G(x),G(y)) < \rho d(x,y) \text{ for all } x,y,\epsilon X,$$

where d(x,y) is a proper metric in X. For strictly contractive mapping ρ is less than one.

<u>One Dimensional Case</u>

For the one dimensional case the simplest possible metric d that can be used to obtain the optimum θ is chosen as follows:

$$|G(y)-G(x_o)| < \rho |y-x_o| \text{ for } \rho<1 \tag{11}$$

Let $y=x_o + \delta$ then

$$|G(x_o + \delta)-G(x_o)| < \rho|\delta| \text{ or } \left|\frac{G(x_o+\delta)-G(x_o)}{\delta}\right| < \rho \qquad (12)$$

So the necessary and sufficient condition for contraction mapping becomes:

$$\frac{d\ (G(x))}{dx} < \rho \qquad (13)$$

Now substitute (10) in (12) to obtain:

$$|\theta(x_o+\delta)+(1-\theta)\ g(x_o+\delta)-\theta x_o-(1-\theta)\ g(x_o)| < \rho|\delta| \qquad \text{or}$$

$$|\theta+(1-\theta)\ \frac{dg(x)}{dx}| \leq \rho$$

Setting $\rho=0$ in the above equation and solving for θ yields:

$$\theta = (dg(x)/dx)/(dg(x)/dx-1) \qquad (14)$$

This value of θ is called the "contraction" factor since it will yield a convergent scheme even in those cases where the basic iterative scheme of equation (7) fails to converge. It should be noted here that in the above analysis θ is treated as a constant when in fact it is a function of x. The reason for that treatment is that θ is solved in the neighborhood of a solution (root) x_o where the values that θ acquires are approximately equal. Therefore, θ can be assumed to be constant within that particular neighborhood.

Two Dimensional Case

In two dimensions, the basic iterative scheme of equation (10) is

given by:

$$\begin{bmatrix} x^{n+1} \\ y^{n+1} \end{bmatrix} = \begin{bmatrix} \theta 11 & \theta 12 \\ \theta 21 & \theta 22 \end{bmatrix} \begin{bmatrix} x^n \\ y^n \end{bmatrix} + \begin{bmatrix} (1-\theta 11) & -\theta 12 \\ -\theta 21 & (1-\theta 22) \end{bmatrix} \begin{bmatrix} g(x^n, y^n) \\ h(x^n, y^n) \end{bmatrix} = \begin{bmatrix} G(x^n, y^n) \\ H(x^n, y^n) \end{bmatrix} \quad (15)$$

Now it is easy to set all four partial derivates Gx, Gy, Hx and Hy equal to zero to obtain:

$$\begin{aligned} Gx &= \theta 11 + (1-\theta 11)\, g_x - \theta 12\, h_x = 0 \\ Gy &= \theta 12 + (1-\theta 11)\, g_y - \theta 12\, h_y = 0 \\ Hx &= \theta 21 - \theta 21\, g_x + (1-\theta 22)\, h_x = 0 \\ Hy &= \theta 22 - \theta 21\, g_y + (1-\theta 22)\, h_y = 0 \end{aligned} \quad (16)$$

Solving this system of equations for θ11, θ12, θ21, θ22 yields:

$$\theta 11 = \frac{h_x g_y + g_x (1-h_y)}{h_x g_y - (1-g_x)(1-h_y)} \quad (17)$$

$$\theta 12 = \frac{g_y}{h_x g_y - (1-g_x)(1-h_y)} \quad (18)$$

$$\theta 21 = \frac{h_x}{h_x g_y - (1-g_x)(1-h_y)} \quad (19)$$

$$\theta 22 = \frac{h_x g_y + (1-g_x) h_y}{h_x g_y - (1-g_x)(1-h_y)} \quad (20)$$

Again, this choice of θ's works very well for the one dimensional problem

but it does not lead to convergence for the two dimensional wire mesh problem.

To explain why this method does not work for the two dimensional problem the theory for constructing convergent iterations for a pair of transcendental equations is invoked. According to this theory the original system of equations

$$x^{n+1} = G(x^n,y^n)$$
$$y^{n+1} = H(x^n,y^n) \quad \text{can be written as:}$$
$$x^{n+1} = x^n+\alpha[g(x^n,y^n)-x^n]+\beta[h(x^n,y^n)-y^n] = G(x^n,y^n)$$
$$y^{n+1} = y^n+\gamma[g(x^n,y^n)-x^n]+\delta[h(x^n,y^n)-y^n] = H(x^n,y^n) \qquad (21)$$

Note the similarity of the above equation with equation (15). The parameters α, β, γ and δ play the same role in equation (21) as the relaxation factors $\theta 11$, $\theta 12$, $\theta 21$ and $\theta 22$ in equation (15). To find the root of equation (21) it is desired to determine α, β, γ and δ, by the four conditions that the first partial derivatives of G and H are zero at some point (x,y) that hopefully is near the root. Note that the unknown parameters enter linearly in the same way as θ's do in equation (15), so the calculation of the partial derivatives G_x,G_y,H_x and H_y poses no problem. For the case of transcendental equations, it is known that this method of constructing convergent schemes works provided that the partial derivatives g_x,g_y,h_x and h_y DO NOT vary very rapidly in the neighborhood of the root (x_o,y_o). Thus, although it is easy to produce a G and an H that are well behaved at the root (x_o,y_o) they may behave quite badly a small distance away. If this strategy is to be successful, G and H must not only have small partial derivatives in some region, but this region must also include the desired root. For the two dimensional wire mesh it

was found that the derivatives g_x,g_y, h_x and h_y vary very rapidly, especially at points close to the edges of the wire. So this fact, and the lack of knowledge of the region within which a root exists, causes this method to fail.

For the Secant Method a different approach is taken. First we define a residue vector F defined by:

$$F(E) = L(E)-E \tag{22}$$

The value of F is actually the error in the solution of equation (7). The secant method technique is applied to equation (22) as:

$$E^{i+1} = E^i-[F(E^i)(E^i-E^{i-1})/(F(E^i)-F(E^{i-1}))] \tag{23}$$

It should be noted that the form of this equation is good only for one dimensional periodic structures (gratings) and that it has to be applied at each sampling point. Numerically, the secant method has an order of convergence of 1.62 [Traub, J. F.].

3. TWO DIMENSIONAL PROBLEM

For two dimensional problems, such as grids, the formulation of the Secant method is more complex. In this case the problem becomes the fitting of a surface at three points [Acton, F. S.]. We actually seek a common root for $E_x(x,y)$ and $E_y(x,y)$. In such a case this method is summarized as follows:

1. Given three points in (x,y) plane, fit planes to the two surfaces, E_x and E_y, and determine the point of intersection, point (x_4,y_4).

2. Substitute one of the first three points by (x_4, y_4).

3. Repeat steps 1 and 2 to convergence.

It should be noted that there are several degrees of freedom in choosing which point to substitute at each iteration. Geometrically, this method fails if all points are collinear due to instability. So one should choose the three points that will maximize some measure of noncolinearity [Froberg, C. E.].

Some Computational Details:

To carry out step one of the above mentioned process we start with the general plane equation:

$$a_1x+a_2y+z = m \tag{24}$$

Substituting the n^{th} point on the E_x surface we get:

$$a_1x_n+a_2y_n+E_{xn} = m \tag{25}$$

Subtracting this equation from the general plane equation on the (x,y) plane yields:

$$a_1(x-x_n)+a_2(y-y_n) = E_{xn} \qquad n = 1,2,3 \tag{26}$$

Similarly, for the E_y surface we obtain:

$$a_3(x-x_n)+a_4(y-y_n) = E_{yn} \qquad n = 1,2,3 \tag{27}$$

After some manipulation these equations can be decoupled and end up with

the following conditions for solving for x and y:

$$\begin{vmatrix} x-x_1 & x-x_2 & x-x_3 \\ E_{x1} & E_{x2} & E_{x3} \\ E_{y1} & E_{y2} & E_{y3} \end{vmatrix} = 0 \qquad (28)$$

and

$$\begin{vmatrix} y-y_1 & y-y_2 & y-y_3 \\ E_{x1} & E_{x2} & E_{x3} \\ E_{y1} & E_{y2} & E_{y3} \end{vmatrix} = 0 \qquad (29)$$

Also, to avoid having colinearity the following condition should be satisfied:

$$a_1a_4-a_2a_3 \neq 0 \qquad (30)$$

In general, stability in two dimensions is a much more difficult quality to handle than in one.

4. NUMERICAL RESULTS

A couple of numerical results are shown here to validate the one dimensional algorithm. Figure 2 depicts the electric field across a unit cell with a large strip size. The result is in good agreement with Brand's result. In Figure 3, the reflection coefficient predicted with this method is compared with those reported by Brand and Wait [Wait, J. R.] for various cell widths. In both examples 128 samples were used.

These results were run on a VAX 11/750 machine. Table 1 shows the number of iterations required for different numbers of sampling points.

The 32 sample points with 8 iterations require 5.25 seconds of CPU time while with 512 sampling points and 20 iterations it takes 38.58 seconds to converge. It was found that a sampling number larger than 128 will not lead to any significant change in the value of the reflection coefficient.

It should be mentioned here that this method solves for both induced currents and aperture fields whereas the FFT conjugate gradient method can only solve for one variable at a time (current or aperture field).

5. SUMMARY AND CONCLUSIONS

An alternative derivative-free method was developed to ensure the convergence of the spectral iteration approach as applied to the electromagnetic scattering from periodic gratings. This method derived from the original S.I.T. method to which a modification was made via the secant method. The two dimensional problem was formulated and its conditions for convergence stated.

6. REFERENCES

Acton, F. S., Numerical Methods that Work. Harper and Row. New York, N.Y., 1970.

Brand, J. C. and J. F. Kauffman, "The application of contraction theory to an iterative formulation of electromagnetic scattering", IEEE Trans. Antennas Propag., vol. AP-33, pp. 1354-1362, Dec. 1985.

Froberg, C. E., Introduction to Numerical Analysis, Addison-Wesley Co., Reading, Mass. 1965.

Harrington, R. F., Field Computation by Moment Methods, MacMillan, New York, 1968.

Middelveen, R. J., G. G. Christodoulou, and J. F. Kauffman, "The secant-corrector spectral iteration method", IEEE/AP-S and URSI Symp., Philadelphia, June 1986, pp. 60. (digest).

Munk, B. A. G. A. Burrell, "Plane Wave Expansion for Arrays of Arbitrary Oriented Piecewise Linear Elements and its Applications in Determining the Impedance of a Single Antenna in a Lossy Half-Space", IEEE Trans. Antenna Propag., Vol. AP-27, No.3, May 1979.

Rus, I. A., "Approximation of Fixed Points of Generalized Contraction Mapping", from Topics in Numerical Analysis II, edited by John J. Miller, Academic Press, New York, 1974, pp. 157-161.

Traub, J. F., Iterative Methods for the Solution of Equations. Chelsea Publishing Co., New York, N.Y., 1982.

Tsao, C. H. and R. Mittra, "A spectral-iteration approach for analyzing scattering from frequeny selective surfaces", IEEE Trans. on Antennas Propag., vol. AP-30, no. 2, pp. 303-308, Mar. 1982.

Wait, R. J., "Theories of scattering from wire grid and mesh structures", in Electromagnetic Scattering, P.L.E. Uslenghi, Ed., New York: Academic Press, 1978, pp. 253-287.

Table 1.

Sampling points Vs. Iterations required

Sampling points	Iterations
32	8
64	8
128	16
256	14
512	20

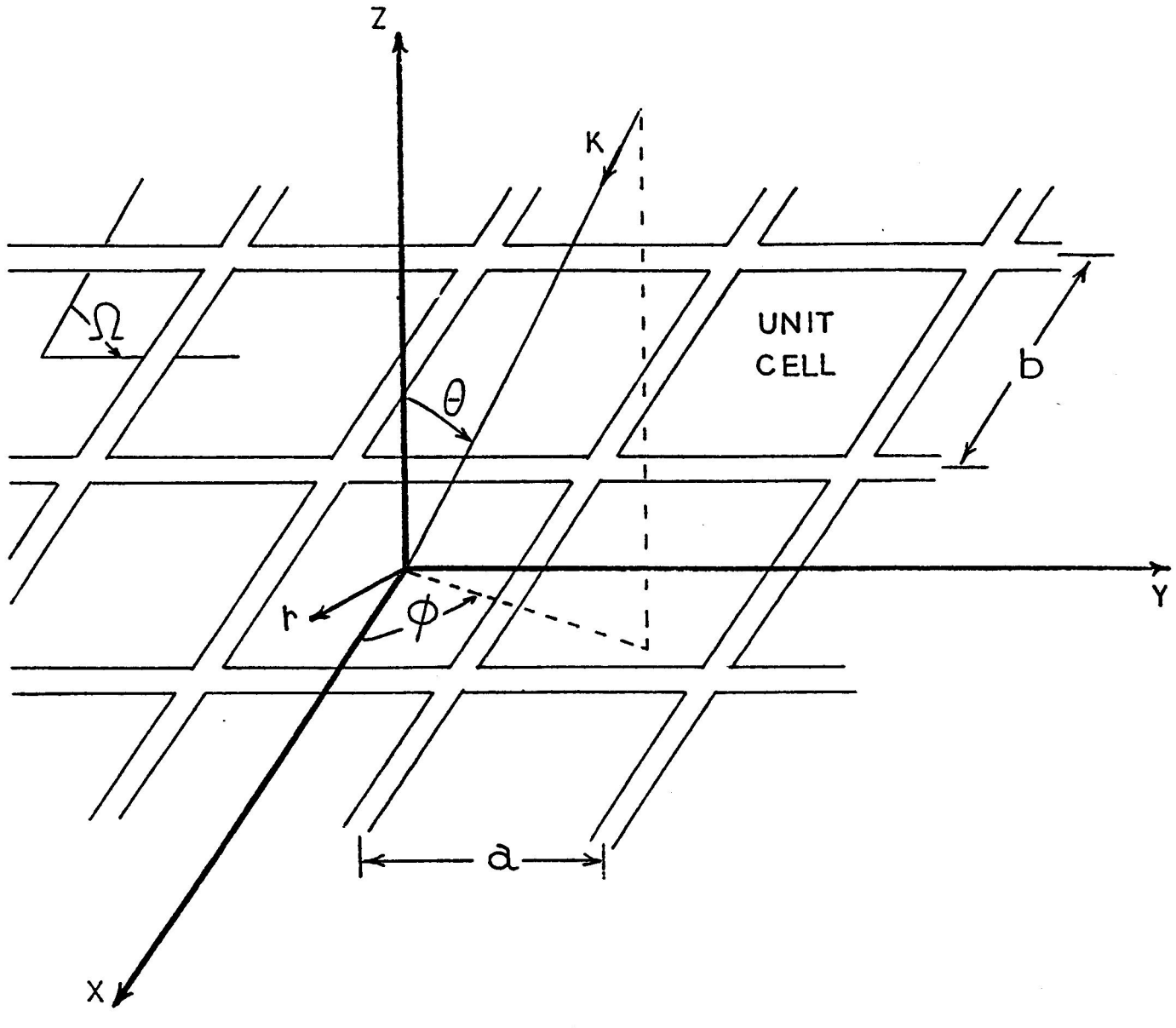

Fig. 1. Geometry of plane

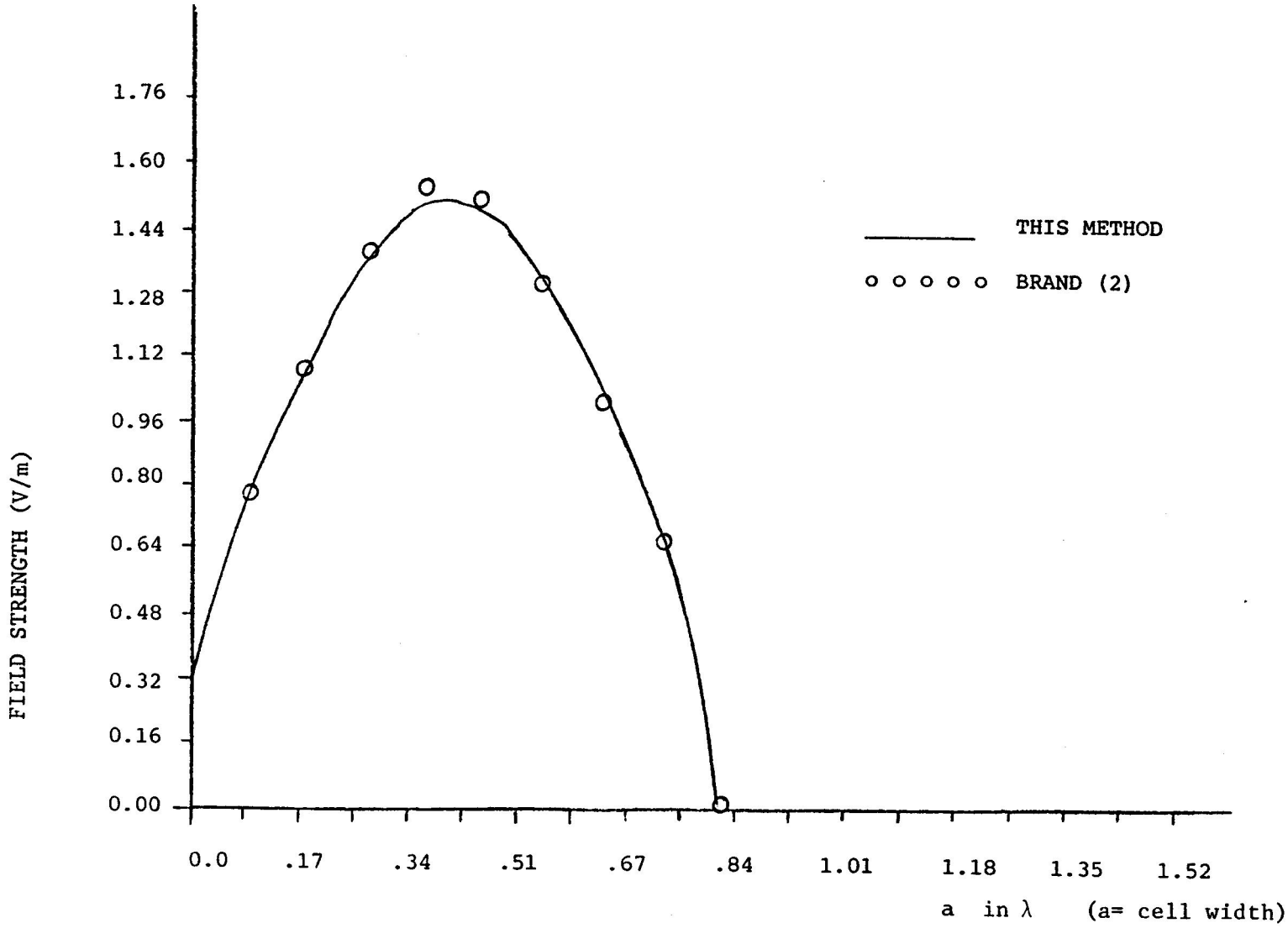

Fig. 2. Electric field across a unit cell with $a=1.4\lambda$, strip width=0.6 a, $b=\infty$, $\theta = 0$.

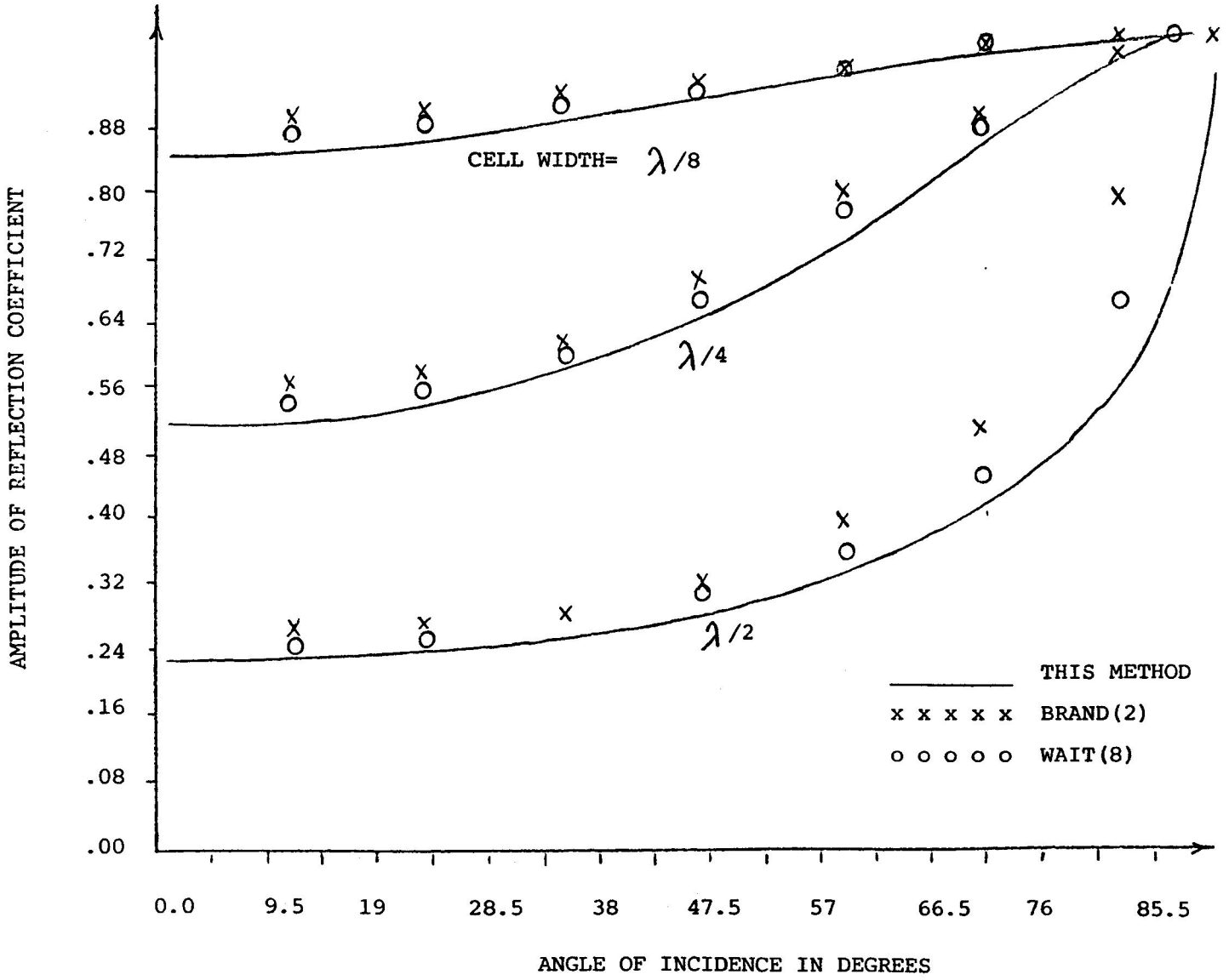

Fig. 3. Reflection coefficient for various angles of wave incidence. Width of strip= 4/600 λ , b= ∞ and (ϕ = 0) .

1988 INSTITUTIONAL MEMBERS

ANTENNA TECHNOLOGIES
6 Shields Dr Box 618
Bennington, VT 05201

NOKIA-MOBIRA
P O Box 86 24101 Salo
Finland

IMAGINEERING LIMITED
95 Barber Greene Rd #112
Canada M3C 3E9

W RICHARD GREEN & ASSOC.
3200 Wilkinson Rd
Cameron Park, CA 95682

HUNTING ENGINEERING LTD
Redding Wood, Ampthill
Bedford England MK45 2HD

ROSEMONT AEROSPACE
14300 Judicial Rd
Burnsville, MN 55337

TEXAS INSTRUMENTS
2501 W University
P O Box 801/MS 8019
McKinney, TX 75069

PRINCIPAL LIBRARIAN
Telecom Australia
Private Bag 37, Clayton
Victoria, Australia 3168

DELFIN SYSTEMS
1349 Moffett Park Dr
Sunnyvale, CA 94089

SCALA ELECTRONIC CORP
P O Box 4580
Medford, OR 97501

THE PILLSBURY COMPANY
311 2nd St. S.E.
Minneapolis, MN 55414

AWA DEFENCE & AEROSPACE
P O Box 96
North Ryde NSW,
Australia 2113

NEW MEXICO STATE UNIVERSITY
Box 3548/Physics/Science Lab
Las Cruces, NM 88003

TRW
One Space Park
Redondo Beach, CA 90278

CULHAM LABORATORY
UK Atomic Energy Authority
Abingdon Oxfordshire
England OX14 3DB

U.S. AIR FORCE
Base Library Bldg 437
485 EIG/EIEUS
Griffiss, AFB, NY 13441

KATHREIN-WERKE KG
Postfach 260
D-8200 Rosenheim 2
West Germany

OAR CORPORATION
10447 Roselle St.
San Diego, CA 92121

SCIENCE APPLICATIONS INTERNATIONAL
5151 East Broadway, Suite 900
Tucson, AZ 85711

U.S.COAST GUARD
2100 2nd St. SW
Washington, DC 20593-0001

STG NATIONAL LIGHT-EN
Ruimtevvart Laboratorium
1059 CM Amsterdam
Netherlands

TELECOM RESEARCH LABS
770 Blackburn Rd
CLayton, Victoria, Australia 3168

MARTIN MARIETTA AEROSPACE
P.O. Box 179
Denver, CO 80201

UNIVERSITY OF CA/BERKELEY
414 Hearst Mining Bldg
Berkeley, CA 94720

FORD AEROSPACE
3939 Fabian Way MS T96
Palo Alto, CA 94303

ITT AEROSPACE/OPT DIVISION
P O Box 3700
Ft Wayne, IN 46801

NYNEX CORPORATION
500 Westchester Ave
White Plains, NY 10604

BUSINESS MANAGEMENT SYSTEMS
Sproughton House
Sproughton, Ipswich
Suffolk, England IP8 3AW

TELEX COMMUNICATIONS INC.
8601 Northeast Hwy 6
Lincoln, NE 68505

ROCKWELL INTERNATIONAL
1745 Jeff Davis Hwy, Suite 1
Arlington, VA 22202

KATHREIN INCORPORATED
26100 Brush Ave, Suite 319
Euclid, OH 44132